DEVELOPMENT OF SUBMERGED ABRASIVE WATER JET SYSTEM AND INVESTIGATION THE PERFORMANCE BY MACHINABILITY OF CASTAMIDE MATERIAL

Salem A. Basher IBRAHIM

2020
DOCTORATE THESIS
DEPARTMENT OF MECHANICAL ENGINEERING

Thesis Advisor
Assistant Prof. Dr. Muhammet Hüseyin ÇETİN

DEVELOPMENT OF SUBMERGED ABRASIVE WATER JET SYSTEM AND INVESTIGATION THE PERFORMANCE BY MACHINABILITY OF CASTAMIDE MATERIAL

Salem A. Basher IBRAHIM

T.C.
Karabuk University
Institute of Graduate Programs
Department of Mechanical Engineering
Prepared as Doctorate Thesis

Thesis Advisor
Assistant Prof. Dr. Muhammet Hüseyin ÇETİN

KARABUK
October 2020

I certify that in my opinion the thesis submitted by Salem A. Basher IBRAHIM titled "DEVELOPMENT OF SUBMERGED ABRASIVE WATER JET SYSTEM AND INVESTIGATION THE PERFORMANCE BY MACHINABILITY OF CASTAMIDE MATERIAL" is fully adequate in scope and in quality as a thesis for the degree of Master of Science.

Assistant Prof. Dr. Muhammet Hüseyin ÇETİN ……
Thesis Advisor, Department of Mechanical Engineering

This thesis is accepted by the examining committee with a unanimous vote in the Department of Mechanical Engineering as a Doctorate of Science thesis. 22.10.2020

Examining Committee Members (Institutions)	Signature
Chairman : Prof. Dr. M. Bahattin ÇELİK (KBU)	.....
Member : Doç. Dr. Okan ÜNAL (KBU)	.....
Member : Doç. Dr. Fuat KARTAL (KU)	.....
Member : Assist. Prof. Dr. Nuri ŞEN (DU)	.....
Member : Assist. Prof. Dr. M. Hüseyin ÇETİN (KBU)	.....

The degree of Doctorate of Science by the thesis submitted is approved by the Administrative Board of the Institute of Graduate Programs, Karabük University.

Prof. Dr. Hasan SOLMAZ .....
Head of the Institute of Graduate Programs

"I declare that all the information within this thesis has been gathered and presented in accordance with academic regulations and ethical principles and I have according to the requirements of these regulations and principles cited all those which do not originate in this work as well."

Salem A. Basher IBRAHIM

ABSTRACT

PhD Thesis

DEVELOPMENT OF SUBMERGED ABRASIVE WATER JET SYSTEM AND INVESTIGATION THE PERFORMANCE BY MACHINABILITY OF CASTAMIDE MATERIAL

Salem A. Basher IBRAHIM

Karabuk University
Institute of Graduate Programs
Department of Mechanical Engineering

Thesis Advisor:
Assist. Prof. Dr. Muhammet Hüseyin ÇETİN
October 2020, 134 pages

This study evaluates the performance of the submerged abrasive water jet turning (AWJT) system, which is used to improve castamide machinability. It comprehensively investigates the concerned materials and process parameters. For minimizing surface roughness and maximizing material removal rate through the mentioned submerged turning process of castamide, we determined optimum parameters. As input parameters, abrasive flow rate (AFR), 3-level traverse speed (TS), and spindle speed (SS) were selected, and the full factorial experimental design was accomplished for this purpose. We statistically analyzed the input parameters' effect ratios using ANOVA, graphic methods, and 3D surface images and examined their interactions. We used TOPSIS and VIKOR methods to determine the optimum testing conditions, and compared the experimental results to the results shown by the conventional abrasive water jet process. Moreover, we obtained regression equation

for mathematically expressing the experimental results, which showed the relations between different variables. Experimental results clearly demonstrated that the submerged AWJT increased the surface roughness of castamide 15% more than the conventional AWJT. It also reduced the rate of metal removal by 5.22%. During the treatment with abrasive water jet, no thermal effect was observed on the surface. We obtained a clean cutting surface, and the sound level reduced to 85dB, which made it environment-friendly. It did not generate any toxic or hazardous substance. The results of ANOVA showed that for castamide machinability, the traverse speed is the most effective parameter. The effectiveness of traverse speed was 85.56% for material removal rate while it was 83.11% for surface roughness. TOPSIS and VIKOR optimization showed 40mm/min TS, 300-rpm SS value and 310g/min AFR, which were optimum test conditions.

Keywords : Submerged turning, Abrasive water jet, Castamide, TOPSIS, VIKOR.
Science Code : 91438

ÖZET

Doktora Tezi

SU ALTI AŞINDIRICI SU JETİ SİSTEMİNİN GELİŞTİRİLMESİ VE KESTAMİD MALZEMESİNİN İŞLENEBİLİRLİĞİ İLE PERFORMANSININ İNCELENMESİ

Salem A. Basher IBRAHIM

Karabük Üniversitesi
Lisansüstü Eğitim Enstitüsü
Makina Mühendisliği Anabilim Dalı

Tez Danışmanı:
Dr. Öğr. Üyesi Muhammet Hüseyin ÇETİN
Ekim 2020, 134 sayfa

Bu çalışmada, su altı aşındırıcı su jeti tornalama (AWJT) sistemi, kestamid malzemesinin işlenebilirliğini artırmak için kullanılmış ve proses parametreleri kapsamlı bir şekilde araştırılmıştır. Su altı kestamid tornalama işleminde yüzey pürüzlülüğünü en aza indirecek ve talaş kaldırma oranını en üst düzeye çıkaracak optimum parametreler belirlenmiştir. Giriş parametreleri olarak 3 seviyeli kesme hızı (TS), aşındırıcı akış hızı (AFR) ve iş mili hızı (SS) dikkate alınmış ve deneysel tasarım tam faktöryel tasarım olarak yapılmıştır. Giriş parametrelerinin etki oranları ANOVA ve grafiksel yöntemler ile istatistiksel olarak analiz edilmiş ve etkileşimleri 3B yüzey görüntüleri ile incelenmiştir. Optimum test koşulu TOPSIS ve VIKOR yöntemleri ile belirlenmiştir. Deney sonuçları geleneksel aşındırıcı su jeti işlemi ile karşılaştırılmıştır. Ayrıca değişkenler arasındaki ilişkileri göstermek ve deneysel sonuçların matematiksel olarak açıklanması için regresyon denklemleri elde edilmiştir. Deneysel

sonuçlara göre, su altı AWJT, kestamid malzemesinin yüzey pürüzlülüğünü geleneksel AWJT'ye kıyasla %15 arttırmış ve metal çıkarma oranını %5.22 azaltmıştır. Aşındırıcı su jeti ile işlem sırasında termal bir etki yoktur, işlenmiş yüzeyde ısıl etki gözlenmez. Ayrıca su altı yöntemde kesme yüzeyi temiz kalır, su sıçramaları önlenir ve ses seviyesi düşürülür (85 dB). Su altı yöntem çevre dostudur, herhangi bir toksik veya çevreye zararlı madde oluşturmaz. ANOVA sonuçları, kesme hızının kestamidin işlenebilirliği üzerinde en etkili parametre olduğunu göstermiştir. Dönüş hızı, yüzey pürüzlülüğü üzerinde %83.11 ve talaş kaldırma oranında %85.56 olarak bulunmuştur. TOPSIS ve VIKOR optimizasyon sonuçlarına göre, optimum test koşulları olarak 40 mm/dk. TS, 310 g/dk. AFR ve 300 rpm SS değerleri belirlenmiştir.

Anahtar Kelimeler : Tozaltı tornalama, Aşındırıcı su jeti, Castamide, TOPSIS, VIKOR.

Bilim Kodu : 91438

ACKNOWLEDGMENT

First, I express my deepest gratitude to my kind and honorable supervisor Assist. Prof. Dr. Muhammet Hüseyin ÇETİN for guidance, motivation, valuable advice, support, and constructive feedback, which helped me accomplish this research.

I am thankful to the committee members for their valuable time, and constructive feedback, which will be certainly helpful for improving my knowledge.

I appreciate my mother for encouraging me to make my life valuable, bringing passion to it, and extending unconditional love. I value her support during my degree programs, and for encouraging me to complete this thesis, for which, I certainly feel very lucky.

I also thank my wife and rest of my family for their patience, support, and encouragement during my studies.

I also thank the university staff for their support, Turkish people for their love, and the Turkish government to offer its educational opportunities to students like me. I also express my deepest regards to my friends, who have been with me.

CONTENTS

Page

Page

Page

Page

LIST OF FIGURES

Page

Page

Page

LIST OF TABLES

Page

SYMBOLS AND ABBREVIATIONS INDEX

SYMBOLS

Pa	:	Pressure
P_h	:	Hydraulic pressure.
Ψ	:	Velocity coefficient of the orifice.
$\emptyset$	:	Coefficient of "vena-contracta."
c_d	:	Discharge coefficient of the orifice.
v_{wj}	:	The volume flow rate.
R	:	loading factor.
η	:	momentum loss factor.
V	:	Head velocity.
f	:	Mass flow rate.
d	:	The depth of cut.
K	:	The index set of utility criteria.
Ci	:	The highest value.
Qi	:	value is calculated.
dB	:	The decibel.

ABBREVIATIONS

AWJM	:	Abrasive Water Jet Machining
Ra	:	Surface roughness value (μm)
ASR	:	Ra (μm)
P	:	Pump pressure(MPa)
ND	:	Nozzle Diameter (mm)
NFR	:	Nozzle Feed Rate (mm min^{-1})

SS	:	Spindle Speed (min^{-1})
AFR	:	Abrasive Flow Rate (g min^{-1})
DOC	:	Depth of Cut (mm)
SOD	:	Standoff Distance (mm)
MRR	:	Material Removal Rate (mm^3 min^{-1})
HDPE	:	High-Density Polyethylene
MRF	:	Material Removal Factor
QCM	:	Quartz Crystal Microbalance
HALS	:	Hindered Amine Light Stabilizers
UPF	:	Ultra Violet Protection Factor
EDM	:	Electrical Discharge Machining
CNC	:	Control Numerical Control
CM	:	Chemical Machining.
CJM	:	Chemical jet machining.
ECM	:	Electro-chemical Machining.
USM	:	Ultrasonic Machining.
LBM	:	Laser–Beam Machining.
WJC	:	Water Jet Cutting.
AWJ	:	Abrasive Water Jet.
TS	:	Travers speed.

PART 1

INTRODUCTION

1.1. HISTORY

Since abrasive water jet machining (AWJM) is a comparatively new machining method, it is now popular and utilized for several industrial purposes. It is an unconventional methodology, which removes material through the effect of erosion induced on a sample through maximized water velocity and grit abrasives' pressure. Many parameters have an impact on the machined surface cut quality carried out thorough this method. Significant factors affecting the cutting quality include standoff distance, traverse speed, hydraulic pressure, abrasive forms, and flow rates. Significant AWJM quality factors include kerf width, kerf tapering, surface roughness (SR), and material removal rate (MRR),

Being a new methodology, AWJM is widely used, and besides, it combines the features of abrasive jet machining technique and water jet. According to experts, it is an unconventional method that uses the erosion impact through water pressure and velocity when the process is carried out on a sample [1].

During the 1970s, waterjet was used for cutting wood and plastic, and it is commercialized in during the late 1980s and examined woodcutting through hi-speed jets. They were initially manufactured for industrial use, and McCartney Manufacturing Company offered them for sale in 1972; they were placed in Alto Boxboard. The abrasive water jet was invented and improved in 1980 and 1983, respectively. Moreover, additional abrasives improved the material range that is possible to be substantially reduced using a Watergate [2]. It is a widely used technique in comparison with other unconventional technologies mainly because it offers various benefits. Industries use it to cut many substances, out of which, some are hard while

others are soft. Experts consider it useful for cutting fibrous, brittle and delicate substances. Over the years, this technique has shown low sensitivity to properties of different materials, as it causes no chatter. It does not generate considerable heat; therefore, the machined surfaces are generally heat-free, and it causes no residual stress. AWJM is a highly versatile and flexible method. This process is not without drawbacks, and its greatest drawback is its noise, and besides, it results in the messier workplace as compared to some other processes [3].

This process has many benefits that result in achieving important milestones in the moulding and manufacturing sectors [4]:

1. Very quick programming and set-up
2. Minimum installation needs for many parts
3. Virtual operations for 2D material shapes
4. Minimum role of extra factors in the machining process
5. Minimum or no heat generation

Capabilities of machining thicker plates: This process is used for removing paint, cutting softer substances, slicing frozen meats, high-level immunization, surgeries, nuclear equipment demolition, drilling specific substances, pocket milling, and leather cutting. AWJM cuts non-iron alloys, some steels, Ti & Ni alloys, some polymers, honeycombs, ceramics, stones, concrete, granite, reinforced plastics, wood, metal/polymer laminations and laminations of glass fibre metals.

There are many differences among researchers on abrasive jets' hydrodynamic aspects, so there are different opinions regarding how to increase the operational effectiveness of this process through variables including abrasive size, type/concentration, speed of impact, and impingement angle. Some researchers tried to find the effect of shapes, sizes and types of nozzles, jet pressure, velocity, and SOD (standoff distance). These researches were based on the performance of this technique and the other contemporary techniques based on geometrical tolerance, rate of removing materials, and finishing of the surfaces of the under-process workpieces [5].

For carrying out the predictions pertaining to the cutting depth, some trials were carried out with varying abrasive mass flow rates, water pressures, SODs, and nozzle traverse speeds while the granite tiles were used for AWJ (abrasive water jet) cutting technique [6].

Researchers conducted many studies to understand how "through pockets" are formed when the milling process is conducted using AWJ. Moreover, some researches were conducted to investigate the AWJ milling. During recent years, researchers are taking an interest in conducting trials on the generation of blind pockets with the help of AWJ, which is termed as "controlled depth milling" [7].

The cutting depth has been a frequently investigated characteristic for predicting AWJM parameter/s. The available literature shows that cut depth reduces when traverse speed increases and when the abrasive size reduces [8] [9]. If we take a look at the other aspects, increased abrasive mass flow rates also deepen the cuts while SOD shows no considerable impact on the cutting depth [10].

The SOD impact on the cutting depth is insignificant, which is so because SOD has a smaller range barely 2-5mm [11]. Moreover, optimal SOD equals 2mm [12].

The surface roughness, which is another aspect that helps to determine and evaluate the product quality, is used as a parameter to assess the plain water jet (PWJ) milling products while the maximum profile-height roughness, average surface roughness, and mean profile irregularity spacing are dependent variables [13]. Moreover, the cut depth is a significant measure that helps to evaluate the effectiveness and quality of the process [9, 14].

1.2. ABRASIVE WATER JET MACHINING

In this study, the submerged AWJM process and optimization has been studied in the light of significant parameters as well as characteristics of the orthogonal array and full factorial experimental design method.

The current study is based on three parameters of machining including spindle speed, abrasive flow rate and traverse speed, which have been optimized using various characteristics of performance, for example, surface roughness and material removal rate. The outcomes suggest that the submerged AWJ machining is possible to improve with the help of this technique [15].

1.3. OBJECTIVES

1. Development of submerged abrasive water jet system systematically.
2. Study efficiency of material cutting process using submerged machining.
3. Investigation of interactions between process parameters and characteristics of submerged AWJ.
4. Study the impact of traverse speed on the machined surface profile.
5. Study the pressure of the fluid and the nozzle-work piece distance.
6. Optimisation of machining parameters.
7. Improving the machinability of castamide material.

1.4. MOTIVATION

Our purpose/motivation is to development of submerged AWJT system and to study three different parameters through submerged AWJM application on castamide material. In this study, optimization of machining parameters by using algorithms such as VIKOR and TOPSIS was studied. The manufacturing problems have been increasing as the technology is growing, which increases the demand for top-performing materials including composites and plastic because, during the conventional processing of plastics, most of the problems emerged in the treated parts by thermal effect or formation of droplets with overheating and burning, which make machining ineffective. Experts and researchers should continue studying it, and they should focus their efforts towards improving industrial materials' strength for meeting the needs of today's industry. Stronger and better materials lead to better machine usage and better output. Also, newer machining techniques are required for meeting industrial needs [15].

1.5. MAINTENANCE WORK CONTINUES INSIDE THE TANKS OF SIDRA TERMINAL

In the industry, regular cleaning/maintenance is necessary to assure continuous work processes and operational safety. The Engineering Department, Sidra Oil Terminal, is in the process of establishing subsidies for the tanks of the crude oil transport line. It is a continuation of the targeted plan that was developed and supervised (by the management committee) to return the tanks of the crude oil centre in the Sidra terminal to raise the storage capacity and achieve high rates of production. It will enhance its role in responding effectively and competitively to the various scenarios of energy markets and improving the schedule for delivering shipments through Sidra Terminal, which has an important strategic location and it is one of the largest oil export terminals. The abrasive waterjet cutting can be used in the dangerously explosive or inflammable circumstances, and besides, sparks are not generated during the cutting process [16].

Figure 1.1. Cutting oil tank by AWJM [16].

1.6. BENEFITS OF USING AWJM IN INDUSTRIAL SECTOR

When high-pressure water jet cutting procedures are used, they do not have any risk of fire, or losing the mechanical properties of a work piece. It does not generate

noxious fumes. Fortunately, it is not a labor-intensive process, and speeding up the work process is possible. Since this process uses just a fraction of abrasive material and water as compared to other water cutting systems, it has comparatively lesser waste. When the risk of fire hazard is ruled out, it is possible to work inside a tank (even an oil tank) using this process. It is possible to make automatic cuts using unconventional arrangements; it is even possible to cut a storage tank shell above the wall ring or roof. In a single pass, multi-layered floors and coatings can be cut [17].

1.7. PROJECT PLAN

Our thesis has been divided into five chapters. In the first chapter, the introduction clarifies the research background. In Chapter 2, a literature survey has been presented about abrasive water jet machining (AWJM), some applications, and some previous researches. Chapter 3 is dedicated to the theoretical background for general AWJM and its application. Chapter 4 introduces the material used in this project. Finally, Chapter 5 sheds light on the research results, its limitations, and the directions for future research. Conclusions and references follow this chapter.

PART 2

LITERATURE REVIEW

The global economy benefits the most out of the accomplishments of the manufacturing industry. Nowadays, the needs of the manufacturing industry include quicker prototyping and production in small batches. This has promoted the need for newer and improved technology that immediately turns raw substances into finally finished goods needing no tooling time [18].

A most recent technology, which develops new non-traditional methods, is AWJ machining, which has provided several advantages such as more flexibility, absence of thermal distortions, machining flexibility, least cutting forces, and quicker machining [11].

More benefits can be achieved if plain water jet (PWJ) technique is used, it will result in a lower cost because of lack no abrasives and surface contamination elimination due to grit embedding [19].

AWJ has been popular for machining substances including stone, steel, brass, aluminium, polymer and titanium. Moreover, it is applicable to various glass types, as well as composite substances [20].

The efficiencies and intensities of machining processes are dependent on many AWJ methodological variables that include abrasive and hydraulic factors as well as material/cutting variables [21-22].

Transverse speed has an impact on surface roughness as it is the most significant factor, which has a definitive impact on surface roughness when the AWJM is applied. The SOD (standoff distance) has a minimum impact on the surface roughness [13].

Veselko Mutavgjic et al. chose aluminium for testing AWJM methodology. They found that the machined surface roughness gets better whenever the abrasive flow rate enhances. Their findings show a great reduction in the machined surface quality as the traverse speed increases [23].

M. A. Azmir et al. studied the impact of AWJM parameters on the roughness of surface (Ra) of aramid fibre reinforced plastics (AFRP). The outcomes of the study show that higher traverse rates allow lesser overlapping machine actions and lesser abrasive components affect the surface that increases the surface roughness. Moreover, higher faster traverse rates lead to more jet deflection that increases the surface roughness magnitude [8].

H. Hocheng and K.R. Chang focused their work on the formation of kerf in a ceramic plate, which was cut using AWJM technique. It must be noted that a crucial combination of abrasive flow, hydraulic pressures, and traverse speed is required for an appropriate cut, which is not possible without a specific thickness. Adequate hydraulic pressure, finer mesh abrasives on a moderate pace result in smoother kerf surfaces. Experiments show that when the kerf width increases as a consequence of the rise in pressure, factors such as traverse speed, abrasive size and flow rates increase as well. The taper ratio becomes higher when the traverse speed is higher, and it reduces when the pressure rises, or the abrasive size improves. It was found that the Taper ratio does not affect the abrasive flow rate [24].

M.A. Azmir, A.K. Ahsan conducted experiments on the kerf and surface roughness of epoxy/glass laminate, which was processed through AWJM. The researchers focused on six parameters having different levels using Taguchi and ANOVA (variance analysis) methodologies to optimize. Some parameters can be termed as abrasive ones (level-2), standoff distance (level-3), hydraulic pressure (level-3), traverse rate (level-3), rate of abrasive flow (level-3), the orientation of cutting (level-3). We find kerf taper ratio by dividing the width of top kerf by the width bottom kerf. Traverse rate and abrasive forms are not significant for the roughness of the surface, but on the other hand, hydraulic pressure is the single most crucial factor in that context. In a nutshell, abrasive mass flow, SOD, and cutting orientation are equally crucial for the roughness

of the surface. Moreover, for kerf taper ratio, abrasive mass flow, hydraulic pressure and cutting orientation have no significance. The kinds of abrasives are significant for kerf taper ratio while traverse rate and SOD are next in the significance. When AWJM's kinetic energy is increased, it results in a high-quality cutting [25].

Researchers, including Hascalik et al. initiated a research study to analyze the impact of traverse speed on AWJM on the alloy Ti–6Al–4V. They took multiple traverse speeds between 60 and 250 mm/min in case of AWJ machining. They conducted studies on the impact of traverse speed on machined surface profiles, kerf geometry and properties of microstructures. The jet's traverse speed is significant for surface morphologies. Different aspects of varying widths and regions of cutting surface should be considered when the traverse speed changes. It was also discovered that the surface roughness and kerf taper ratio rise when the traverse speed increases. It happens because traverse speed during the AWJM lets only a small number of abrasives collide against a targeted jet target that creates narrower slots. After accomplishing their study, they have identified 3 distinct zones. The following factors are important in this context [26]:

1. The initially damaged region (IDR) is a cutting zone on a shallower angle.
2. Smoother cutting region (SCR) that helps to cut on large angles.
3. Rougher cutting region (RCR) where the jet deflects upwards.

Researchers such as Khan and Hague have analyzed many abrasive substances and their performances during AWJM processing of the glass workpieces. The comparative analyses of performances of different materials were conducted such as silicon carbide, garnet and aluminium oxide abrasives through the same AWJM processing of glass. The abrasive hardness was 1350, 2100 and 2500 knops. Hardness plays a very significant role for abrasives, which have a definitive impact on cutting geometry. The penetration depth of a jet is more when the abrasive hardness increases. The impact of abrasives on taper is observed using different cutting characteristics such as SOD, pressure and rate of work feed. They discovered that the garnet abrasive produces the highest proportion of taper while silicon carbide and aluminium oxide abrasives are next in proportion. Every type of abrasives leads to the taper of cut

increase through standoff distance. On the other hand, every kind of abrasives reduces taper when the jet pressure rises. The cut taper is small in case of silicon carbide abrasive while garnet and aluminium oxide is next to it [27].

Babu and Jegaraj researched the quality and efficiency of cutting using AWJM based on the orifice and nozzle-diameter variations for cutting aluminium alloy 6063-T6. It was discovered that orifice sizes and nozzle-diameter have an impact on the cutting depth, rate of material removal, efficiency, the roughness of the surface and the kerf. They suggested that 3:1 is an appropriate ratio between nozzle-diameter and orifice size that best suits as compared to other ratios between the nozzle-diameter and the orifice size, which helps to achieve more cut depth. Moreover, they also suggested 5:1 ratio between the mentioned variables. They noticed that when the hydraulic pressure rises for different orifice-nozzle size ratios, it deepens the cut. Material removal increases when the focusing nozzle size is approximately 1.2 mm; however, when it is increased, material removal reduces. Abrasive flow rate has lesser significance for the width of the kerf. The current study recommends that the industrial workers should maintain both variables, including the orifice size within 0.25–0.3 mm and nozzle size 1.2mm because it maintains lesser taper. Rising orifice size or diameter of the focusing nozzle has no considerable impact on the quality of the surface or a workpiece; however, large orifice produces a much better quality of finishing/cutting surface [28].

Wang and Wong conducted a study on cutting metallic coated steels through AWJ. They have thrown light on the link between the parameter and kerf characteristics. In this context, they have introduced empirical kerf geometrical models for predicting AWJ quality with the help of 3-level 4-factor trial. They took different parameters to understand the link. Upper and lower widths of kerf rise with rising water pressure. Both the kerf widths rise as a result of SOD enhancement, but the lower one changes a little. Traverse speed generates a negative impact on both the kerf widths; however, kerf taper is positively linked with the traverse speed as they fall and rise with each other. The roughness of the surface reduces when the abrasive flow rate improves. Table 2.1 illustrates that burr height quickly reduces when there is a fall in the traverse speed [29].

Table 2.1. Properties of the Kerf/process parameters [29].

	Water Pressure	**Standoff Distance**	**Abrasive Flow Rate**	**Traverse Speed**
Kerf with	Increase	Increase	Not significant	Decrease
Kerf taper	Not significant	Increase	Not significant	Increase
Surface roughness	With a minimum	Increase	Decrease	Increase
Burr height	Decrease	Increase	Not significant	Increase

Mahabalesh Palleda investigated the impact of various chemical atmospheres such as polymers, acetone or phosphoric acid in a 30-70 ratio. He also studied SOD, water on taper angle and material removal rate out of AWJM holes. It was noted that the removal of materials was maximum when single slurry was added to the polymer as compared to the addition of 3 slurries. MRR value rises when the SOD rises as a consequence of the momentum gained by the affecting abrasive components on a sample surface. The taper holes, which are part of the total drilled holes, decrease when SOD enhances. It was found that the taper holes existed in lesser numbers when phosphoric acid was combined with slurry as compared to using either water slurry or the one with acetone. In polymers, the taper was almost non-existent. The rate of material removal enhances along with enhancing concentrations of phosphoric acid and acetone. As far as polymers are concerned, there is a continuous rise in material removal in the slurry. There are fewer chances of having a taper of the hole if there is phosphoric acid combined with the slurry rather than the presence of acetone in it [22].

Ray and Paul conducted a study on why MRR rises along with increasing grain size, air pressure, and nozzle diameter. MRR rises when SOD rises on a specific pressure. Their research shows that first MRR rises then stays with little change for some time, and later it reduces when SOD rises. They brought material removal factor (MRF) in the equation, which is a dimensionless parameter and shows the weight of removed material using gram as a unit for abrasive components. MRF declines while pressure

rises, which indicates low pressure of abrasives materials, while the removal quantity is more on high pressure [30].

It happens when high air pressure carries large numbers of abrasive components/particles from the nozzle, which results is a higher collision between the particles that loses substantial energy, as indicated in Figures 2.1 and 2.2.

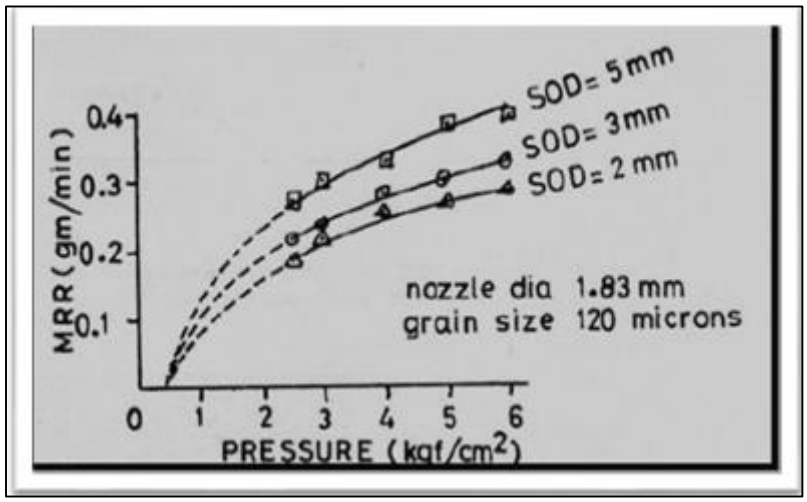

Figure 2.1. MRR vs pressure at 120-micron grain size [30].

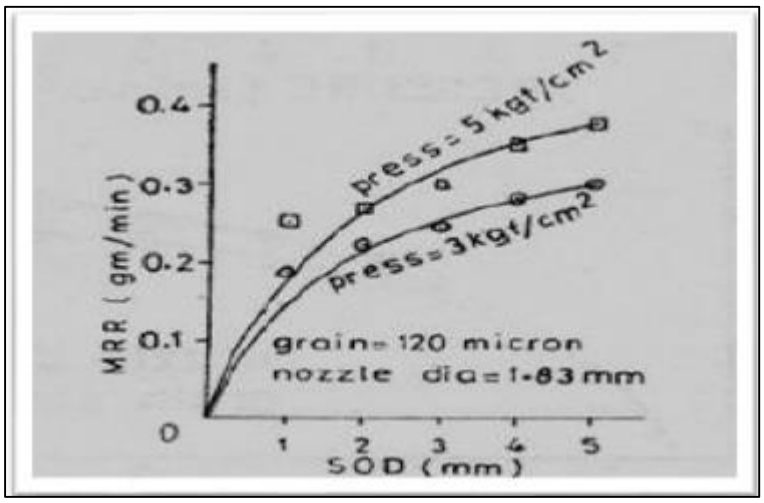

Figure 2.2. MRR vs SOD [30].

Kartal, conducted a study on the effect of AWJ parameters in the context of material removal while machining aluminium alloy 6061. The mentioned study touched upon certain machining parameters, including nozzle feed rate, pump pressure, and abrasive

flow rates. It must be noted that the abrasive size and spindle speed are constants. Generally, the rate, at which, the material removes, increases with the increase in abrasive flows as well as pump pressure (Figures 2.3, 2.4, and 2.5) [31].

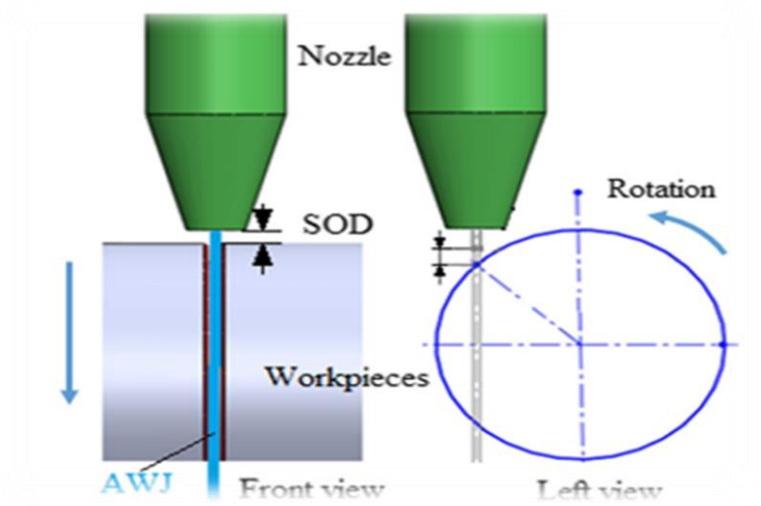

Figure 2.3. Schematic illustration of AWJT method [31].

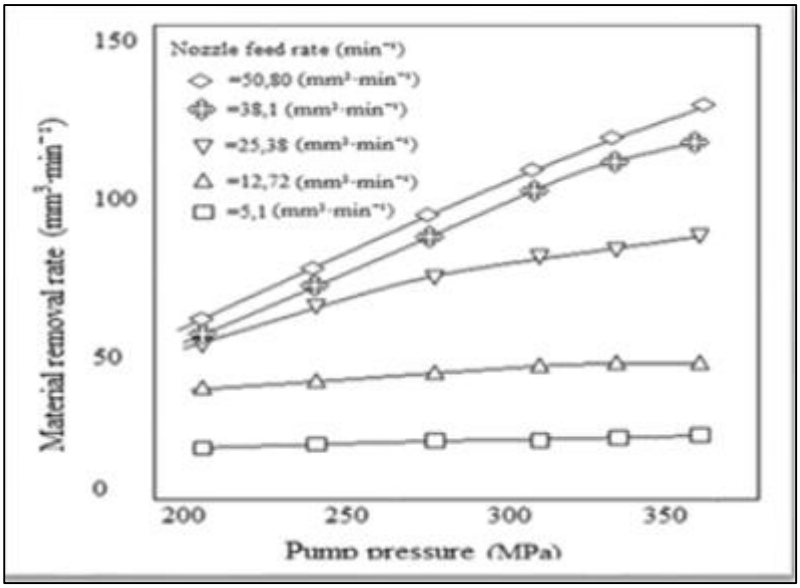

Figure 2.4. Pump pressure variations on rate of material removal [31].

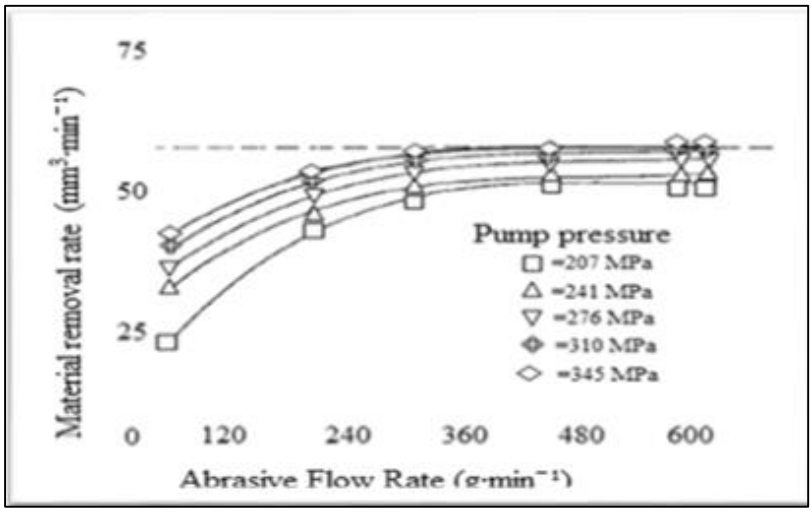

Figure 2.5. Impact of abrasive flow rate variations on the removal of material [31].

Hashish conducted trials and investigated machined surfaces left after AWJT processing and observed macro-characteristics of the resulting surfaces. He took aluminium workpieces having 25 mm diameter each. He found out that the surfaces of those workpieces became rough when they were removed after processing. An image of the workpiece after AWJT process has been illustrated in Figure 2.6. On the other hand, Figure 4b shows the roughness of the surface at a higher nozzle feed rate. The study assumes that the SOD is constant even at variable nozzle feed rate. Experiments show that the rate of material removal reduces when the performance of the jet is dissatisfactory or when SOD (standoff distance) from a workpiece increases. Experts believe that the roughness of the surface is more when the nozzle feed rate is increased [32].

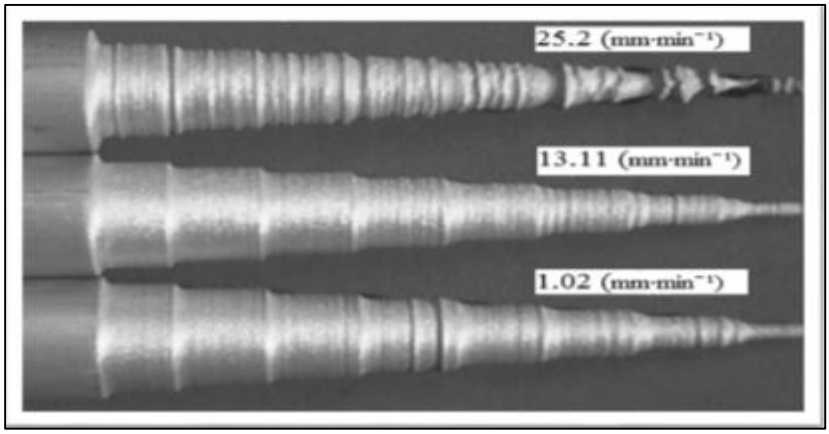

Figure 2.6. Macro-surfaces obtained at different feed rates [32].

Zhong and Han experimented on glass materials and for that, they first developed a testing apparatus for experimentation. This apparatus includes the connection between an electric motor and a spindle while intermediary transferring equipment was not chosen. Before the experiment, the insulation process was carried out on the spindle to resist the pressure of abrasive components and water. The workpieces were cylindrical, and they were made up of 25mm glass. Major machining factors include SOD, spindle speed, pump pressures, abrasive flow rate, and nozzle feed rates. The roughness of the surface and waviness increased when the rotation pace was raised. A low roughness is obtainable at higher rotation and lower nozzle feed rate. It was observed that the more the SOD was, the more surface roughness values were found. Higher pump pressures increase waviness as well as surface roughness [33].

Andersson et al. conducted a comparative study that analyzed AWJ and drew comparisons with orthodox methodologies. They prepared a sample workpiece with the help of AWJ process. The testing apparatus has been illustrated in Figure 2.7. Researchers found almost no thermal effect when the sample was prepared, so now, it was feasible to prepare many workpieces made up of different materials having less cost and machining time [34].

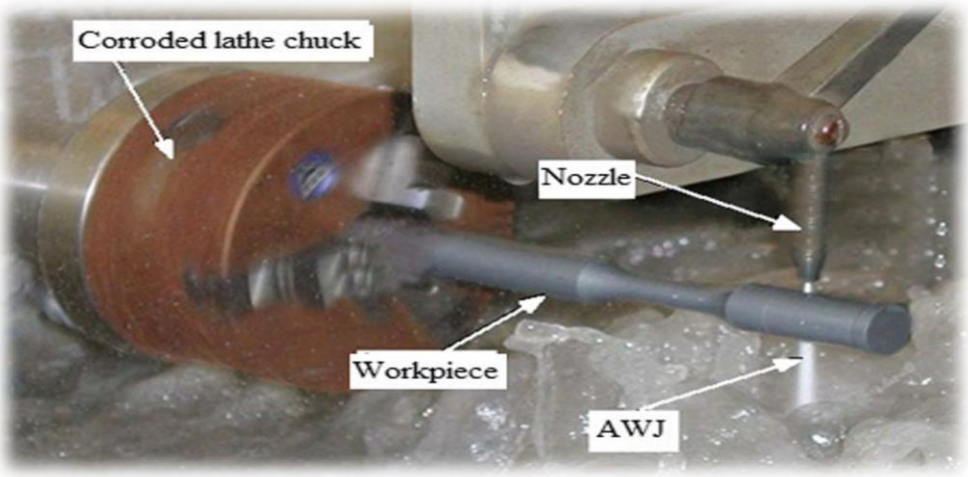

Figure 2.7. AWJ testing apparatus required for machining [34].

Uhlmann et al. machined titanium-aluminium workpieces both through AWJ and conventional turning processes. They used six-axis AWJT for machining. For the sake

of experiment, specific AWJ testing equipment was used. The AWJT method has been illustrated in Figure 2.8. Researchers controlled abrasive flow rate within 100-600g min^{-1}, and they used an 80 mesh garnet as an abrasive substance. They limited nozzle feed rate at 10 mm min^{-1}, SOD 50 mm, pump pressure 550 MPa, and angle of the nozzle at 30° while all of them were kept constant. The outcomes demonstrated that conventional machining leads to accumulation of material around the cutter. It happens because of friction. The researchers documented those results. They noted the material removal volume, which showed that AWJT removed higher material volume, which was 13 cubic centimetres. Ra values for AWJT existed within 5-20 µm. Moreover, Ra = 5 µm shows a material removal of 0.3 cm^3 min^{-1}. The preliminary experiments show that the diameter 4.98 mm and cut depth 3.3 mm was found, which means that the result had similar surface quality, which is demonstrated in Figure 2.9 while MRR was 0.8cm^3 min^{-1} [35].

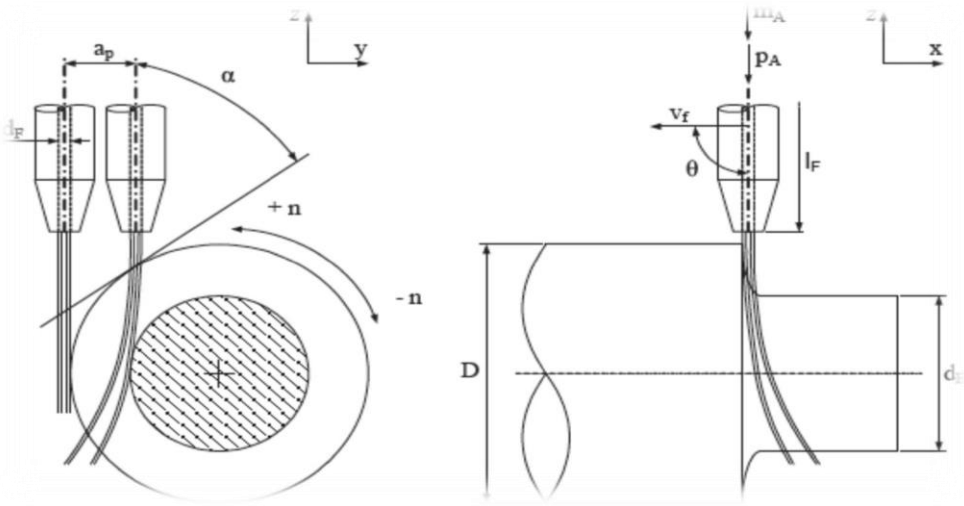

Figure 2.8. Schematic representation of AWJT [35].

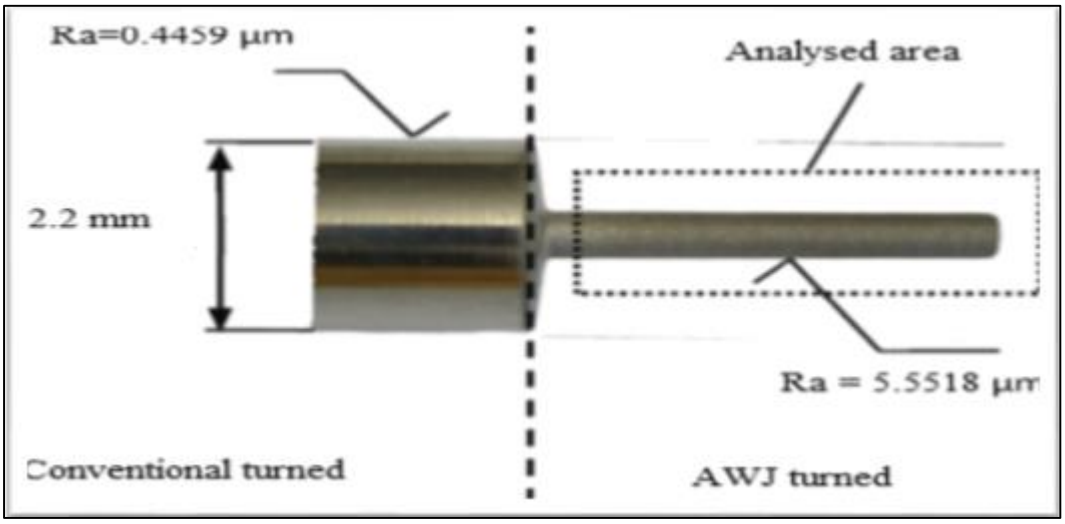

Figure 2.9. Conventional and AWJ turning of TNBV5 specimen [35].

Axinte et al. have investigated the effects of AWJ machining on grinding disks. The researchers conducted experiments using turning testing apparatus for performing a turning trial. They reported that for them, AWJ was a new process, in which, they used a couple of aluminium grinding disks having different sizes having 140 and 50 mm diameters. They used 5-axis KMT and a pump with 413-MPa ultra-high-pressure capacity for testing. The orifice diameter was 0.3 mm, and the nozzle diameter was 1.1 mm. They maintained spindle speed between 90-168 min^{-1}, nozzle feed rate on z-axis between 1-120 mm min^{-1}, SOD between 5-60 mm, pump pressure between 69-415 MPa, and abrasive substance with 80 mesh garnet. The outcomes of the research also indicate that the machining width was lowered from 3.6 to 2.6 mm as nozzle feed rate raised from 10 to 30 mm min^{-1}. The profile accuracy of the grinding disk cross-section depleted when the higher SOD was acquired. Therefore, we can deduce that precision relies on jet focus and diameter while the outcomes are achieved through the scattered jet formation. Research shows that jet having 285 g min^{-1} abrasive contents shows the formation of linear as well as scattered jet [36].

Zohourkari and Zohoor presented a mathematical concept/model for estimating a ductile material's final diameter when the material is removed through AWJ. Some researches and experimental studies on AWJ have conducted a comparative analysis of the precision and the reality behind the theoretical findings through practical production. Some researches prove the theoretical findings of the presented models.

The outcomes show that the nozzle feed rate should be 2 mm min^{-1} for finding out the impact of traverse speed and for finding the effectiveness of a suggested model. Figure 2.10 illustrates the estimated diameters, which were estimated using Manu model and the proposed model is compared to the experimental data [37].

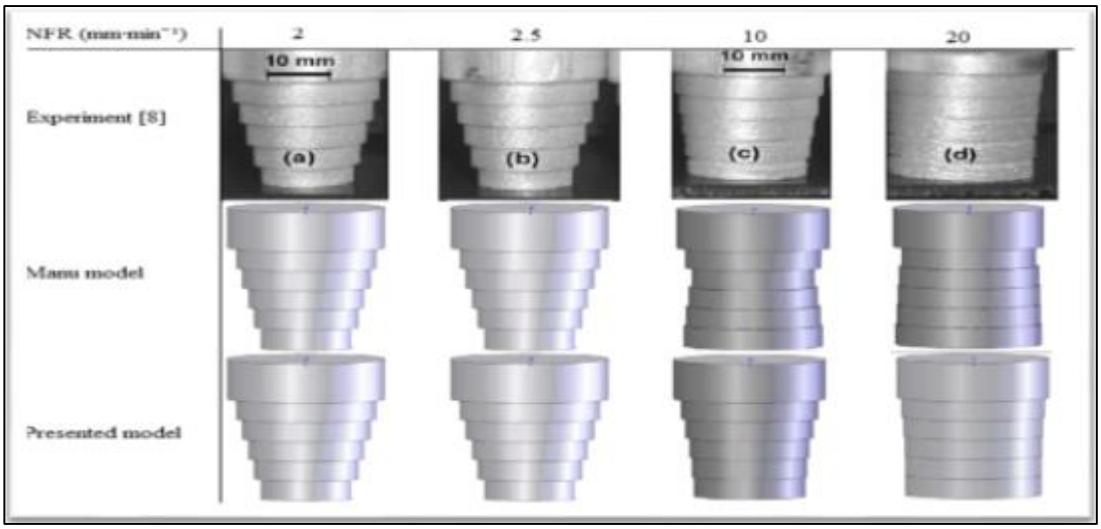

Figure 2.10. AWJ & conventional turning of TNBV5 specimens [37].

Kartal and Gokkaya conducted tests using specifically developed turning-testing equipment to machine cylindrical workpieces with the help of AWJ, which is illustrated in Figure 2.11. The mentioned research has a specifically designed safety cabinet to protect the spindle and motor and spindle from water and abrasive particles, which are commonly observed in AWJ machining. This safety cabinet eliminates inappropriate conditions that occur when the machining process is in progress [38].

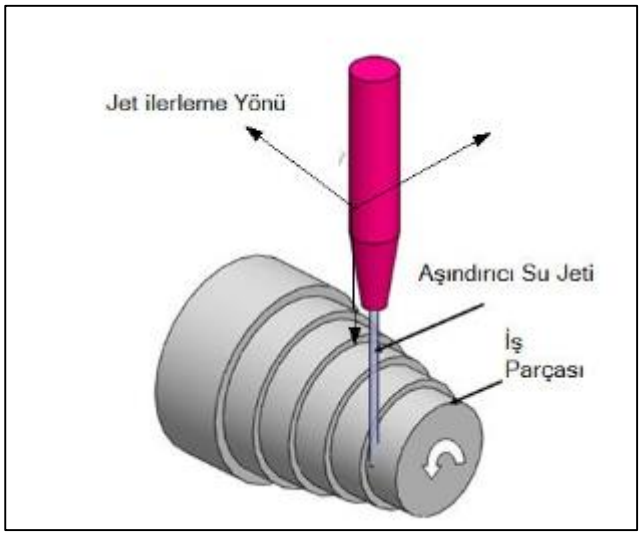

Figure 2.11. Turning test apparatus used for AWJ process [38].

Kartal et al. researched the effects of parameters of machining on the roughness of the surface during turning copper alloy "Cu-Cr-Zr" with the help of AWJ, which is illustrated in Figure 2.12. 350 MPa pump pressure, abrasive garnet with 80 mesh size, and 1.2 mm nozzle diameter were the constants, and they remained unchanged during the trials. The researchers used copper alloys, having 240 and 30 mm sizes for conducting experiments. These samples were processed through AWJ machining with 4 nozzle feed rates including 10, 15, 20 and 25 mm min^{-1} while the abrasive flow rates were 50, 150, 250 and 350 g min^{-1}. Other parameters include nozzle distances 2, 5, 8, and 11 mm and spindle speeds, which were 25, 50, 75, and 100 rpm. The empirical study shows that the nozzle approach distance and feed rate enhanced Ra, which is evident because Ra values existed in the range 2.5–5.5 μm [39].

Figure 2.12. Grinding disk during experimental turning [39].

Kartal et al. studied low-density polyethene materials while conducting the AWJT process having L18 orthogonal array. The research indicates that the material was removed with the help of a conventional turning procedure. The outcomes of the study show that the workpiece surface was very rough because the material, which should be removed, got stuck on the surface. Researchers also claimed that the AWJT method does not create unwanted situations that conventional turning processes create. This is so because the machining components do not deform or melt during the AWJ processing. Figure 2.13 illustrates low-density polyethene workpiece, which was machined using conventional turning methods. Figure 2.13 (b) illustrates the low-density polyethene material processed using AWJ [40].

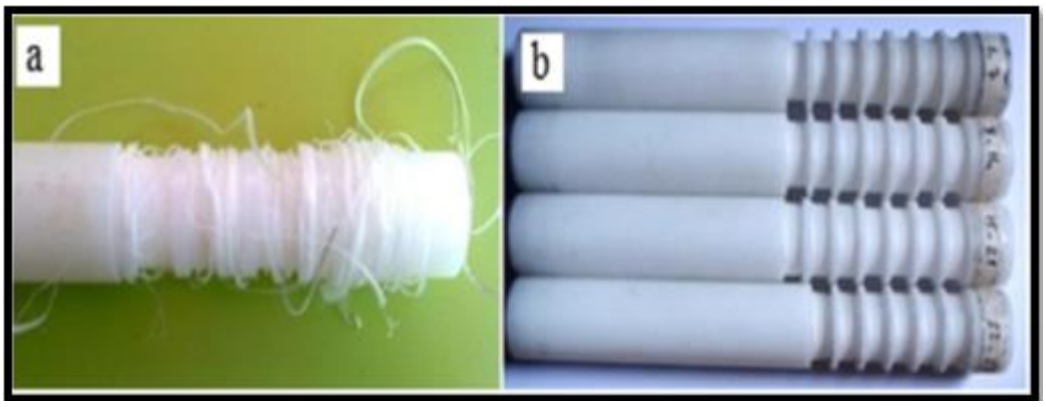

Figure 2.13. AWJT processed polyethylene [40].

Kartal and Gökkaya analyzed the effects of AWJT both on machining depth of AISI 1040 steel and the material removal. They noticed that the AWJT parameters have a positive effect on the removal of material as well as machining depth. It is shown in (Figure. 2.14) [41].

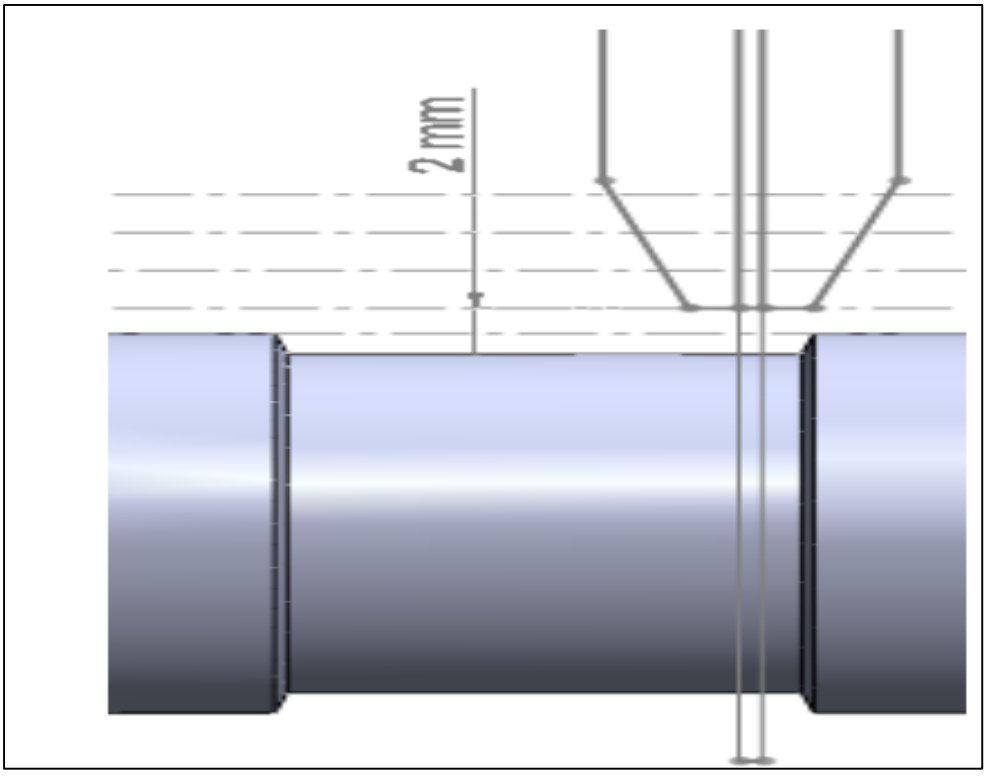

Figure 2.14. Effect of nozzle feed rate and spindle speed on rate of material removal [41].

Hloch et al. conducted experiments on 55 mm titanium workpieces through AWJ. They used 60 mesh garnets. They used selective parameter including spindle speed

(60 rpm), pump pressure (400 MPa), abrasive flow rate (400 g min^{-1}) and SOD (10 mm). Since they were maintained at a fixed rate, we can consider them as constants. Here, five varying nozzle feed rates were used, which are 1.5, 3, 4.5, 6, and 7.5 mm min^{-1}, so it is a variable. The researchers mentioned that a workpiece was linked with the turning-test equipment having no safety materials, and this way, the machining process was carried out. Findings show that using AWJT for processing titanium is best when the nozzle feed rate is maintained at 1.5 mm while Ra should be 6.984 μm. It was noticed that the greatest nozzle feed rate results in a Ra value of 8.308 μm. Researchers opined that the rate of material removal reduces when Ra increases along with the increase in the rate of nozzle feed; therefore, they mentioned that AWJT has a definitive advantage while processing hard-to-machine materials as compared to conventional and orthodox techniques/methods [42].

Li et al. also researched the use of AWJ for machining very strong steel category AISI 4340 workpieces. Researchers conducted experiments to find out the effect of AWJT machining parameters on material removal and Ra in case of steel workpiece AISI 4340. During the process, nozzle feed rates were 3, 6, 12 and 24 mm/min, pump pressure values were 200, 260, 320, and 380 MPa, abrasive flow rates remained 228, 333, 420, and 498 g/min, nozzle angles were 45°, 60°, 75°, and 90°, and spindle speeds were reported as 97, 194, 389, and 777 rpm. Based on findings, the mathematical model has been created, which makes use of the Bernoulli's equations for estimating material removal rates and Ra values. Error rate, which was observed in the mentioned mathematical model is 2% [43]. The kind of equipment used for testing is shown in the following Figure (2.15).

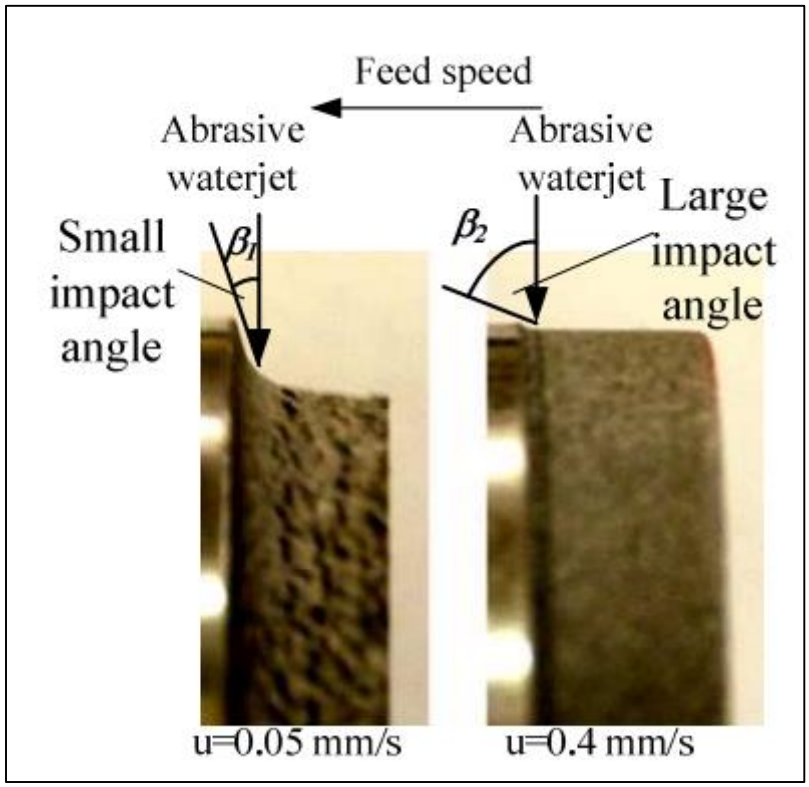

Figure 2.15. Apparatus for turning AWJ test apparatus [43].

Li et al. studied nozzle feed rates and found that a rate of 6 mm/min, 380MPa pump pressure, 90° AWJ impact angle, 498 g/min abrasive flow rate, and 777 min^{-1} spindle speed substantial to remove materials optimally. It was noticed that the machining depth increases with increasing spindle speed. Figure 2.16 shows radial mode and offset mode, which researchers have used for comparison with AWJT experimentation for identifying the one that is beneficial for material removal and surface roughness. Researchers indicated that radial mode causes rougher surface in comparison with the offset mode, so, the offset mode is useful for obtaining surfaces having lower roughness [43].

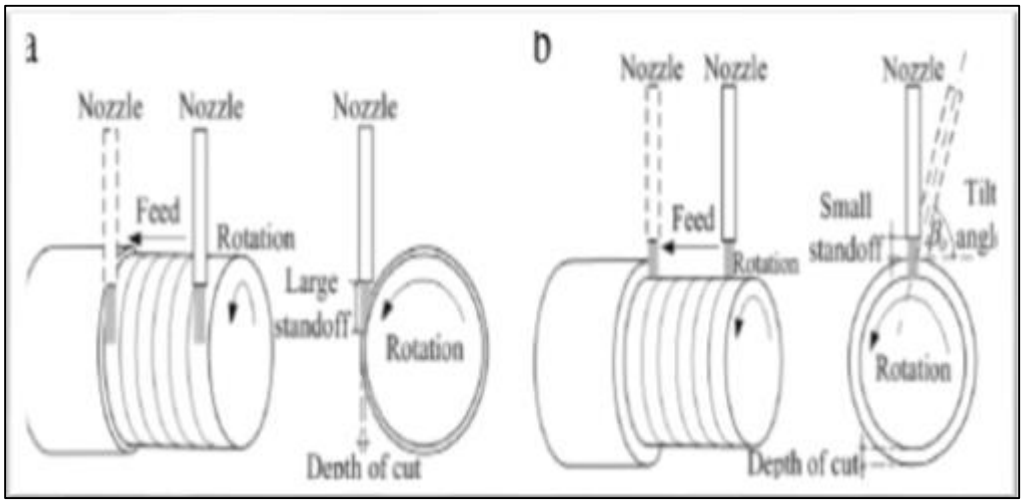

Figure 2.16. AWJT method: a) offset mode, b) radial mode [46].

Zohourkari et al. conducted trials for investigating the effect of AWJT characteristics on the rate of material removal. The mentioned AWJT characteristics/parameters include pump pressure that assumes values such as 130, 200, 250, 300, and 370 MPa, abrasive flow rates such as 106, 230, 324, 422, and 557 g/min, nozzle feed rates 3, 5, 7, and 9.8 mm/min while spindle spinning at 160, 300, 400, 500, and 640 rpm. They used aluminium alloy AA 2011-T4 with Ø=30 mm as a testing sample. In this case, the researchers utilized specific turning test equipment, which has been illustrated in Figure 2.16 for alloy mentioned above [44].

Kartal and Gökkaya tried a custom-made turning device for investigating steel AISI 1050 and its machining in the context of AWJT. They maintained nozzle diameter between 0.7-1.3 mm, rates of nozzle feed at 5, 25, and 45 mm/min, abrasive flow rates 50, 200, and 350 g/min, spindle speeds 500, 1500, and 2500 rpm, and SOD 2, 10, and 18 mm. The experimental design was based on Taguchi L18. The effect of AWJ machining depth was investigated with the help of statistical variance analyses. The researchers presented a linear regression model using the link, which was established between the characteristics affecting machining depth. The mentioned study declares that it is quite possible to remove large quantities of material using AWJT. Researchers focused mainly on abrasive flow rate, nozzle feed rate and spindle speed to check the AWJT machining depth. The rates of nozzle feed and abrasive flows respectively affected machining depth by 75% and 14%, which was obtained through the

percentage of variance impact. With the help of characteristics, which affect machining depth, they suggested a linear regression model. The obtained data were used to compare the data that is obtained using various trials [45].

Hashish and du Plassis suggested a model that discusses strength zones and jet spreading. They researched to understand the impact of SOD [46].

It was found that the particle velocity on any jet cross-section can be between 0 and nozzle wall and at most until the jet centre. The distribution of velocity is consistent with the strength/energy distribution of a jet. A jet's internal contour areas that witness high and converging velocities. These velocities end up as tapered cuts on \material. In this context, the kerf width depends on jet width/diameter [46].

Chen et al. stated that the velocity of the particle at any cross-section of the jet must differ from zero at the nozzle wall to the greatest jet centre. This speed delivery agrees to an energy or strength distribution in the jet. The kerf width depends on the efficient width (or diameter) of the jet that in turn relies on the jet strength in that region and the target material. The main interests in sheet steel processing are the kerf shape (kerf width and kerf taper) and kerf quality (cut surface roughness) in addition to the burrs that may be configured at the jet exit. These features are presented in the study [47].

Vikram et al. developed a differential equation-based model for predicting surface topography by simulating the equation of the trajectory of the jet. They used Bitter's erosion theory as well as Ballistics theory and found that the jet trajectory is curvilinear. Highly random nature of striking the abrasive particles was discussed through power spectral density analysis. This random nature of the cut surface was generated due to the intersection of striation marks and steps formed by the trajectories [48].

A final conclusion was drawn, which RBFN network model precisely anticipates as compared to the BPNN/regression models. Caydaş et al. (2008) applied 3 forms of sigmoid function to predict the surface roughness, and later, they conducted a comparison with the regression. In the case of surface roughness model, they created

its integration with the ANN model. Optimal controlling parameters are adjusted through annealing stimulation with the value of the function anticipated using ANN. In this context, researchers consider two integration forms. They found out that the integrated model shows more accuracy as compared to the ANN model for the prediction of surface roughness, which Figures 2.17 and Figure 2.18 are showing [49].

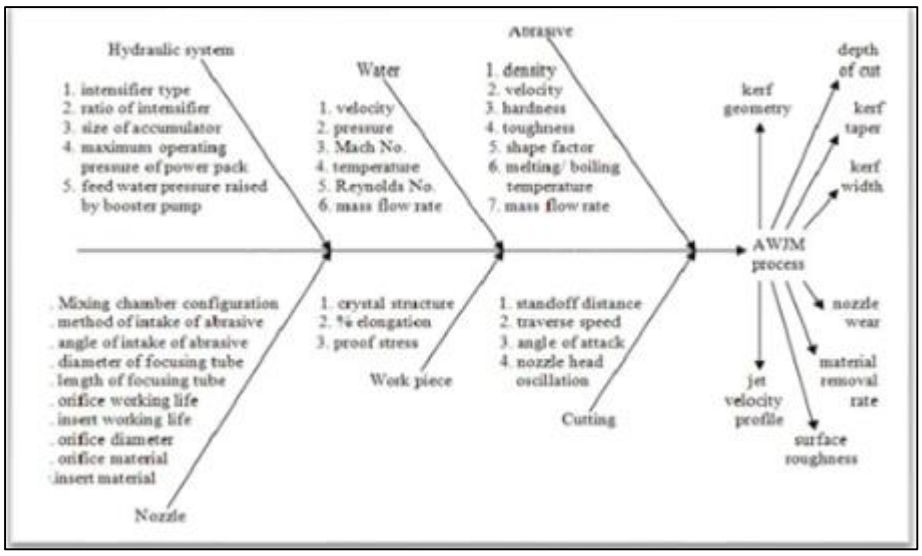

Figure 2.17. Cause – effect diagram of AWJM process [50].

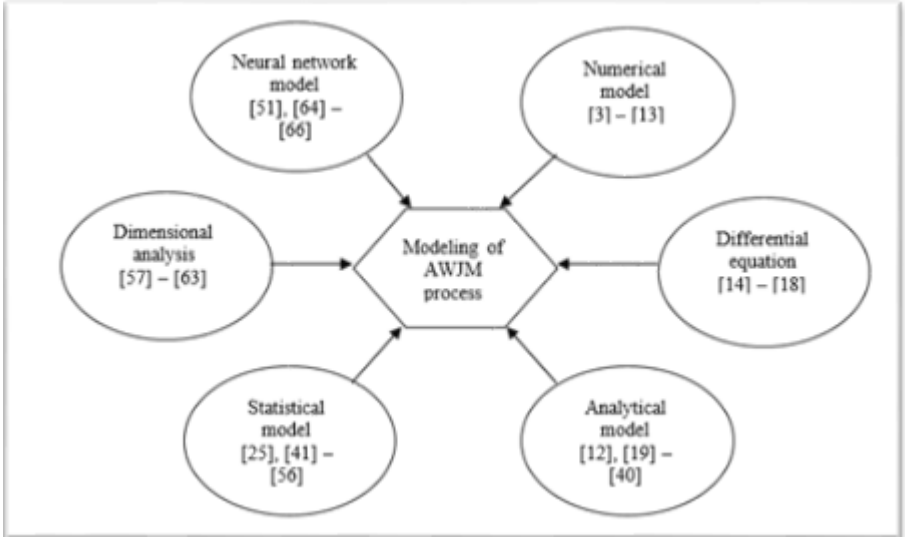

Figure 2.18. Modelling techniques applied for AWJM process [50].

Manu and Babu constructed a mathematical model based on Finnie erosion model for developing AWJT-based erosion model. It was initiated using the abrasive angle and

nozzle-water delivery as functions of reduced diameter. Figure 19 depicts the AWJ impact angle. The mentioned experiment includes aluminium AA-6063 workpiece. Figure 13 shows the turning text apparatus for AWJT process [51]. The experiment focused on fixed parameters such as 5 g/s abrasive flow, 250 MPa pump pressure, 80 mesh garnet abrasive size, 13, 25, 37, and 50 rpm spindle speeds, nozzle feed rates such as 1, 1.5, 2, 2.5, 3, 4, 5, 10, 20, 30, 40, and 50 mm/min, nozzle diameters 0.76, 1.2, and 1.6 mm, and SODs such as 11.7, 10.7, 9.7, 8.7, and 7.7 mm. Researchers found that they found the same values, which were earlier calculated using mathematical model [51].

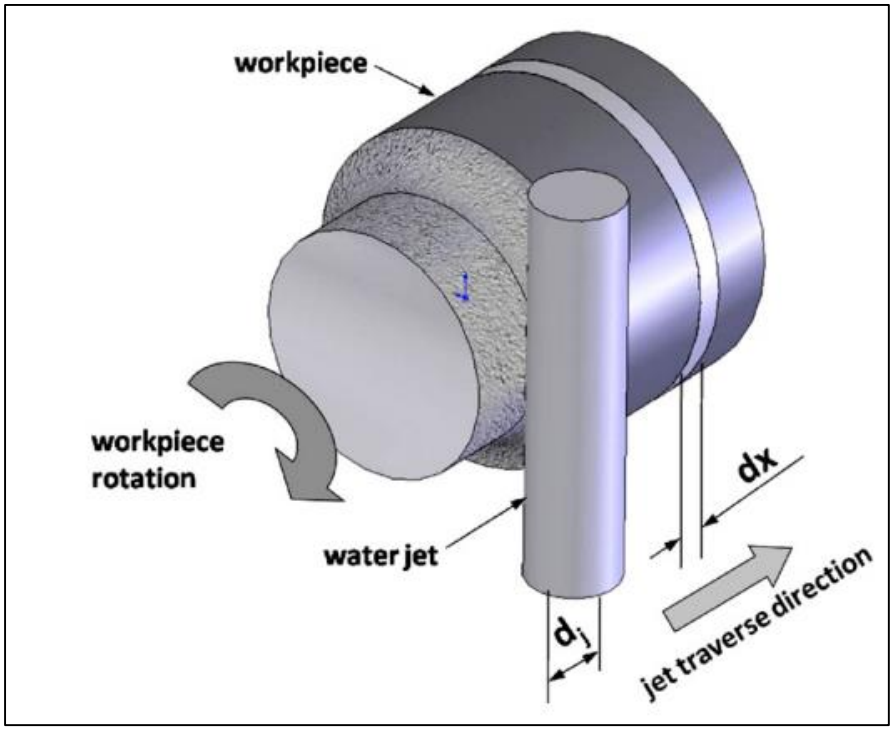

Figure 2.19. The AWJ turning apparatus [51].

Selvan et al. considered surface roughness as a quality parameter. With the design of experiments, they set up the process parameters for machining aluminium. Through experimentation, they found that for good surface finish, more abrasive flow rates and hydraulic pressures is required having lower traverse speeds as well as standoff distance. As far as AWJ turning is concerned, the under process sample rotates, and AWJ has to be axially and radically traversed for producing needed turned surface [52].

Borkowski presented a new method for the 3D sculpturing of various substances with the help of peak-pressure AWJ. He proposed a mathematical model for shaping the material as well as the experimental testing to test this novel approach [53].

Kök et al. investigated AWJ cut surfaces' roughness as well as genetic expression programming (GEP) that helps to predict surface roughness when AA-7075 alloy is machined using the AWJ process. In the case of developed conceptualizations, material characteristics including sizes or weight-fractions of reinforced substance, cut depth/s are almost always variable. Researchers compared forecasted results with the outcomes of the experiment, which met the satisfactory condition. Some researches show that AWJ technique can machine different types of materials by considering various combinations of process parameters [13].

Rajyalakshmi et al. specified that abrasive waterjet machining (AWJM) is one of the latest machining processes for complex to cut materials. It is environment friendly and comparatively reasonable process with a sensibly high material removal ratio. In all the machining processes, the workpiece quality relies on many design parameters. The process parameters that primarily influence the quality of cutting in AWJM are hydraulic pressure, traverse speed, stand-off distance, abrasive flow rate types of abrasive. The quality parameters considered in AWJM are (MRR), Surface Roughness (SR), Depth of Cut, kerf Features and Nozzle wear. Since its diverse benefits, it gains more significance recently. Many statistical and modern methods are applied to enhance these process parameters to enhance performance features. However, most of the researchers considered collective process parameters such as hydraulic pressure, traverse speed, standoff distance and abrasive flow rate. Other parameters can also be taken into account for enhancement that affects the quality parameters. The study attempted to present the research work carried out so far in AWJM area [54].

Hocheng et al. have discussed the feasibility of AWJ milling for fibre-reinforced plastics. They conducted studies on the impact of different parameters on the removal of material as well as the surface roughness of single-pass cutting using dimensional analysis, which later extended the studies to multi-pass cutting [55].

Arola and Ramulu used microstructural analysis and microhardness measurement for studying the impact of material properties such as on-the-surface integrity as well as texture [56].

Hloch et al. conducted an experimental study on macro-geometric cutting AWJ cutting quality. They considered level quality as a process parameter and applied regression equations using ANOVA [57].

Zhu et al. found that by using a ductile erosion method, accurate surface machining becomes possible using AWJM on smaller erosion angle and less pressure [58].

Gursewak Kesharwhani conducted experiments on non-spherical sharp-edged ceramic abrasives to machine samples of materials used in the aerospace industries. They concluded that traverse speed significantly affects controlled-depth milling for AWJ machining. They also discovered that in case the setup is modified, 20% time reduces for milling of a titanium alloy. The waviness on the surface is possible to reduce when traverse speed increases with the help of abrasive feeding system modifications [59].

Sidda Reddy et al**.** investigated optimizing input parameters for AWJ machining with the help of Taguchi process. They used variance analysis (ANOVA) and S/N (signal-to-noise ratio) for optimizing certain parameters to predict/find appropriate surface roughness and material removal rate (MRR) [59].

Derziza Bagic-Hajdervic et al. studied the effect of thickness of the material, abrasive flow rate and traverse speed during abrasive water jet machining of aluminium for surface roughness. It was concluded that traverse speed has a significant effect on surface roughness at the bottom of the cut and relation between surface roughness and other variables [59].

Jai Autrin and M. Dev Anand researched on how to optimize machining parameters for AWJ machining for workpiece made up of copper alloy using regression. They

also found the impact of SOD (standoff distance), the diameter of the nozzle, and the pressure of water on surface roughness and material removal [59].

Paul et al. mentioned the impact of air on the material removal rate (MRR). They used silicon carbide for abrasive components on varying air pressures. They discovered that the MRR enhanced when the grain sizes and nozzle diameter were increased. MRR shows a positive relation with SOD, as Figure 2.2 shows [59].

Woolak and K.N. Murthy found that beyond the threshold pressure, MRR and cutting depth increase with more nozzle-pressure. The peak MRR value for ductile/ brittle substances can be achieved on impingement angles. In the case of ductile materials, 15-25 degree impingement angle leads to higher material removal rate. In the case of brittle materials, these small angles also speed up material removal [59].

Ghobety et al. conducted experiments on AWJM repeatability. Using the mixing chamber improves the repeatability of the process. They calculated machined surface depth to find out repeatability of the process [59].

Domiaty et al. conducted glass drilling for varying thicknesses in order to find out control parameters' machinability. A larger nozzle diameter results in the more abrasive mass flow that results in higher MRR while smaller abrasive size results in lower MRR [59].

Aliraza Moridi et al. conducted experiments on the impact of different parameters on AWJM cutting performances. When the abrasive mass flow becomes higher, it improves inter-particle collisions that decreases the overall material removal [59].

Oiseth researched the impact of ozone-generating ultraviolet light treatment while processing dense polyethene (HDPE) films. She continuously monitored the process through quartz crystal microbalance (QCM) method with and without ozone. Those films were later processed through optical microscopes X-ray photoelectron spectroscopy and atomic force microscopes. The researcher declared that ozone re-modified the properties of HDPE film surface but etched off polymer. She determined

0.48nm/min etching rate. The argon atmosphere, in which, ultraviolet rays for processing the polymer film, creates little film degradation; ozone is applied for destruction and for getting rid of material. In this case, the QCM method was a solution that helped to monitor ablation kinetics created through UV-ozone treatment [60].

Duvall et al. researched conventional HDPE compound that has HDPE resin as well carbon black, which was included 2-3% of the total weight for protecting the material from oxidation degradation when it is exposed to UV rays. When stabilizers such as antioxidants for preventing during pipe extrusion oxidation at 350-400 degree Fahrenheit as well as other antioxidants, they protect against corrosive effects of water, which exist in the air. Some disinfecting compounds are also added [61].

Singh & Joshi conducted a study on HDPE monofilament photo stabilization through hindered amine light stabilizers (HALS) as well as ultraviolet ray absorber on different stabilization concentration. He assessed those filaments to understand UV resistance when it is exposed outdoors as well as when it is applied to artificial weathering conditions and when it is tested based on regular intervals for tensile property retention. HDPE films have different thicknesses because they have different photo stabilizing concentrations. The films have UV protection capability that can be found through Ultra Violet Protection Factor (UPF). Experimental outcomes show that UV absorbers substantially enhance filaments' stability [62].

Kamweru et al. observed UV-light absorption through traditional PE films. Some films were taken as samples, and they were exposed to the ultraviolet fluorescent lamp at 20˚C temperature with 40% relative humidity for 2 hours. Absorption was observed during reflection, transmission, and emission spectra, which took place through the optical analyzer. The researchers also investigated facts about natural degradation in the presence of sunlight in PE films for 150 days. DMA instrument was used to analyze degradation through storage modulus changes. The proof of chromophoric sites was ultraviolet light absorption that takes place from 250 to 400nm [63].

Brandalise et al. conducted research on the evolution of hardness observed in high-density polyethene (HDPE) at high temperature. It increases when gamma rays,

annealing time and temperatures rise. Some factors, which play a role in the hardness levels, follow first-order structural relaxation. These issues, which influence hardness after annealing HDPE, improve when the dose and temperature increases. HDPE structure relaxation shows less mixing energy within crystalline parts rather than amorphous parts [64].

Barbosa et al. studied and found HDPE mono-filaments with the help of several extruder/post-extruder equipment. Some undrawn and drawn mono-filaments (drawing ratio: 7:1) irradiate at 10 MeV electron beams on normal room temperature with 25, 50, 75, 100 and 125 kGy doses that create network structures. These fibres have been studied for their mechanical aspects and measurements. It was observed that irradiated fibres' tensile properties reduced; however, elongation for undrawn and at the break for drawn fibres increased when irradiation dose boosted to 125 kGy [65].

Wu et al. discovered that the structure of the system for water jet cutting machine fault diagnosis depending on the multi-information fusion had been provided that takes the time-varying, termination and doubt of the multi-fault features information into account. They used the neural network's capability for better fault tolerance, strong generalization ability, features of self-organization, self-learning, and self-adaptation, and take benefit of multi-source information fusion technology to recognize the total processing for doubt information. The feature layer-fusing model of the water jet cutting machine fault diagnosis that using the fuzzy neural network to understand feature layer fusion and D-S evidence theory to complete the decision layer fusion. The results of the simulation of water jet cutting machine fault diagnosis present that the technique can efficiently enhance the diagnostic reliability and decrease diagnostic indecision [66].

Johan Fredin discovered that **a**brasive waterjet cutting (AWJ) is a highly effective technique for cutting nearly any type of materials. When holes are cut the waterjet first needs to pierce the material. The research offers an extensive experimental analysis of piercing parameters influence on piercing time. Results of the experiment on feed ratios, thicknesses of the work-piece, abrasive flow rates, impasse distances and water pressure have been presented as well. Moreover, they presented studies on three

techniques of the dynamic piercing. It is exposed that a large amount of time and resources can be saved by selecting the parameters of piercing correctly. A large number of experiments puts strains on the experimental setup. An automated experimental setup comprising piercing detection has been provided to allow a large series of experiments to take place effectively [67].

Aich et al. conducted experiments to cut the borosilicate glass by AWJM. Cut depth has been measured with different machine parameter settings as water pressure, abrasive flow ratio, traverse speed and standoff distance. Optimal circumstances of control parameter sets have been searched too through particle swarm optimization (PSO). Furthermore, scanning electron microscopic (SEM) image shows some extent and the cut surface nature and erosion behaviour of formless material qualitatively [68]

PART 3

THEORETICAL BACKGROUND

3.1. NON TRADITIONAL MANUFACTURING PROCESSES

3.1.1. Introduction

Non-traditional manufacturing consists of methods and procedures, which helps getting rid of excessive materials through thermal, mechanical, electrical, or chemical energy as well as their combinations. They do not involve the use of sharp cutting tools, which are applied in traditional cutting/manufacturing methods. Rigid materials are not easy to process through conventional processes, including drilling, cutting, shaping, turning, and milling. The unconventional machining methods are also termed as advanced manufacturing methods, which work well wherever conventional methods fail, become uneconomical, or unfeasible for any reason. These reasons may be toughness, which makes it almost impossible to machine through conventional processes. Many unconventional machining methods have been introduced so far to meet the machining requirements. If they are correctly employed, they have certain benefits as compared to conventional machining. General conventional machining systems have been elaborated in the following section [69].

3.1.2. Electrical Discharge Machining (EDM)

It is a commonly utilized unconventional machining method, which has several advantages. Its main benefits include grinding and cutting metals with the help of several tools because this process uses thermo-electrical processes, which can erode unnecessary substances to get a cleaner workpiece through electrical spark applied between the electrode and the workpiece [70].

Conventional machines depend on tougher and denser tools/abrasive materials for eliminating materials while unconventional ones like EDM makes use of electrical sparks/thermal power for eroding unnecessary materials for creating a definitive shape; therefore, material hardness cannot be considered as a dominating factor any more to carry out the EDM technique. EDM schematic diagram has been given below (Figure 3.1), which shows that the workpiece and the tool have been put in a di-electrical liquid.

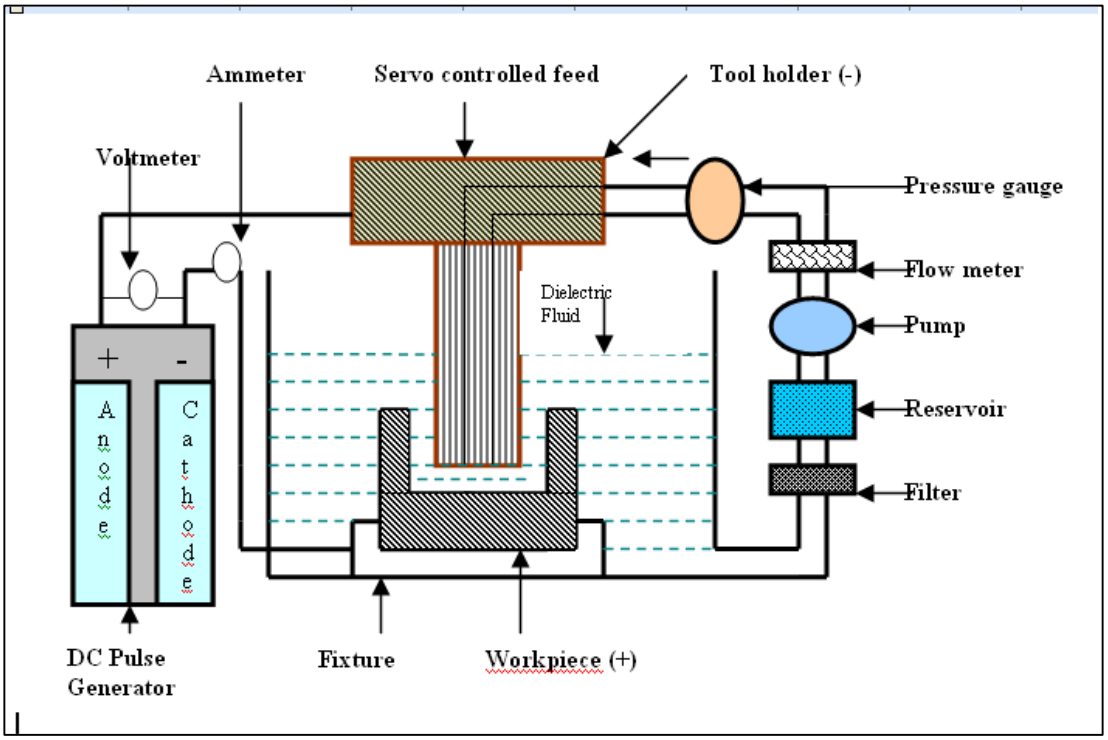

Figure 3.1. Schematic of the EDM process [70].

EDM gets rid of the unwanted materials when it discharges electrical signal or when it stores in a capacitor bank, which lies across a little gap between the workpiece and the cathode with a capacity to apply 50 volts/10 amps in general [70].

3.1.3. Working Principle of EDM

The EDM principle is used to create eroding effect on the electrodes, through which, controlled electric spark discharges are done; therefore, it is a type of thermal erosion. A dielectric liquid creates the spark, which is generally either oil or water existing

between the electrode and the workpiece; so it acts like a cutting tool. Mechanical contact is absent between the electrodes in this process. Since electrical discharges produce erosion; therefore, both the workpiece and the electrode must have sufficient electric conductivity. During machining, small specs of workpiece material are successively removed, melted, or vaporized while discharging. The single spark removes very small volume (104-106 mm^3); however, after 10000 repetitions/second, it is possible to remove large numbers of tiny specs. A basic explanation of erosion, which happens as a consequence of a single EDM discharge, has been given in Figure 2 (a-e). When the electrodes receive 200V, moving them towards the workpiece breaks the workpiece. It increases within-the-gap electric field and acquires the appropriate value needed for the breakdown process. The breakdown location normally exists between the closest points of the workpiece and the electrode; however, this also depends on the presence of particles in the gap. After the breakdown, the current abruptly rises while the voltage falls. Current is needed at this stage because of the creation of a plasma channel between the electrodes and the ionized dielectric. Then maintaining the discharge current leads to continuous ion and electron bombardment, which rapidly heats up the workpiece (besides heating up the electrode), which creates a small pool of molten metal. If a small metal quantity is to be removed, it can be vaporized when heating takes place. When the discharge occurs, it results in plasma channel expansion; so, the molten metal pool expands and its radius increases. The workpiece-electrode distance is a significant parameter, which should be within the range 10-100μm (the gap increases with increasing discharge current). The voltage and current shut down at the end of the discharge. Under immense pressure exerted by the surrounding dielectric implodes the plasma; so, the dielectric sucks the molten metal pool, which leaves only a small crater at the surface of the workpiece [70].

.

3.1.4. Advantages of EDM

The advantages of EDM can be described as follows [71]:

1. Using this method, materials having any hardness level are possible to the machine.
2. It leaves no burrs on the surface of the workpiece.

3. A major benefit of this system is its ability to machine fragile as well as brittle components with no distortion.
4. It helps to machine complicated internal shapes.
5. Less prone to arcing.
6. Stray currents make it possible to be eliminated unwanted machining.

3.1.5. Disadvantages of EDM

The disadvantages of EDM can be described as follows [71]:

1. It is only applicable to electricity conducting substances.
2. Its MRR is less in volume, and it is a slower technique in comparison with conventional machining.
3. It might result in unnecessary erosion as well as over-cutting. Rough surfaces finish at high material removal rate.
4. Tool wear, mechanical stresses, micro-fissures caused by heat transfer or the need for subsequent deburring operations.
5. Gentle transitions and top-quality surfaces without burr formation

3.2. WIRE EDM

Wire electrical discharge machining (WEDM) was introduced because it can cut intricate shapes and too tapered geometries with high performance, especially in precision, efficiency, and stability. EDM is available for commercial use in the shape of wire-cutting machines/wire EDM and die-sinking machines. This procedure includes a slowly-moving wire that moves on a specified path for removing materials from the surface of a workpiece (Figure 3.2). It utilizes an electro-thermal mechanism for cutting electricity conducting substances. It removes materials through a sequence of discharges between the workpiece and the wire (electrode) while the dielectric liquid is present that results in ionization of the fluid in the gap. This area is heated up on a very high temperature to melt the surface and remove particles, which can be flushed through the dielectric fluid. It is used in coordination with the CNC, and so it is used for complete cuts throughout the object or workpiece. The main parameter for

this process is the melting temperature of components, which is essential; therefore, it does not rely on hardness or strength. MRR and surface quality obtained after wire EDM machining depends on many factors and parameters, for example, the material used in the wire and the peak current applied. The most important control parameters for this process are discharge current, discharge capacitance, pulse duration, pulse frequency, wire-speed, wire tension and voltage [70].

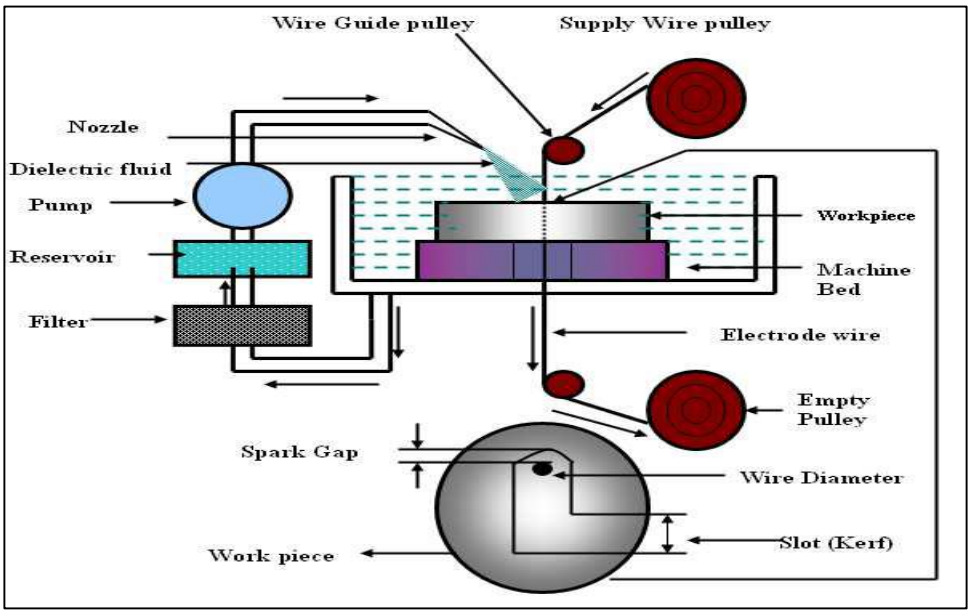

Figure 3.2. Wire cut EDM [70].

3.3. CHEMICAL MACHINING

The chemical machining performs based on the principle of chemical etching, which implies that the workpiece metal parts should be removed using a strong corrosive "etchant" chemical (Figure 3.3). When the etchant reacts with the material workpiece, it is cut, and solid material is removed from it. Metal removal is done through the etchant attack. The material portion, which is needed, is protected from the chemical attack using the coating of maskants. The chemical machining of all metal and ceramic substances is done using the mentioned process. When the workpiece material chemically reacts with the chemical, this process requires a chemical reagent that assures the desired reaction, and after the reaction, it is easily removed. When the

workpiece surface is etched away, the lower layers get exposed, but the process carries on until removing the desired amount of material [72].

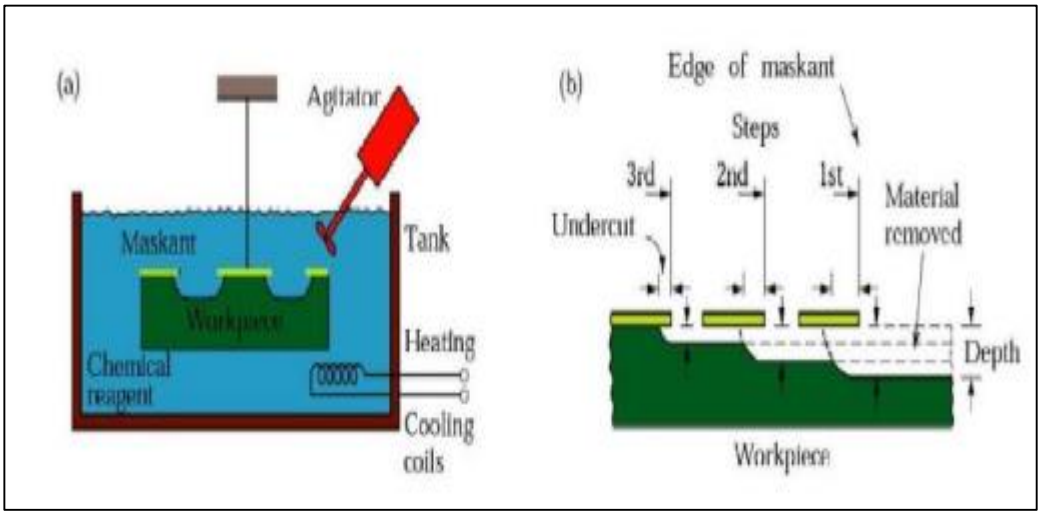

Figure 3.3. (a) Schematic diagram of chemical machining (b) Stages to produce profiled Cavity through chemical machining [72].

3.3.1. Chemical Milling

In chemical milling, shallow cavities are produced on plates, sheets, forgings and extrusions. The two key materials used in the chemical milling process are etchant and maskant. Etchants are acidic or alkaline solutions maintained within controlled ranges of chemical composition and temperature. Maskants are specially designed elastomeric products that are hand strippable and chemically resistant to the harsh etchants [72].

3.3.2. Steps Involved in Chemical Milling

Residual stress relief: When a component needs machining, its residual stress takes place through earlier processing, which needs relief for preventing against post-chemical milling warp formation [72]:

1. Preparation: Before processing, the workpieces are cleaned and de-greased to assure appropriate adhesion of a masking material, which results in uniform removal of materials.
2. Mask application: Mask is applied on the surfaces, which do not need CM, and they are not etched.
3. Etching: Etchants are applied to exposed surfaces, which need chemical machining.
4. De-masking: When machining is over, the machined components need a thorough wash for preventing reaction/s with etchant residue. Later the masking materials are peeled off, and the surface undergoes cleaning and inspection.

3.4. ELECTRO-CHEMICAL MACHINING (ECM)

ECM removes metals through the reverse-electroplating process. Through this method, tiny specs move from the anode (the sample/workpiece) towards the cathode (machine component). The electrolyte liquid takes the de-plated substance before letting it reach a machine tool. A cavity produces, which shows a process called as "female mating" of a tool as in Figure 3.4 below [73].

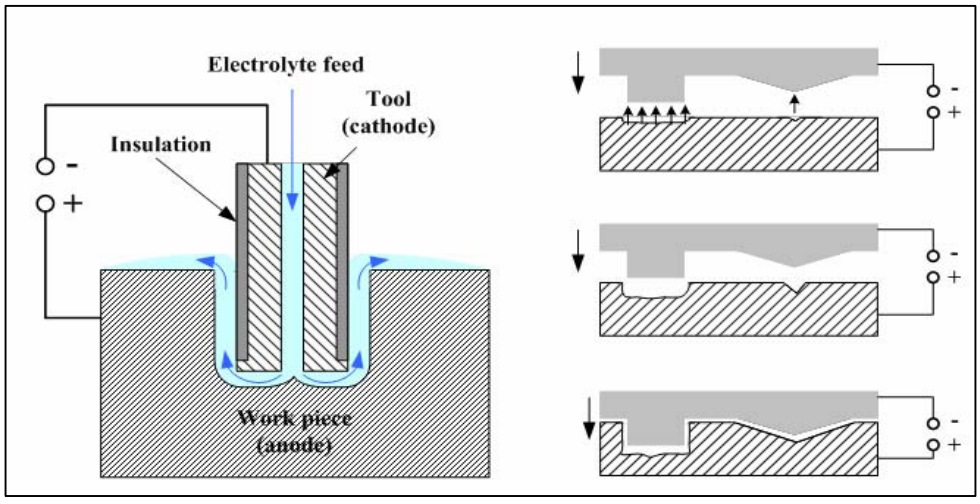

Figure 3.4 The principle scheme of Electro-Chemical Machining process [73].

Just like EDM, the hardness of a workpiece does not act like a factor, which makes ECM useful for tough machining substances and complicated shapes. This process is

used to carve complicated shapes on several substances irrespective of their hardness or other challenging physical properties [73].

3.4.1. Advantages of ECM

Advantages of ECM can be illustrated as follows [73]:

1. Parts do not have thermal/mechanical stresses.
2. Tools do not wear out in the ECM. Delicate components are possible to machine because stress is not involved. ECM's deburring function deburrs inaccessible components of a workpiece.
3. It is possible to have a quality surface finish (about 25μm) through ECM.
4. Less prone to arcing,
5. Clean operating environment and
6. This process involves the formation of deep holes.

3.4.2. Limitations of ECM

Limitations of ECM can be described as follows [73]:

1. It is unsuitable for the production of sharp squared edges and plain bottom as it causes electrolytes to erode sharp shapes.
2. ECM applies to the majority of metals; however, it is not economical, so it is applied in specific situations.
3. For electro-chemical machining, material removal rate MRR = C.I.h cm3/min. Here C stands for specified MRR (nickel has 0.2052 cm3/amp-min), I represents current in amperes and h stands for the efficiency of the current (such as 90 to 100%). The rate of metals' electrochemical removal is proportional to the operational elapsed time as well as current, which is transmitted through an electrolyte.
4. Several factors have an impact on the machining rate, including the type of electrolyte used, electrolyte flow rate, and conditions of the process.
5. Tool wear, mechanical stresses and micro-fissures caused by heat transfer

3.5. ULTRASONIC MACHINING (USM)

USM is a method of mechanically removing material. It is also considered as a viable solution that uses abrasives for eroding cavities or holes in tough workpieces through specifically designed tools, peak frequency mechanically-managed movement and abrasive material. This method is an answer to the growing requirement of processing brittle substances, including glass, crystal, poly-crystalline ceramic materials, and workpieces having detailed profiles and forms. Today, it is extensively utilized for tough machining workpieces, which are almost impossible or uneconomical if they are machined through conventional methods. Tough particles in the slurry are moved to the workpiece surface through an oscillating tool having a maximum frequency of 100 kHz with the help of repeated abrasion—this kind of tool processes cross-sectional cavities. Figure 3.5 is the schematic diagram of USM [74].

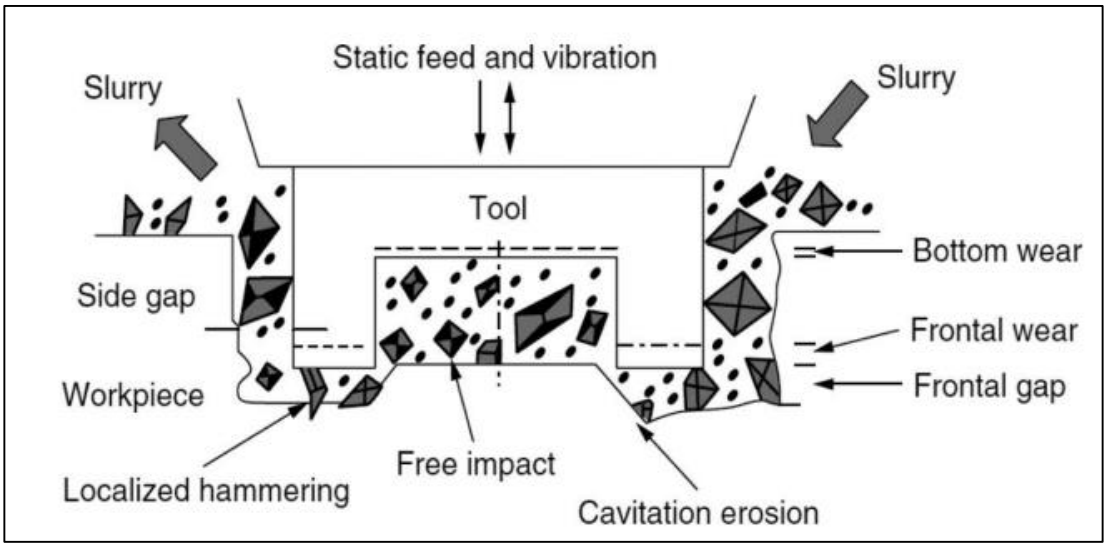

Figure 3.5. Schematic diagram of USM [74].

USM process targets brittle materials for machining, which may be conductive or dielectric, including ceramics, titanium compounds, ruby, boron carbide, and quartz. Its versatility is evident from its usefulness for substances having multiple properties. This method machines all those substances irrespective of their electrical conductivity. To carry out a useful cutting procedure, a machinist must be careful about the following:

Machining tools should be resistant to wear and tear. Steels with high carbon content serve this purpose very well. Abrasives should have 25 to 60 mm diameter and those, which are water-based, should have 40% volume. The slurry should have additives such as boron and silicon carbides and aluminium oxide [74].

3.5.1. Applications

Application of USM for establishing cost-effective machining solutions for hard and brittle materials, such as; glass, tungsten carbide, cubic boron nitride. Performance measures in USM process are dependent on the work material properties [75].

3.6. LASER BEAM MACHINING (LBM)

Laser-beam machining thermally removes material, which uses a high-energy laser beam for melting/vaporizing substances on both metallic as well as other surfaces. The laser helps cutting, welding, drilling, and marking. This process is specifically useful to make holes on precise spots. Schematic diagram of LBM has been illustrated in Figure 3.6 [76].

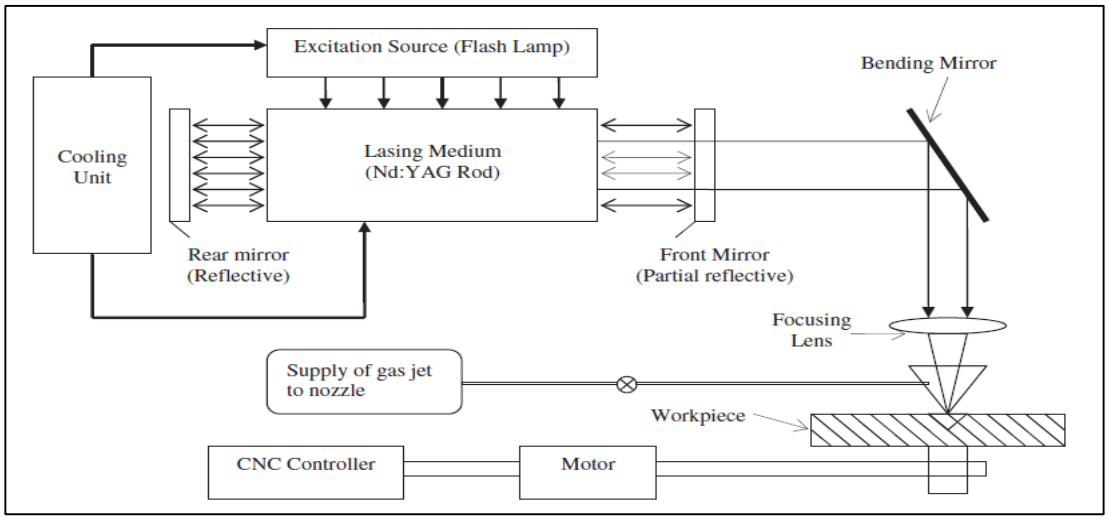

Figure 3.6. Schematic of Nd: YAG laser beam cutting system [76].

3.6.1. Different Laser Types for Manufacturing Operations

Laser beam drilling has two forms: percussion and trepan drilling. In case of trepan drilling, the cutting is made around the circumference of the hole; on the other hand, percussion drilling directly 'punches' through a workpiece while there is no relative movement in the workpiece or the laser, as Figure 3.7 shows [76].

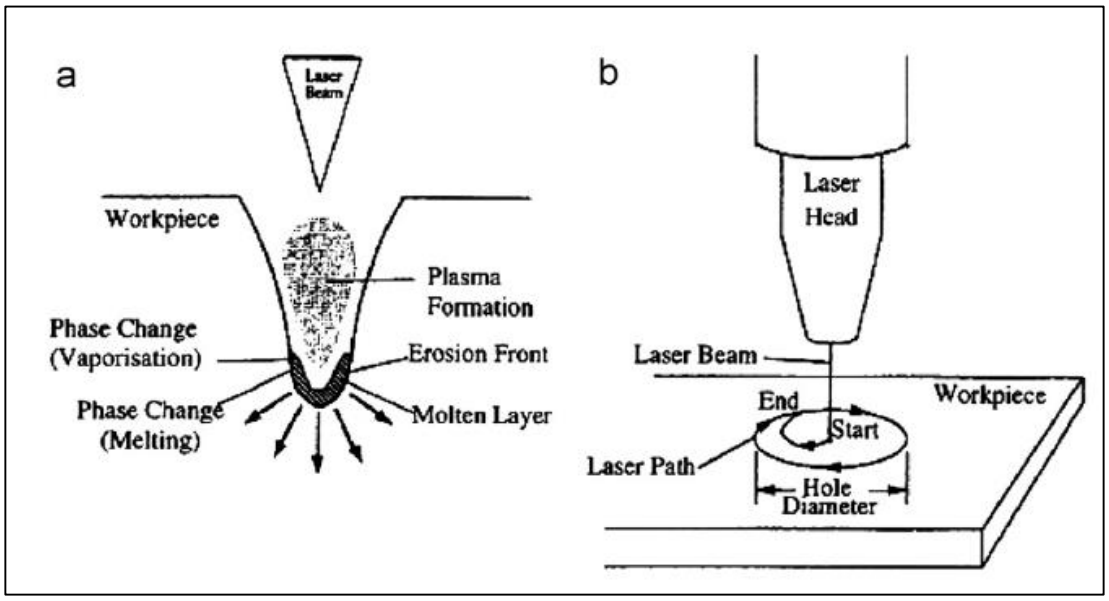

Figure 3.7. LBM schematic diagram [76].

3.6.2. Applications

In the aircraft industry, automobile sectors, civil structures, electronic industry, house appliances, and nuclear sector, LBM has substantial applications. In the automobile sector and home appliances, stainless steel is commonly used, and laser beam cutting is very suitable to cut it with precision [76].

3.6.3. Laser Beam Cutting (Drilling)

When LBM is used for drilling, the transfer of energy through Nd: YAGs melts a workpiece only on the point where the laser comes in contact with the workpiece that later converts into plasma and releases. Gas jets also help this process when a laser transforms a workpiece and leaves a substance. Laser drills are generally used for

drilling more rigid substances and workpiece geometries, which are not easy through other processes [76].

3.6.4. Laser Beam Cutting (Milling)

When a laser is diverted towards a workpiece, it moves through a specified trajectory for cutting material. Continuous-wave or CO2 lasers are helpful for higher-than-average electricity, greater material-removal, and smoother cuts [76].

3.6.5. Advantages of Laser Cutting

Absence of cutting path limitations because lasers can be moved or diverted anywhere. Stress-less operations, which allow cutting fragile substances with no need for extra support [77]:

1. Possibility to cut tough abrasive materials.
2. Possibility to cut sticky substances.
3. Economical and flexible method.
4. Very high precision cutting and machining.
5. No need for lubrication before cutting.
6. No wear and tear of tools.
7. Limited heat-affected areas around the cut.

3.6.6. Limitations of Laser Cutting

Limitations of laser cutting can be described as follows [77]:

1. Less economical when cutting is performed on a large scale.
2. Thickness limitations because of taper.
3. More investment needs because of the high cost of equipment
4. High maintenance costs.
5. Need for cover gas.
6. Heat related problems.

3.7. WATER JET CUTTING (WJC)

It is a beneficial method that reduces cost and increases the work speed through removing/eliminating/reducing the need for pricy secondary machining. Since heat is not used on substances, the edges cut very clean leaving least burr. Issues including cracks and defects on edges, crystal formation, low weld-ability, hardness and less machinability have been substantially decreased with this method. WJC is based on the rule that when extreme water pressure is applied by letting it come out of a narrow nozzle or "orifice," also named as "jewel." This type of cutting utilizes water-exiting beam for cutting fragile substances. It is unsuitable for cutting tough substances. In this technique, water inlet pressure remains typically from 1300 to 4000 bars, which moves through a tiny hole called as a jewel that generally has 0-0.4 mm diameter. Figure 3.8 shows how WJC works [78].

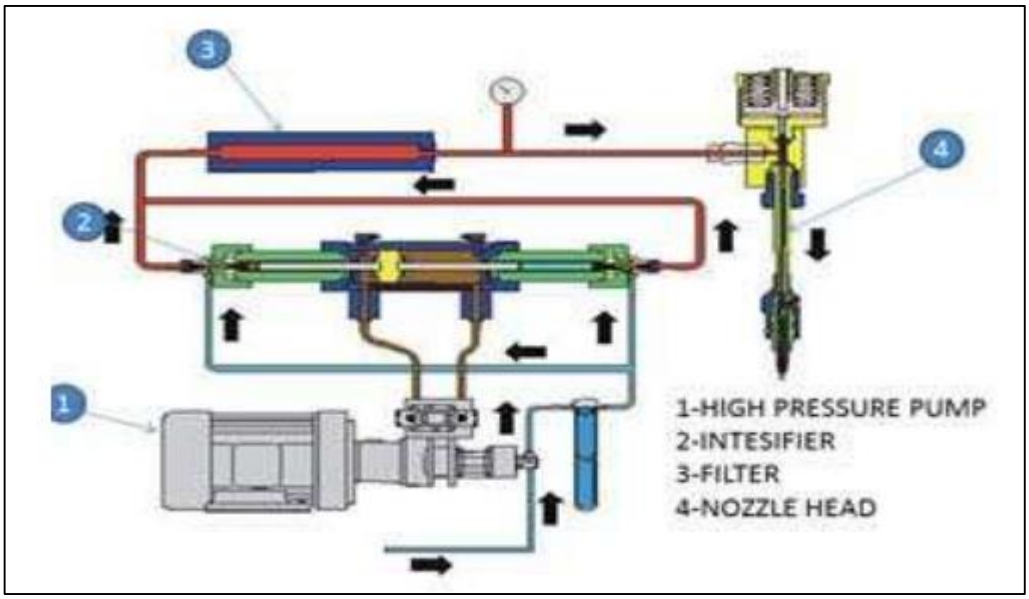

Figure 3.8. Water jet cutting [78].

3.7.1. Applications

WJC is a helpful technique for cutting low-strength substances including plastic, aluminium and wood. If we add abrasives, it becomes abrasive WJC, which works for even tougher metals and alloys, including steels and tools [78].

3.7.2. Advantages of Water Jet Cutting

Since WJC does not involve heat, it is beneficial for cutting materials such as tool steel and alloys in situations where extra heat changes the physical/chemical properties of a workpiece. WJC leaves no residual particles and releases no dust, so it is the healthier and safer method as compared to grinding or machining. Remaining benefits have been mentioned under the topic "abrasive water jet cutting" [78].

3.8. ABRASIVE WATER JET CUTTING (AWJC)

This method is a type of previously mentioned water jet cutting with only a difference that in this case, water has abrasive components/specs including silicon carbide/aluminium oxide, which increases the rate of material removal even more than typical water jet. It can cut any form of substance from hard-to-machine to softer ones, including glass, ceramics, rubber, and foam, to mention a few. A narrow cut sequence and computer-aided movements support this method for producing better quality and more quantity. It is an ideal machining process for those substances, which are not possible to cut using thermal or laser-based techniques. It can cut metals, alloys, non-metals and other complex materials having varying thicknesses. It is appropriate for those substances, which are sensitive to heat, and it is impossible to machine them with heat-releasing techniques [79].

Figure 3.9 is the schematic diagram of AWJ cutting that is just like water jet cutting other than features such as abrasives, mixing tube, and guard. When this process is initiated, water comes out of the jewel (nozzle) that causes a vacuum to suck abrasive particles, and later, they mix up with water to prepare a high-speed abrasive beam [79].

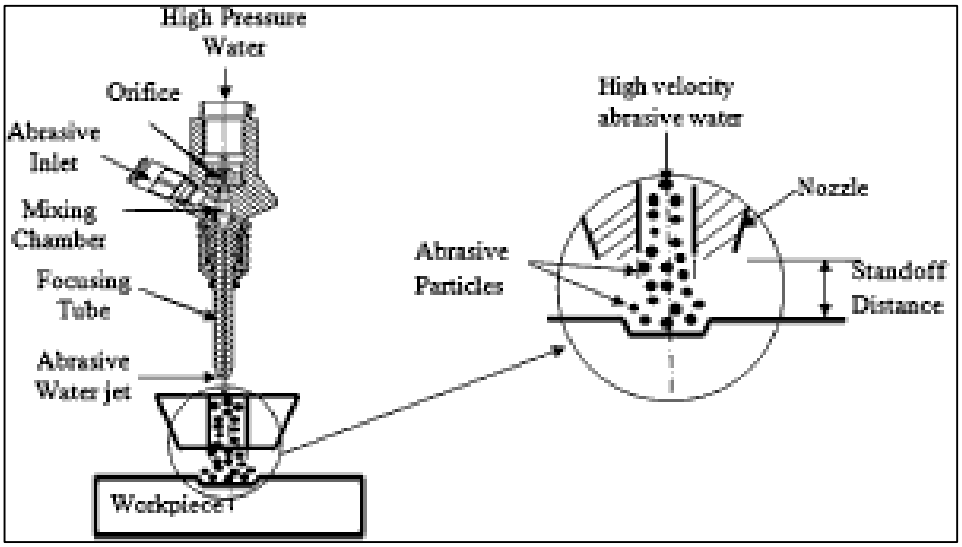

Figure 3.9. Abrasive water jet machining [79].

3.8.1 Applications

AWJ cutting is popular in industries such as automobile, aerospace, and electronics. Aerospace manufacturing, for example, titanium covers of fighter jets, engine parts, aluminium bodies and interior cabins are generally manufactured with the help of AWJ cutting. In the case of automobiles, internal parts such as liners, panels and bodies of fibreglass are manufactured using this method. In the same way, certain electronics products, including cable strips and circuit boards, are cut through AWJ [79].

3.8.2. Advantages of Abrasive Water Jet Cutting

Advantages of Abrasive Water Jet Cutting are as follows [79]:

1. It does not need a secondary finishing in many cases.
2. No distortion during cutting.
3. Application of limited cutting force on a workpiece.
4. Fewer tools are needed.
5. A less or no burr after cutting.
6. Its normal finish is between 125-250microns.
7. Less kerf size decreases material waste.
8. Least heat impact.

9. Localized structural change.
10. No metal contaminants, which appear because of cutting.
11. Elimination of thermal distortion.
12. Operation without slag/cutting dross.
13. Precise, multi-plane cutting, shaping, and possibility of bevel creation.

3.8.3. Disadvantages of Abrasive Water Jet Cutting

Disadvantages of Abrasive Water Jet Cutting are as follows [79]:

1. Not possible to drill flat bottoms.
2. Not possible to cut degrading materials having moist surfaces that reduce the cutting speed. They are normally used for rough cutting.
3. The main flipsides of AWJ cutting include high cost and noisy operations.

3.9. DETAILS OF ABRASIVE WATER JET (AWJ)

It is a fast-growing machining technique, which has gained worldwide popularity. AWJ removes excessive materials with the help of a complicated phenomenon that has many parameters. These parameters affect the AWJ machining performance as they include finishing on the surface, accuracy, material removal etc.

A few decades ago, the scientists and researchers were conducting experiments and researches on the water jet system. In the 1980s, abrasive jet technology was introduced, which was an improved form of the water jet. Inclusion of abrasive components is the only difference both the processes have. These abrasives improved material range, which could be machined with AWJ, and they could not be machined with water jets [80].

3.9.1. Water Jets

Many forms of jets, including abrasive water jets (AWJs) and pure water jets (PWJs) are utilized to conduct several operations including drilling, cutting, turning and

milling. AWJs are more popular than other types as they are utilized in many types of industrial processes including aerospace engineering, production, and mining because they are fully capable of cutting tough and thick metals, and they provide the facility of operating the jet using the jet nozzle. This method has gained popularity despite the fact that it is an uncommon technique as compared to other metal processing techniques as it provides some advantages including cutting-edge precision with least possibility of thermal degradation of metal during cutting [80].

3.9.2. Classification of Water Jets

Nowadays, many types of jets are available. Some high-velocity water jets are used for the same purposes as the common water jets do. They include abrasive jets, pure water jets, pulsed jets, continuous water jets and cavitating jets. On the other hand, AWJs further include injecting as well as abrasive wear suspension jets. The types of jets are shown in Figure 3.10.

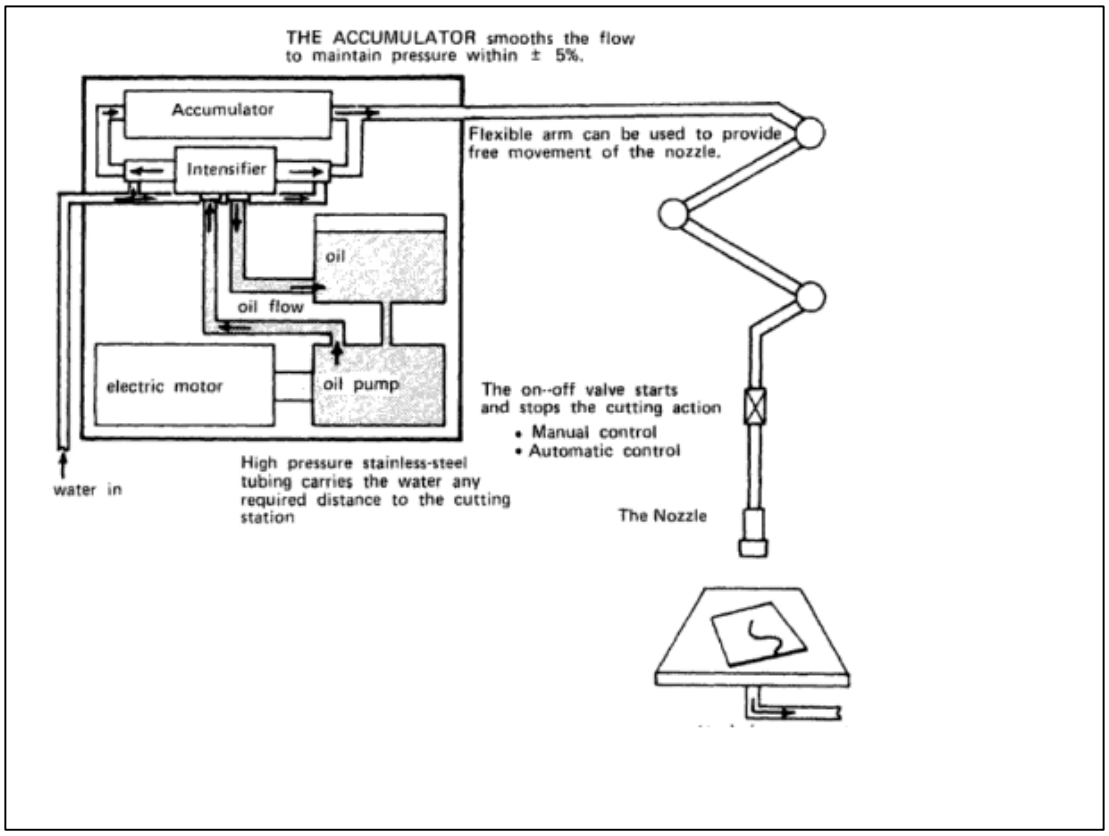

Figure 3.10. Types of water jets [80].

AWJM and simple WJM have undeniable beneficial properties that make them popular for common use in manufacturing.

Very quick installation and programming.
Few fixtures needed.
Capability to machine all 2D shapes using any substance.
Least extra factors and forces while machine operations.
No heat generation and impact on the workpiece.
Capacity to process thick sheets/plates [80].

3.9.3. Machine

In case of any AWJ machining, having entrained AWJM has the following components, which are exhibited in Figure 3.11 [79].

1. LP booster pump.
2. Orifice.
3. Hydraulic unit.
4. Mixing Chamber.
5. Mixer for additives.
6. Focusing insert/tube.
7. Catchers.
8. CNC table/s.
9. Abrasive meter.
10. Intensifier.
11. Accumulator.
12. Peak-pressure transmission line.
13. Valve for turning on/off**.**

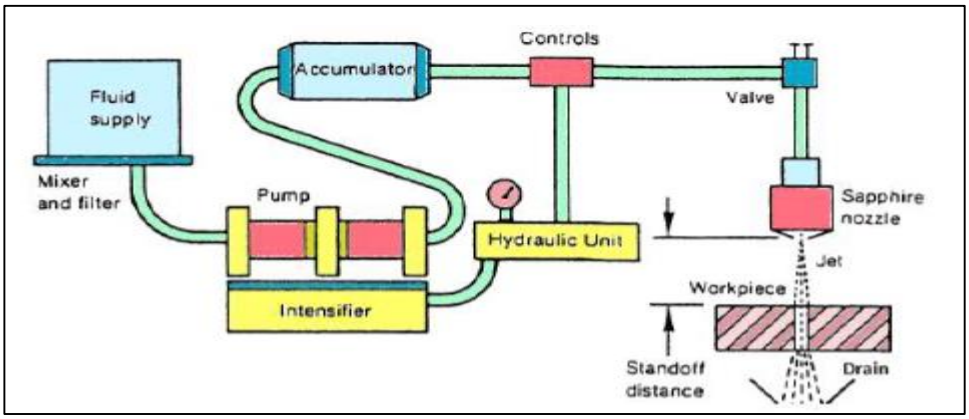

Figure 3.11. Schematic diagram of WJM [79].

Intensifier, shown in Figure 3.12, is generally operated through the hydraulic power pack, which works for positive displacement using a hydraulic pump. A power pack, which is used in industries, is operated through computers for controlled pressure [80].

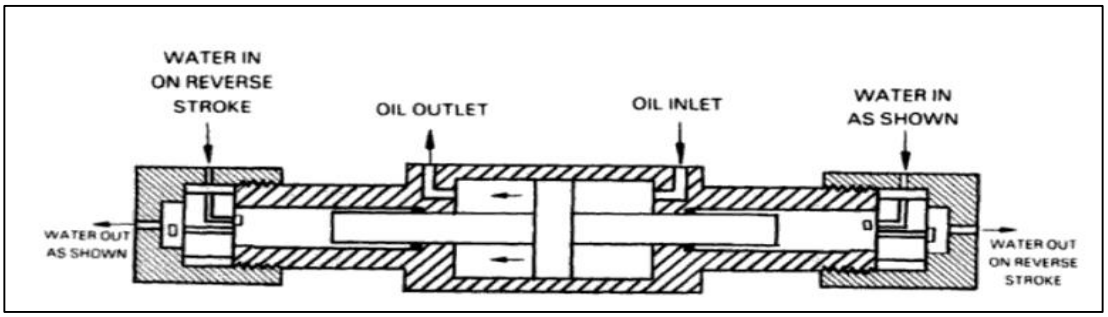

Figure 3.12. Intensifier schematic [80].

A hydraulic system takes the hydraulic oil and delivers it to an intensifier on a pressure. If the ratio between the two intensifier cylinders' cross-section is A where A = A-large/A-small. This means that the pressure amplification in a small cylinder will be (Eq 3.1):

$$P_o \, X \, A_o / \, A_w = \, P_W \tag{3.1}$$

In this case, if we set the hydraulic pressure at 100 bars while the area ratio is 40, then: pw = 100x40, so pw=4000 bars. Now, if we utilize direction controlling valve, intensifier is run through hydraulic devices. This is taken to a small cylinder, or it may be sent using a booster pump that normally increases water pressure until 11 bars

before it reaches intensifier. Normally, water softening is done using complex polymers by adding them to the additives unit. When an intensifier is operated, it transmits water at peak pressure (Figure 3.13). When the bigger piston moves its direction in the intensifier, the delivery pressure generally drops. For countering that, normally a thick cylinder is used for accommodating high-pressure water. It is considered as an accumulator that performs like the engine flywheel to minimize water-pressure changes. That high-pressure water is shifted to steel pipes, from where it moves towards cutting head. Such pipes can take water at 4000 bars (or 400 MPa) having in-built flexibility that does not allow leakage to take place. The cutting part has a mixer, orifice, and a focusing insert, which form water jet and mix it with abrasive components to make the AWJ ready [80].

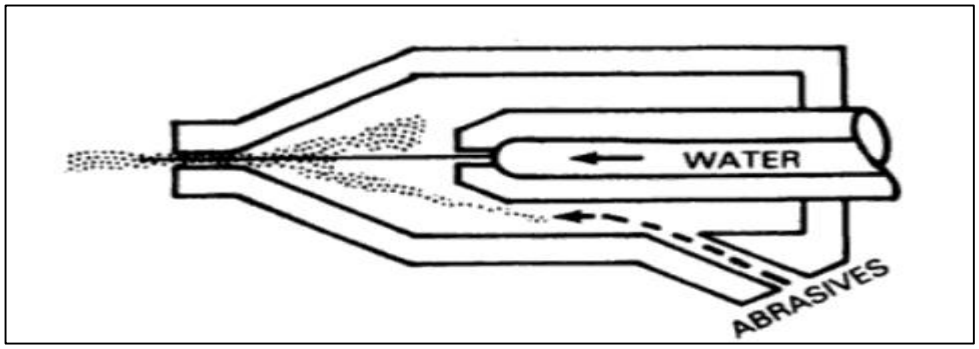

Figure 3.13. Abrasive water jet nozzle [80].

The cutting head/jet former are shown in Figure 3.13. Flexible steel pipes have a diameter 6 mm, and they carry water towards cutting head/jet former [80].

3.9.4. AWJM PARTS

3.9.4.1. Hydraulic System Components

Using abrasive water for cutting and using laser beams have been proven as far better methods as compared to conventional cutting. AWJC has been popular for cutting tough or hard-to-machine substances such as ceramics, Ti alloys, metals and concrete. AWJ machining normally utilizes a multi-dimensional reciprocation pump as a main source of energy. High pressure is applied to treated water, and that is passed through

4000-6000 bar (or 400-600 MPa). Abrasives such as garnet are added to the water through a hopper, so it was diverted towards a chamber that mixes it in the cutting head. These abrasives are moved on a high speed through the nozzle having small orifice diameter (0.1-1.0 mm). Water that exits from the orifice moves on high speed (more than 1000 m/s) that finally cuts a substance even as tough as steel. The Ti and Kevlar polymers are processed through this method. It is illustrated in Figures 3.14 [79].

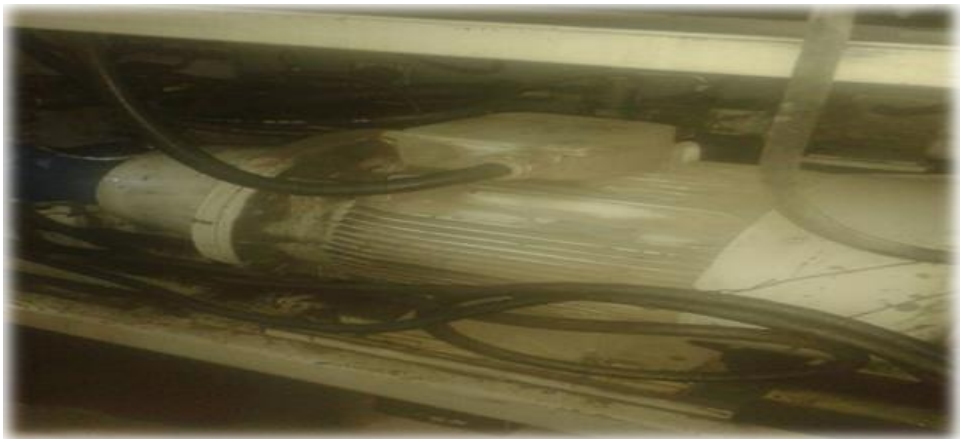

Figure 3.14. AC motor and oil pump (machine apparatus).

3.9.4.2. High-Pressure System Components

It contains a hydraulic cylinder, hydraulic piston. Photograph of high-pressure cylinder assembly was given Figure 3.15.

Figure 3.15. Hydraulic cylinder with high-pressure water (machine apparatus).

3.9.4.3. Oil Evaporator

The oil comes from the pump is very hot and oil evaporator must be used (Figure 3.16) before the oil goes to the tanks [79].

Figure 3.16. Oil evaporator (machine apparatus).

3.9.4.4 Mixing

Figures 3.17 throw light on how mixing is carried out. Here mixing implies abrasive components' successive entrainment in water jet, which helps abrasive water jet pressure to come out of the narrow opening [79].

Figure 3.17. Slurry tank.

When mixing is initiated, abrasive substance slowly accelerates because of momentum transfer from plain water to abrasive water, so jet leaves the focusing tube, so in both cases, plain water and abrasive liquid emerge with the same speed. Figures 3.17 illustrates the need for inserts/focusing tubes. That tube is manufactured using tungsten carbide having internal diameter 0.8-1.6mm while its length range is 50-80mm. Generally, tungsten carbides are utilized to provide resistance against abrasive particles, which move towards the jet during mixing, and they are forced to move away because of dragging force and buoyancy. They come in contact with the internal part of the mixing tube and jet before they speed up with the water jet pressure [79]. The process of mixing is modelled mathematically as under. For that, we consider the loss of energy when water jet forms in the orifice.

3.9.4.5. Abrasive Metering System

Supplies the cutting head with the quantity of abrasive and mixing abrasive, air and water together in the chamber [79] as shown in Figure 3.18.

Figure 3.18. Abrasive metering systems (machine apparatus).

3.9.4.6. Water Jet Nozzle

This cutting technology has proved low production cost, high cutting speed and low material loss [79] as showing in Figure 3.19.

Figure 3.19. Water jet nozzle (machine apparatus).

3.10. THE PROCESS PARAMETERS

They include jet pressure, traverse speed, SOD, size of abrasive grit and abrasive flow. The mentioned parameters are normally in good proximity with complicated non-linear relation between inputs and outputs, as Figure 3.20 indicates below [54].

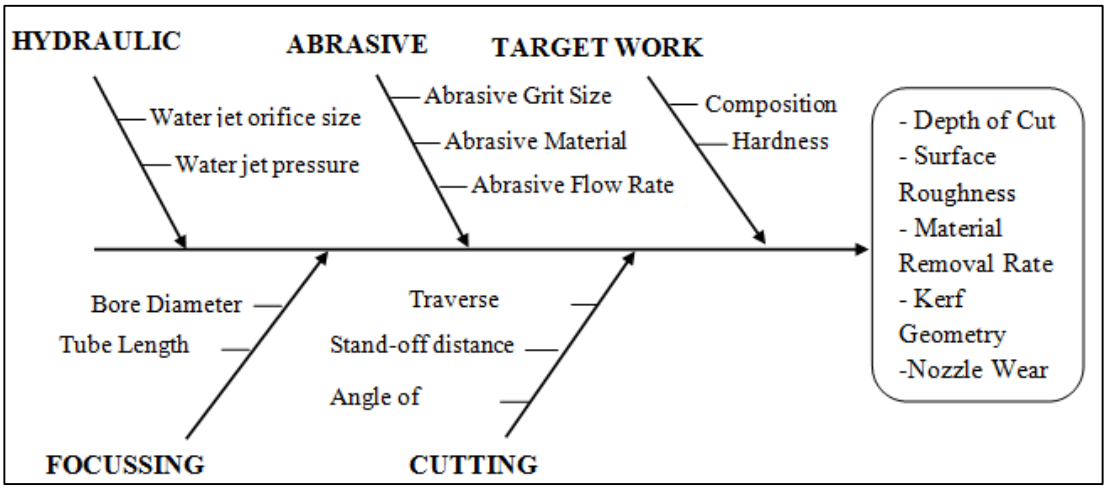

Figure 3.20. Classification of process parameters influencing the AWJM [54].

3.10.1. Cut Depth

3.10.1.1. The Impact of Traverse Speed on Cut Depth

Cut depth was assessed on various traverse speeds (f) in the range 1000-2000 mm/min. Tests were repeated for two abrasive flow rates of 100 and 150 g/min. Stand-off distance is 2 mm. The relation between cut depth and traverse speed has been shown in Figure 3.21 that proves the fact that the cut depth reduces with the increasing traverse speed that is so because the time when a workpiece exposes to the cutting abrasive jet reduces. The relation is of a power function form with a high regression ratio R2. This relation is nearly similar irrespective of the considered abrasive flow rates. Also, the figure shows that the higher jet traverse speed results in, the less deep cut on lower abrasive flows. It means that the increases in the traverse speed cause the impact on the workpiece that decreases exposure time, thus reducing the cutting depth. Jet traverse speed increases two times, which reduces the cutting depth by 70%. In order to get a higher regression factor R^2, the power formula is used [82].

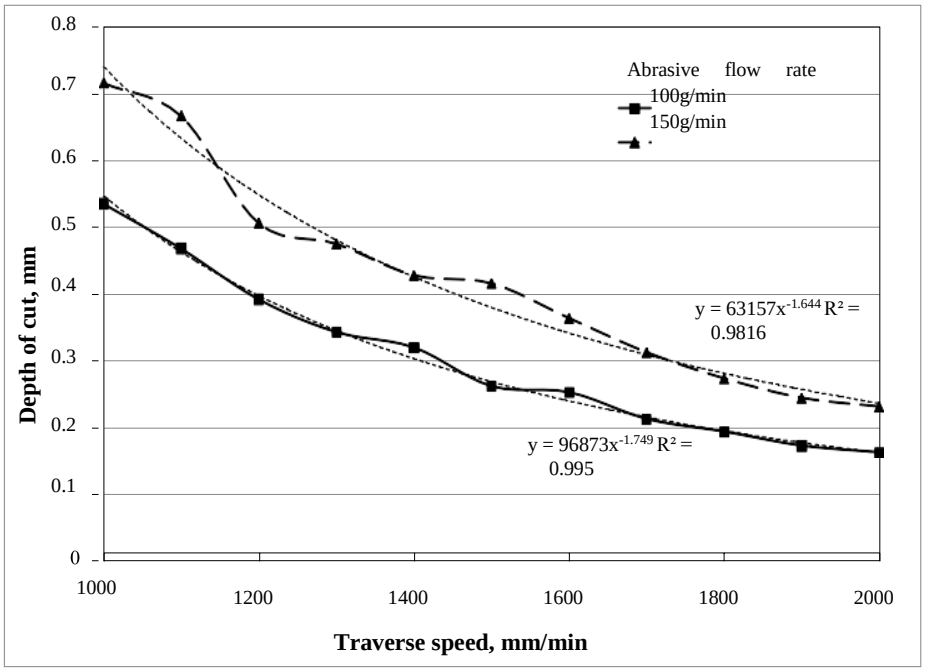

Figure 3.21. The impact of traverse speed on the roughness of the surface on varying [82].

3.10.1.2. Effect of Jet Pressure on Cutting Depth

Impact of jet pressure (p) on cutting depth has been tested at different pressures, ranging from 20 to 100 MPa. Tests were repeated for two abrasive flow rates of 150 and 250 g/min. The relation between jet pressure and a cutting depth of cut is obvious in Figure 3.22. It is clear from the given figure that when the jet pressure increases, the depth of cut has slight random changes around a fixed value. This means that the jet pressure has no impact on cutting depth within the testing range [82].

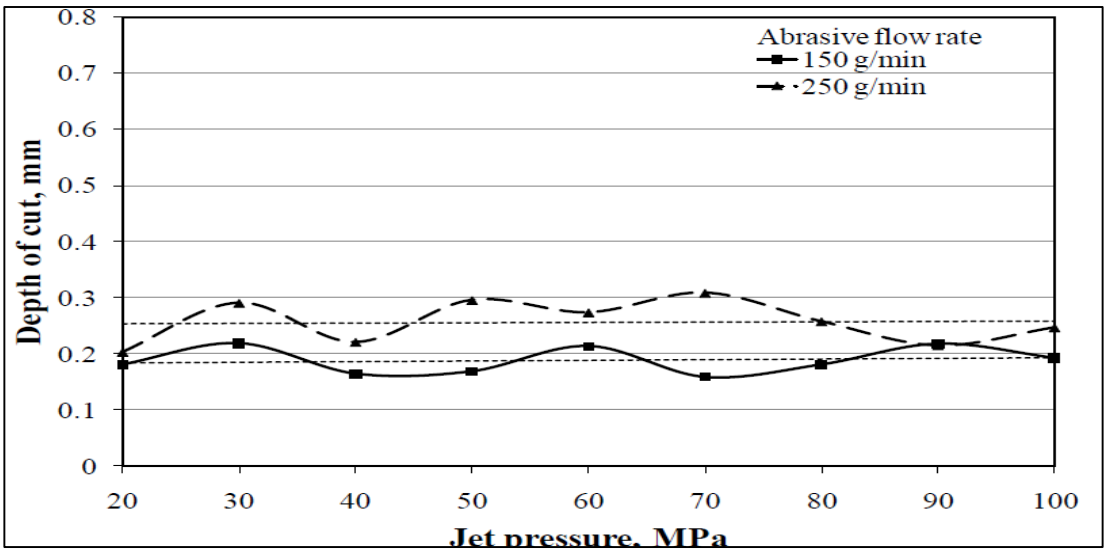

Figure 3.22. The impact of jet pressure on cutting depth of different abrasive flow [82].

3.10.1.3. Impact of Abrasive Flow Rate on Cutting Depth

The effect of rate of abrasive flows on cutting depth was tested. The tests were conducted at different abrasive flows in the range of 60-220 g/min. The tests were repeated at traverse speeds of 1600 and 2000 mm/min. Figure 3.23 shows the test results and trend curves. It is found that increasing abrasive flows enhance the cutting depth. The general trend of the mentioned relation is a polynomial function with high regression ratio R^2. If abrasive flows increase 3.5 times, cutting depth increases about 3.8 times [82].

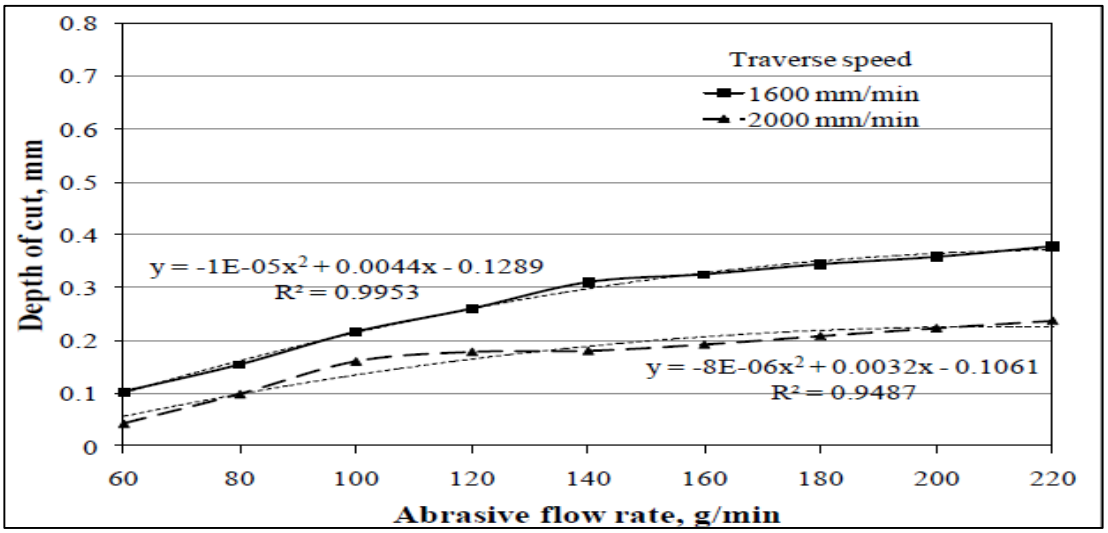

Figure 3.23. Impact of the rate of abrasive flows on cutting depth of cut at different rates [82].

3.10.1.4. Impact Standoff Distance (SOD) On Cut Depth

The impact of SOD on cut depth was tested. This test was conducted at four different stand-off distances and repeated at three abrasive flow rate values. The results are illustrated in Figure 3.24. The depth of cut values barely changed with SOD increase. Therefore, we can conclude that SOD has no impact on cut depth [82].

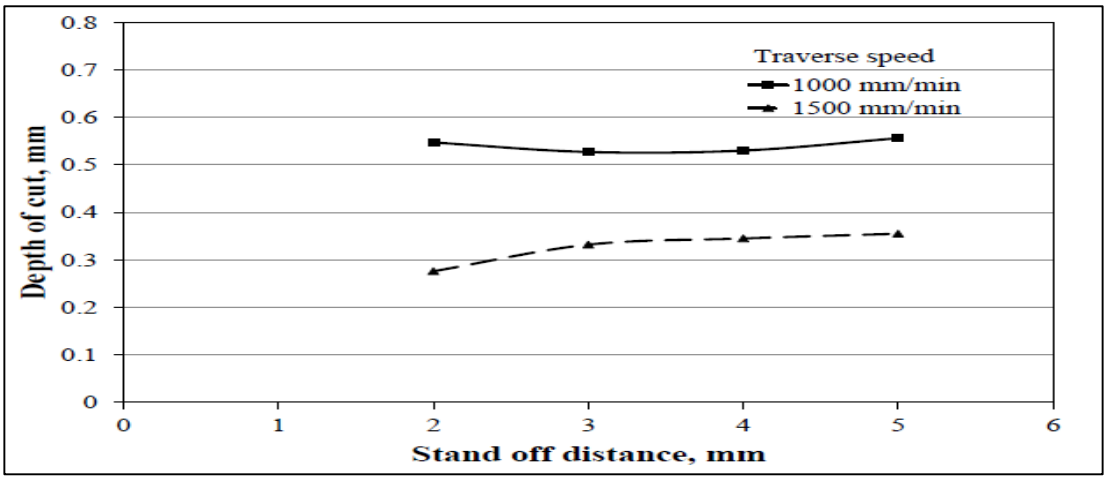

Figure 3.24. Impact of SOD on cut depth at different traverse speeds rates [82]. .

3.10.2. Material Removal Rate (MRR)

3.10.2.1. Effect of Traverse Speed on MRR

The relation between TS and MRR was given in Figure 3.25. There is a high correlation between those parameters [82].

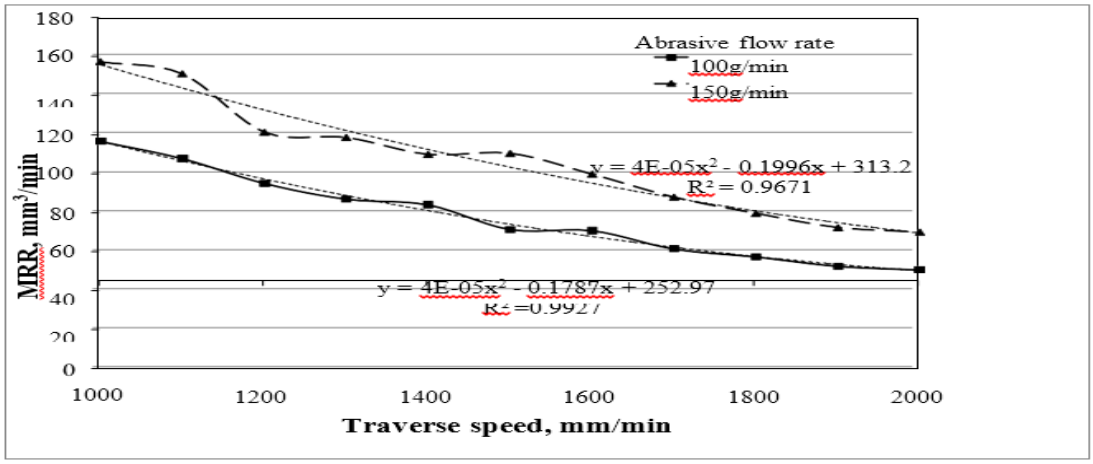

Figure 3.25. Impact of traverse speed on MMR at different abrasive flow rates [82].

3.10.2.2. Impact of Jet Pressure on MRR

It was tested whether jet pressure has any impact on MMR between 20-100 MPa pressures. In this range, results show that whenever jet pressures increase; the MRR has almost a fixed value. The tests were repeated at two abrasive flow rates; therefore, they show no effect impact of jet pressure on MMR in the tested range. Figure 3.26 shows the link between MRR and jet pressure on the MMR with varying abrasive flow rates [82].

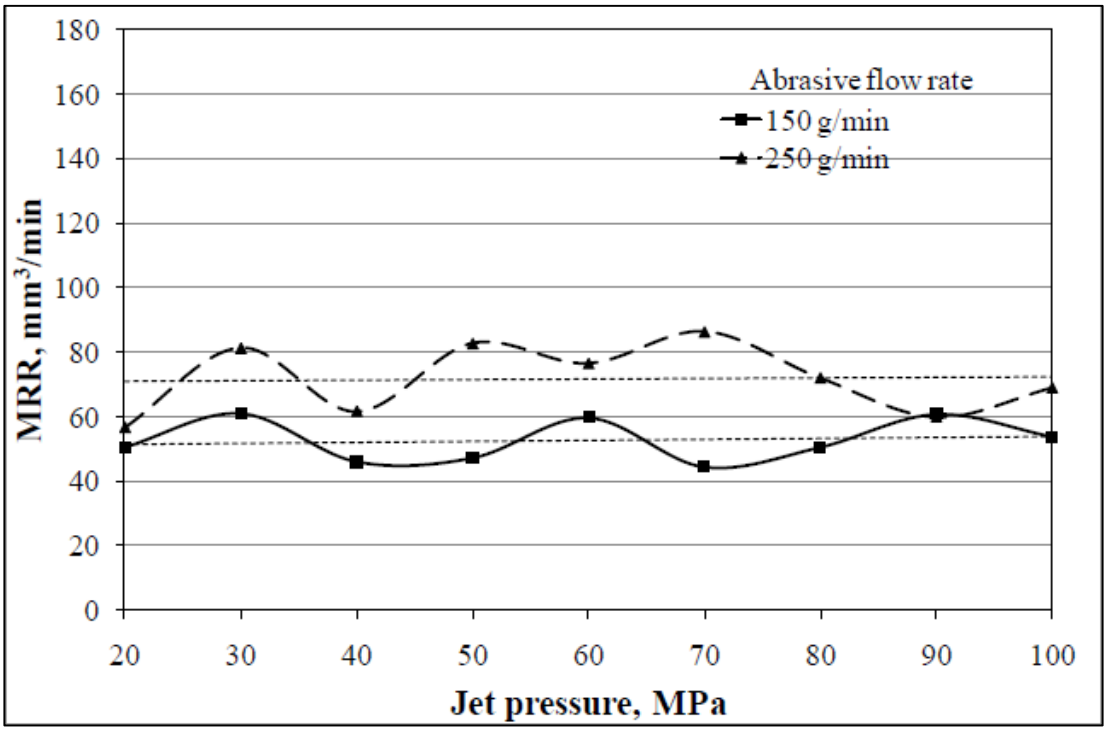

Figure 3.26. Impact of jet pressure on MMR at different abrasive flow rates [82].

3.10.3. Impact of Abrasive Flow Rate on MRR

Many trials have been conducted to explore the link between MRR and abrasive flows. During these tests, the abrasive flow rate ranges between 60-220 g/min, so, the tests were repeated for two traverse speeds 1600 mm/min and 2000 mm/min. Figure 3.27 shows the test results with their trend curves. It is obvious that MRR rises when the abrasive flow rate increases. The trend is of a polynomial function with high regression ratio R2. As an abrasive flow, rate increases by 3.5 times, MRR increased three times [82].

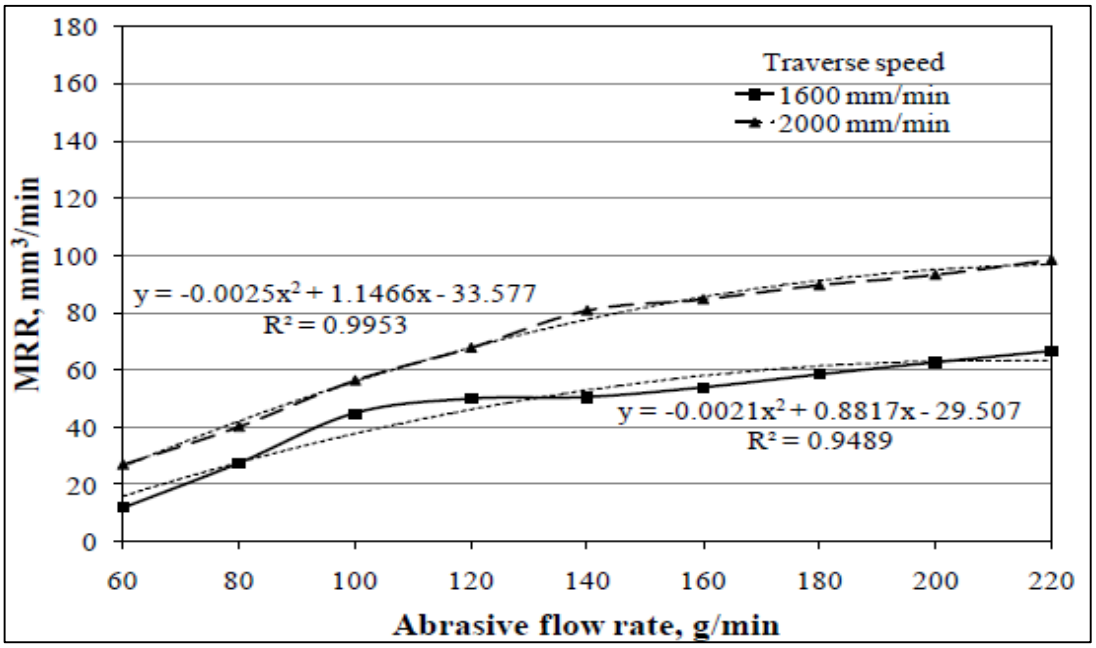

Figure 3.27. Impact of abrasive flow rates on MRR at different traverse speeds rates [82].

3.10.4. Impact of SOD on MRR

MRR values were tested at four different stand-off distances. The tests were repeated at two different traverse speeds 1000 mm/min and 1500 mm/min. The test results are illustrated in Figure 3.28. The tests show that the MRR values are nearly constant at different stand-off distances. Therefore, it is concluded that SOD causes no impact on MRR value [82].

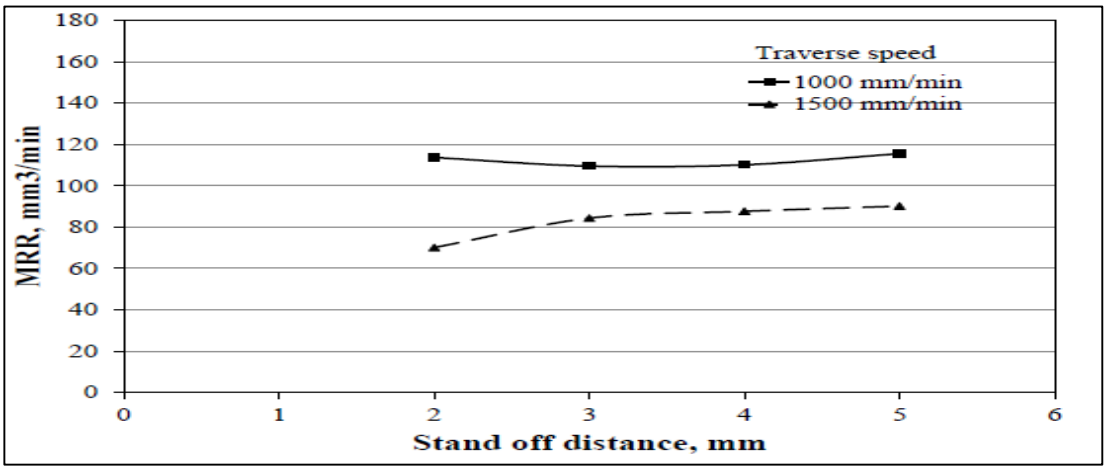

Figure 3.28. Impact of SOD on MRR at different traverse speeds [70].

3.10.5. Surface Roughness

3.10.5.1. Traverse Speed and Its Impact on Surface Roughness

The roughness of the surface (Ra values) was estimated on many traverse speeds between 1000-2000 mm/min. This test was repeated with two varying abrasive flows 100 and 150 g/min. The test results show that when traverse speed increases, on-the-surface roughness rises. Increasing traverse speed twice results in a decrease in the surface roughness by two times. The relation trend has a power function with a medium regression ratio R^2. Figure 3.29 shows the test results and their trend curves. This is due to the fact that higher traverse speeds result in less overlapping machine performance while a few materials have an impact on targeted materials for a given exposure time [82].

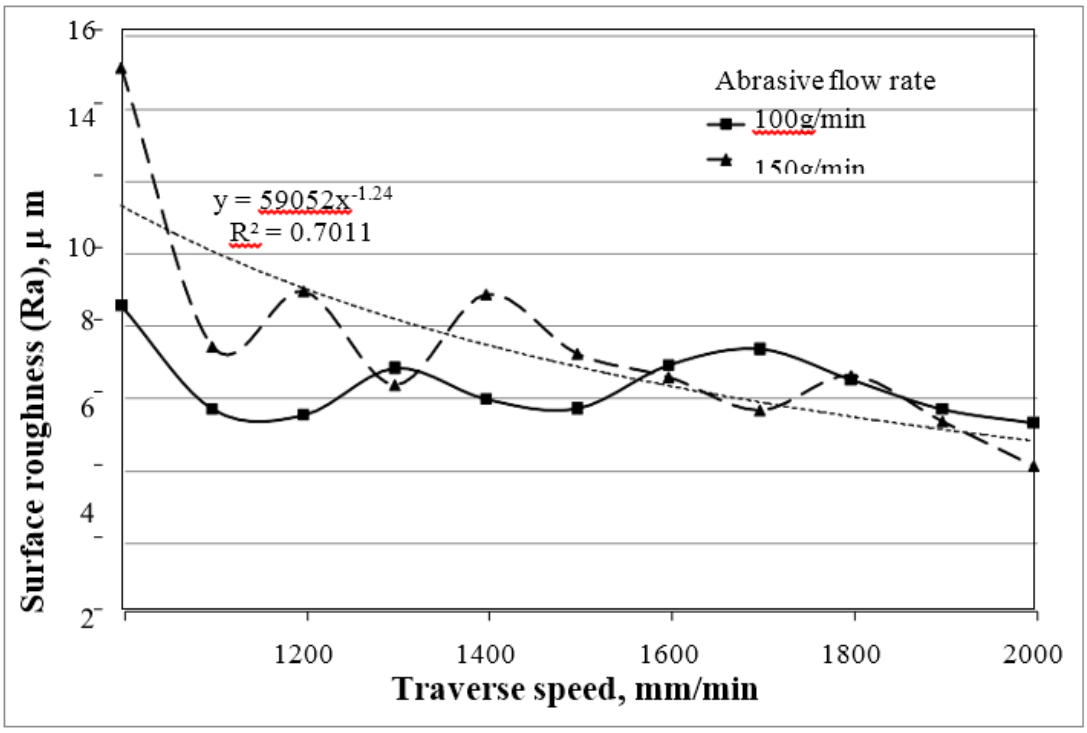

Figure 3.29. Impact of traverse speed on the roughness of surface with varying [82].

3.10.5.2. Impact of Jet Pressure on Surface Roughness

In order to check jet pressure impact on the roughness of the surface, the Ra parameter was tested under ranges of pressures from 20 to 100 MPa. In this range, results show that when jet pressure increases, the surface roughness Ra parameter almost had a fixed value. The tests were repeated at 150g/min and 250g/min rates of abrasive flow. Therefore, we can conclude that jet pressure does not affect surface roughness Ra parameter in the test range. Figure 3.30 shows the test results of the jet pressure impact on surface roughness Ra parameter on various abrasive flow rates [82].

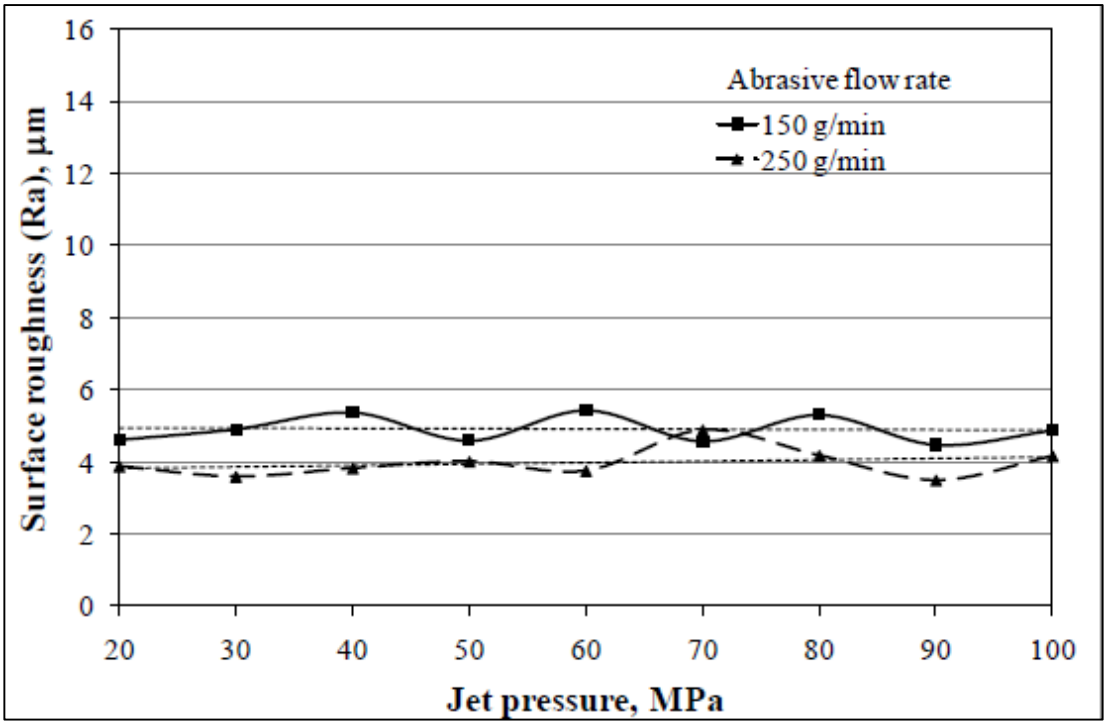

Figure 3.30. Jet pressure impact on surface roughness at different abrasive flow rates [82].

3.10.5.3. Impact of Abrasive Flow Rate on Surface Roughness

The surface roughness Ra parameter values were tested at a range of abrasive flow rates from 60 to 220 g/min. Those tests were repeated at two different traverse speeds 1600 mm/min and 2000 mm/min. The test results are illustrated in Figure 3.31, and the tests show that the surface roughness Ra values showed a slight decrease when the abrasive flow rate was increased. Increasing of abrasive flow by 3.5 times leads to

decrease the surface roughness 25% when the traverse speed was 1600 mm/min, and it is 45% at 2000 mm/min traverse speed. When the rate of abrasive flow increases, it allows extra elements to impinge and produce a smoother surface [82].

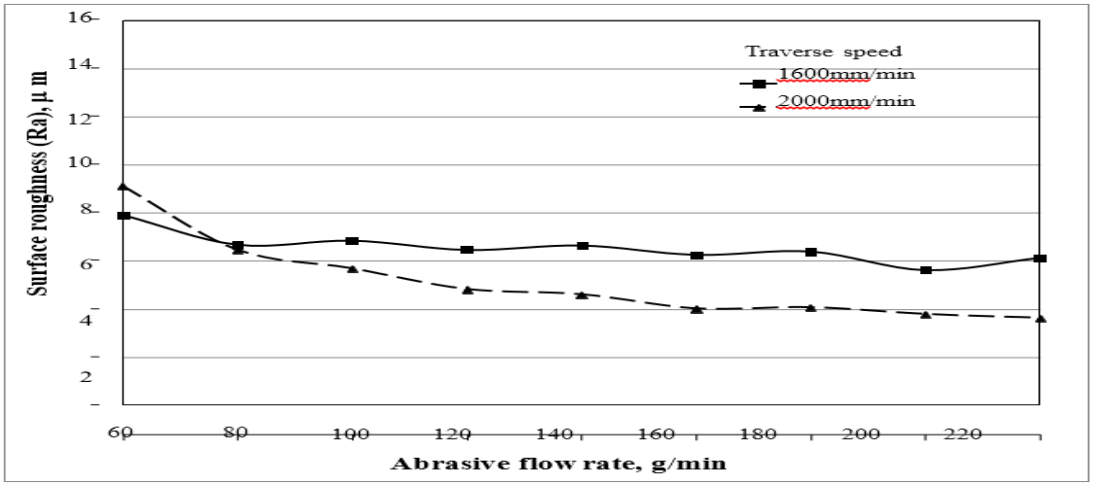

Figure 3.31. Impact of abrasive flow rate on the roughness of the surface at different [82].

3.10.5.4. Impact of SOD on Surface Roughness

To understand the impact of SOD on the roughness, the test was conducted at four different SOD parameters and repeated at two traverse speeds. The results are illustrated in Figure 3.32. We can conclude that the SOD bears no impact on cutting depth as the tests indicate [82].

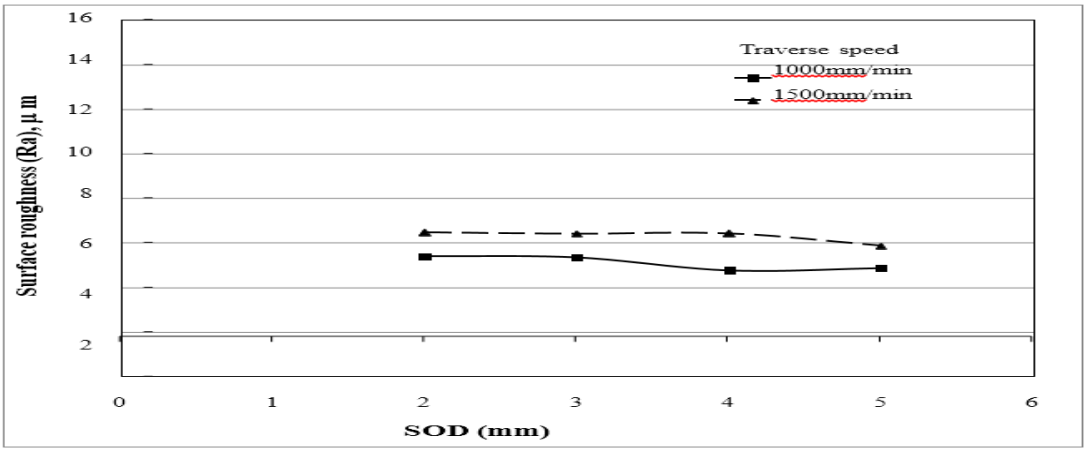

Figure 3.32. Impact of SOD on surface roughness at different traverse speeds [82].

3.11. UNDERWATER ABRASIVE WATER WET MACHINING

3.11.1. Contraction Parts of Underwater Abrasive Water Jet Turning

Water jet turning mechanism consist of [83]:

1. A conical space.
2. Connection apparatus.
3. Drive motor.
4. Sealing components.
5. Holder clip.
6. Connecting piece.
7. Roller bearings.
8. Shaft.

As can be seen from Figure 3.33, the water jet turning mechanism, according to the invention, comprises a shaft allowing rotation of the workpiece around its axis by driving the connection apparatus. It comprises roller bearings which bear the shaft and allow rotation of the shaft without vibration. The drive motion is provided to the shaft via the drive motor. A small pulley is found before the drive motor, which transfers the motion of the drive motor to the large pulley. Then transfers the rotational motion coming from the small pulley to the shaft. Our experimental work using a turning lathe setup which operated underwater with a maximum sound level of 85 dB developed in order to be used in abrasive water jet machining as mention in (Figure 3.33 and Figure 3.34). Figure 3. 34, including the main parts:

1. Cutting head.
2. Water tank level.
3. Workpieces.
4. Stepper motor and belt-driven pulley.
5. Stainless steel body.
6. Holder for material.

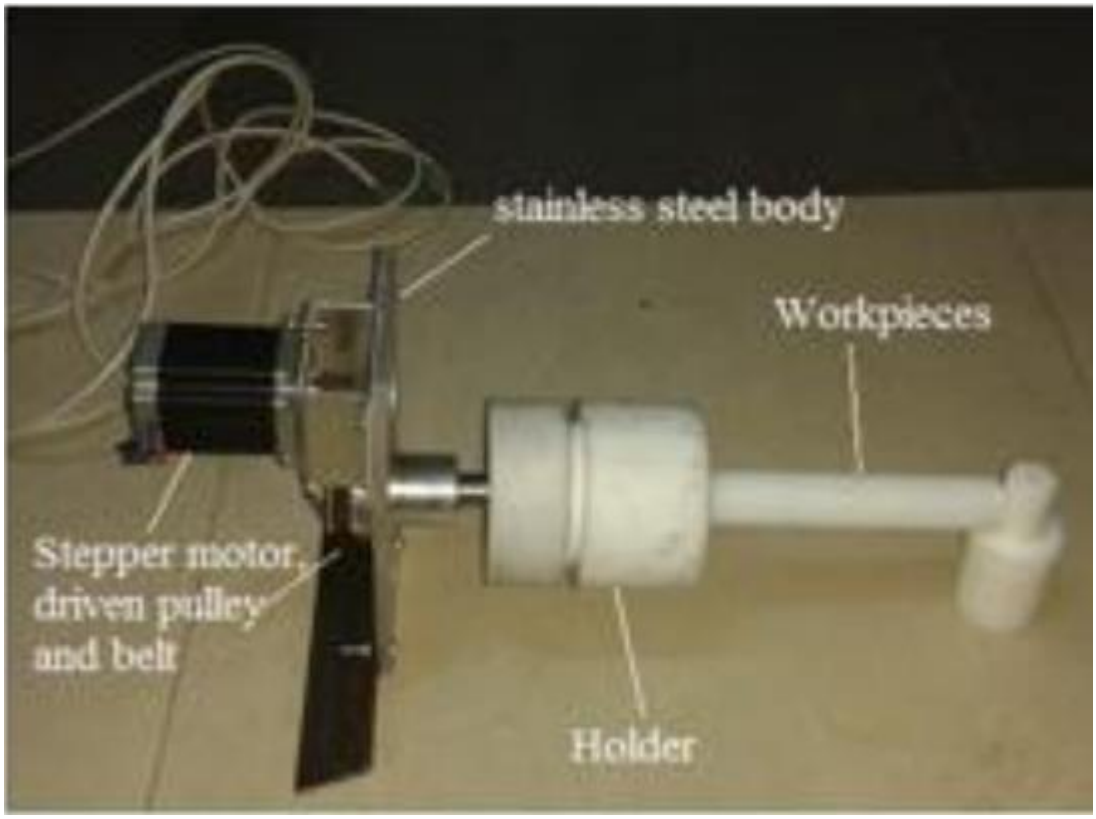

Figure 3.33. A schematic and prototype view of the developed turning mechanism [83].

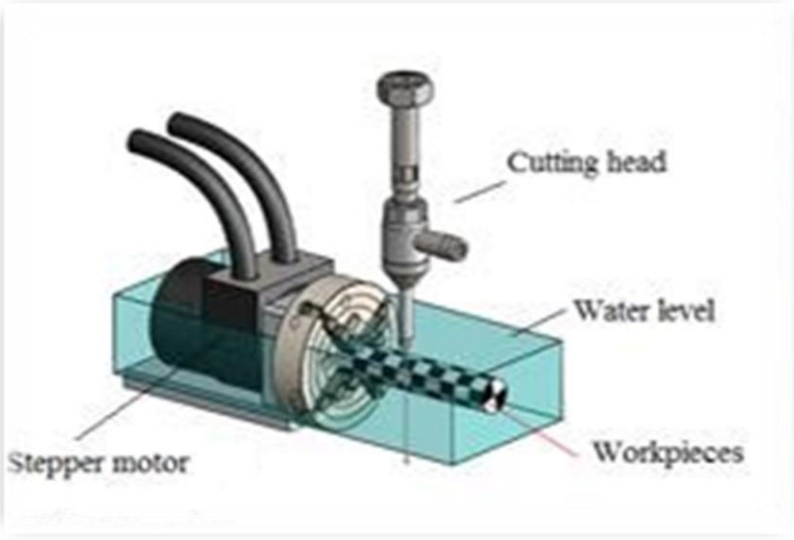

Figure 3.34. A schematic and prototype view of the developed turning [83].

3.11.2. Comparing Between Above and Under Water AWJM

3.11.2.1. Above Water AWJM

Use of the lathe chuck without protection makes the already difficult turning operation even more difficult. Since the abrasive water, the jet nozzle is above water level; the noise level is quite high and can reach up to 110 dB. This hearing loss may be temporary, permanent or both. Temporary hearing loss also called hearing fatigue, is eliminated after getting away from the short term exposure of a loud environment (usually in a few hours). Permanent hearing loss may be caused by Personal sensitivity [50]:

1. Level of noise (total energy of sound).
2. Frequency distribution of noise – sound.
3. The total amount of daily exposure.
4. Length of noise exposure.
5. Type of noise, such as continuous, intermittent, or pulsed etc.

3.11.3. Submerged AWJM

Noise level below water becomes lower, and the great advantage can be provided in terms of occupational safety. This process does not form waves/agitation in the water jet pool. Operates underwater makes resistant against corrosion since the parts are made of stainless steel and plastic and have a long service life. Abrasive sand does not go into the workpiece that is connected to the holder clip. Moreover, it has a modular structure that can easily be attached and detached. Ensures easy installation and removal in water jet machines and prevents loss of time. The mechanism is formed of the gasket-closed system and felt beds [84].

3.11.3.1. Cutting Parameters of Submerged Water Jet Machine

Cutting parameters from the above descriptions, the parameters of abrasive water jet cutting can be identified as follows [84]:

1. Abrasive mass flow rate.
2. Water mass flow rate.
3. Standoff distance of cutting head from work piece.
4. Pump operating pressure.
5. Speed of cut.
6. Number of passes.
7. Angle of abrasive attack to the work piece.
8. Type and size of abrasive material.
9. Focusing tube length.
10. Focusing tube diameter Mixing abrasive materials with the water jet 'or the degree of mixing of abrasive with jet' can be considered as dependent on the cutting head design.

Waterproof problems in the development of underwater abrasive water jet turning workers who operate high-pressure water jetting equipment should maintain their competency. This can be assessed and revised by providing refresher training or by evaluating and documenting an assessment of the high-pressure water jetting operation. Furthermore, these may be caused many problems concerted to the main points [84]:

1. System Operation: Explain how to safely operate all components of the high-pressure water jetting system, including the potential dangers, problems and emergency actions to be taken if the equipment fails or malfunctions.
2. Cutting Action: Demonstrate the cutting action of a pressurized jet of water and the potential hazard it poses by using audio-visual aids or using the equipment.
3. Control Devices: Explain how to operate all relevant control devices safely.
4. Part Compatibility: Explain how important it is to check all parts, fittings and hoses are compatible and are the correct size and rated equal to or greater than the maximum operating pressure of the high-pressure pump unit. Using the correct parts reduces the possibility of equipment failures and resulting injuries.
5. Hoses: Explain the correct method of inspection before use as well as connecting hoses, including laying them out without kinks, protection from wear and the correct tools to use on couplings and fittings.

6. Nozzles: Explain how to choose the correct nozzle use and size to check the maximum reaction force of 250 N or 25.5 kg is not exceeded during manual gun operations. The manufacturer's nozzle charts should be used for this.
7. Personal Protective Equipment: Give instructions about when and how specific PPE should be worn.
8. Maintaining Equipment: Explain that water jetting components like valves and seating surfaces in pressure-regulating devices experience high rates of wear during operation and that the equipment should be inspected often and maintained to ensure it can be used safely.

PART 4

ENGINEERING POLYMERS

4.1. INDUSTRIAL IMPORTANCE OF POLYMERS

When polymers are heated, they are passed in a soft and moldable state, but when they cool down, they become solid. In the fused deposition modelling process, they are melted and then extruded through a nozzle, which forms layers in the final part. Engineering thermoplastics is a subset of plastic materials, which are frequently used in applications requiring high performance in areas such as heat resistance, chemical resistance, impact or mechanical strength. In engineering sciences, some substances are called thermoplastics simply because they can be used in high-performance engineering applications. We can define layered production as a manufacturing process that can produce complex geometric parts with low energy and time consumption. It is a method for rapid prototyping highly complex parts, and in some cases, it is impossible to fabricate them using conventional methods. Despite the advantages offered by layered production, it is not yet included in the industrial mass production lines as an alternative to traditional production techniques due to repeatability and lack of process stability.

In some cases, this may not be a significant problem, but for some industrial purposes requiring high precision, this process may cause rough surfaces of the outer layer and lack of precision. Additional finishing is required to meet these limitations. Contrary to other machining processes, water jet cutting uses water at high speed and pressure for cutting substances ranging from plastic to hard metals. For soft materials, no additions are required for water jet cutting, whereas for hard metals, abrasive particles should be added to the cutting water. Thus, it becomes more effective. Advantages of water jet include its ability to cut both soft as well as rigid materials. Heating does not occur during the cutting process. Such cutting tools with a high frequency of change

are not used; thus, they save money. The cutting surface remains clean and does not require additional treatment. It is environment friendly because it does not create any toxic or hazardous substance. It works at low tolerances. Disadvantages of the water jet: Installation costs and prices of water jet machines are high. Abrasive materials and water can be mixed to cut hard metals. Water jet cutting process is time-consuming: therefore, in this case, production is slower as compared to the traditional methods [85]. It causes distorted geometries when thick parts are cut, which limits water jet cutting thick parts.

4.2. HISTORICAL POLYMER DEVELOPMENT

Natural polymers exist since the beginning of life, which shows that they played significant roles in the human, plant, and animal lives. Throughout the history of time, humans have been using natural polymers for clothing, shelter, decoration, weapons, tools, and writing materials but today's polymer industry evolved in 19th Century after significant discoveries, which modified some natural polymers. Thomas Hancock presented an idea in the 18th Century to modify natural rubber by adding some additives. After that, Charles Goodyear changed the natural rubber properties by vulcanization with sulfur. In 1909, Bakelite was recognized as the first synthetic polymer, after which, a synthetic fibre Rayon was developed in 1911. The polymer science was adequately studied just a century ago when Herman Staudinger presented his pioneer work. According to the 2-page definition by Staudinger (1919), high molecular mass compounds have long molecules with a covalent bond between them [85].

4.3 CLASSIFICATION OF POLYMERS

The word polymer is a generic term, which stands for several materials, which have high molecular weights. They exist in large numbers and forms, and they have a specific type of atoms. Polymers can acquire different physical properties, chemical structures, thermal characteristics, and mechanical behaviours [86]. Based on such diverse properties, polymers have been classified into different categories, which have

been presented in Table 1.1. The broad and main classification of polymers has been given in the next section.

Table 4.1. Classification of Polymers [86].

Basis of Classification	Polymer Type
Origin	Synthetic, Natural, and Semi-synthetic
Thermal Responses	Thermosetting and Thermoplastic
Formation Mode	Condensation, Addition
Line structures	Branched, Linear, Physical, and Cross-linked Application
Properties	Plastic, Rubber, and Fibers
Tacticity	Syndiotactic, Sotactic, Atactic
Crystallinity	Semi-crystalline, Non-crystalline (amorphous), Crystalline
Polarity	Non-polar, Polar
Chain	Hetro/Homo chain

4.4. PHYSICAL PROPERTIES OF POLYMERS

It is a commonplace knowledge that polymers show unique physical properties among all the non-metals. Some of them are tough, and they can tolerate large permanent deformations, but even then, they do not break. Some of them are strong and stiff, while others are flexible and soft. Some of them can withstand high impact without being damaged. The mentioned mechanical properties are specifically true for polymers, and the monomers, which are used to manufacture polymers, do not have them. Ethylene cannot form good films because it is different. Polymers are so different from each other because they acquire unusual physical properties because of large numbers of interactions among its chains. Such interactions have various kinds of inter-molecular bonds as well as complex physical entanglements. These interactions have a magnitude that depends on the molecular weight, the intermolecular bonding forces, the flexibility of the polymer chain, and the arrangement of chains. Certainly, the interactions are different for different kinds of polymers, and they are often different even in different samples of the identical polymer [87].

4.5. CHARACTERISTICS OF POLYMERS

The polymers' characteristics are illustrated below [88]:

1. High specific strength but low specific gravity
2. Electrical and thermal insulations
3. Weather and corrosion resistances
4. Easy manufacturing/designing complex structures
5. Aesthetic appearance because of easy-to-color property
6. Possibility of mass production using low-energy manufacturing techniques
7. Easy-to-print and easy-to-handle
8. The tremendous scope of chemical/physical modification for meeting industrial and commercial requirements
9. Possibility of low-cost production

4.6. APPLICATIONS OF POLYMERS TO DIFFERENT ASPECTS OF OUR LIVES

Polymer applications is illustrated as follows [89]:

1. Health
2. Medicines requiring high specific strength and modulus
3. Clothing that requires high resistance to corrosion
4. Transportation that requires high thermal and electrical conductance
5. Housing that requires insulation/conductance
6. Defence requirement of energy-conserving, fast, and easy processing to make intricate shapes
7. Electronics, which require an aesthetic appeal
8. Surfaces that require fungus and moth protection
9. Products that require low water and gas permeability
10. Need for biodegradable and non-biodegradable substances

4.7. STRUCTURAL POLYMERS

The materials of familiar categories, including fibres, plastics, adhesives, and rubbers, have diverse arrays of natural as well as synthetic polymers. These materials have a general rubric of specific structural polymers because their mechanical behaviour helps to perform their function. When they are compared with metals, they have broader use. Table 4.2 shows that synthetic fibres, rubber and plastics were produced in large quantities in the US, which was worth 71 billion pounds back in 1992, and the production tripled during the last two decades. The original manufacturers received roughly $0.50 per pound, but this return was different based on the type of material. When the price of crude oil is $20 per barrel, it means that oil costs almost $0.06 per pound; therefore, conversion to polymers adds considerable value. These materials require many manufacturing steps before they acquire their final forms. Their national economic impact is in the hundreds of billions of dollars every year [90].

Table 4.2. US production of structural polymers [90].

Substances	**Pounds (billions)**
Rubber	4.20
Fibres	9.10
Plastics	57.60

PART 5

MATERIAL AND METHOD

5.1. MATERIAL AND METHOD

5.1.1 Characterization of Experimental Material

Mechanical, thermal and physical properties of the castamide material used in the study are given in Table 5.1 [91, 92]. Castamide is one of the most preferred engineering plastics due to its ~85 MPa strength, 1.10 g/cm^3 density and high hardness. Also, castamide is used in bearings with high stability in wear conditions [93]. For this reason, it is of industrial importance to increase the machinability of castamide material which is directly related to surface quality.

Table 5.1. Engineering properties of cast-polyamide [92].

Property	Unit	Value
Density	*g/cm^3*	1.15
Water absorption	*%*	6-7
Tensile strength	*MPa*	90
Modulus of elasticity	*GPa*	4
Tensile elongation	*%*	>20
Impact strength (Izod, notched)	*kJ/m^2*	5.6
Hardness (Shore D)	*Shore D*	84
Melting temperature	*C°*	220
Thermal elongation	*1/K.10^5*	8-9

However, due to the high temperature during the conventional machining process, the castamide material melts, the surface form of the material deteriorates, and the surface roughness increases. Also, the melted plastic material smears back onto the material

surface by the cutting tool, which makes it hard to obtain an acceptable surface quality (Figure 5.1). In order to increase the machinability of castamide, methods not producing heat effect are required. AWJT is one of such machining processes and can be used to improve the machinability of castamide.

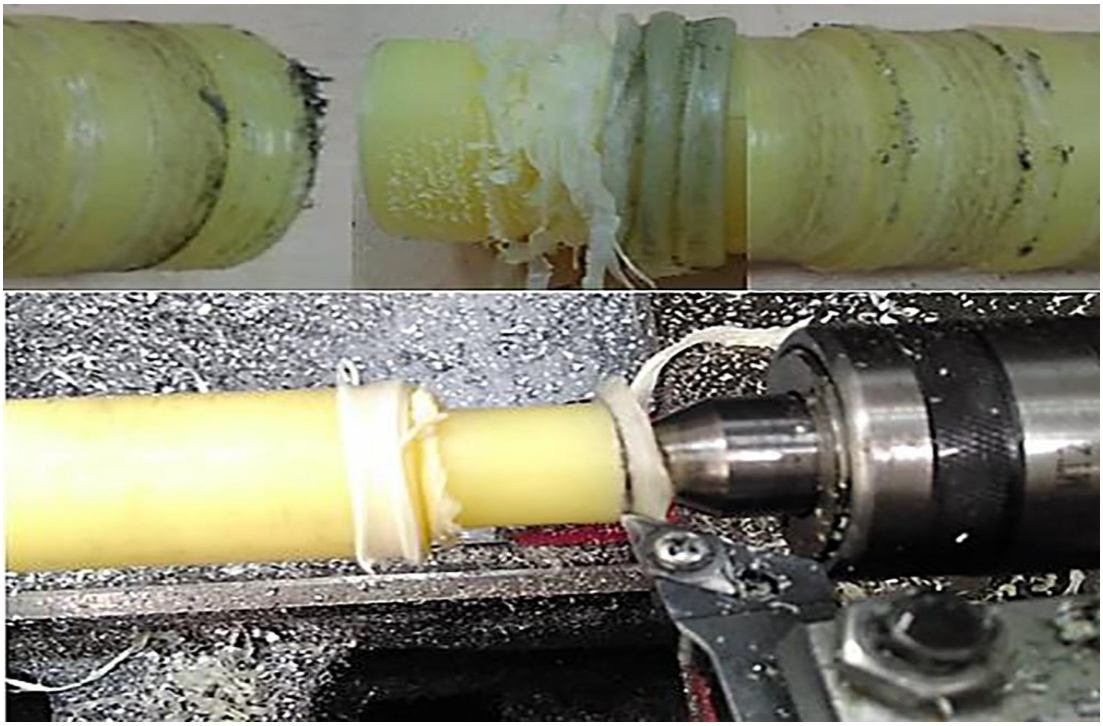

Figure 5.1. Surface quality deterioration due to melt spinning.

5.1.2. Introduction of Submerged Abrasive Water Jet System

In this study, a submerged AWJ turning assembly was used to minimize the problems above (Figure 5.2). The AWJ lathe is made by combining a conventional lathe with a water-jet machine. In the assembly, the abrasive-added water jet works as a cutting tool, and the lathe apparatus rotates the workpiece. Submerged assembly passes the abrasive jet from the high-pressure zone to the hydrostatic pressure zone and thus minimize the expansion of the jet producing a better cutting profile (Figure 5.3). Submerged AWJT experimental setup uses a 0.37 kW electric motor and ATV 12 380 V–220 V control card for the motor speed control which can turn the motor at a constant speed and torque at the desired direction. The turning mechanism was constructed using a belt and pulley and key coupling. A surface hardened chrome shaft

is used as a spindle. The roller bearing is used as a bearing element. In the lathe, a 100 mm diameter three-jaw chuck was used to hold the workpiece. A digital dial gauge with a precision of 0.001 mm was used to detect the deviation of the system axis. In the designed system, the axial offset value of spindle and lathe chuck was measured as 0.001 mm. SL-V 50 KMT model pump is used, and the tests were conducted under 3800 bar constant pressure. For sealing mechanical and electronic equipment, liquid gasket and protective cover are used. Mineral-based garnet material of ~80 mesh size was used as an abrasive particle. Garnet material is a preferred abrasive due to its antitoxic properties and having no corrosive effect. Garnet material's SEM images are given in Figure 5.4, which shows the multiple sharp-edged structures of the garner. This form enables the many contact areas with high tensile values, and the material can be cut rigidly.

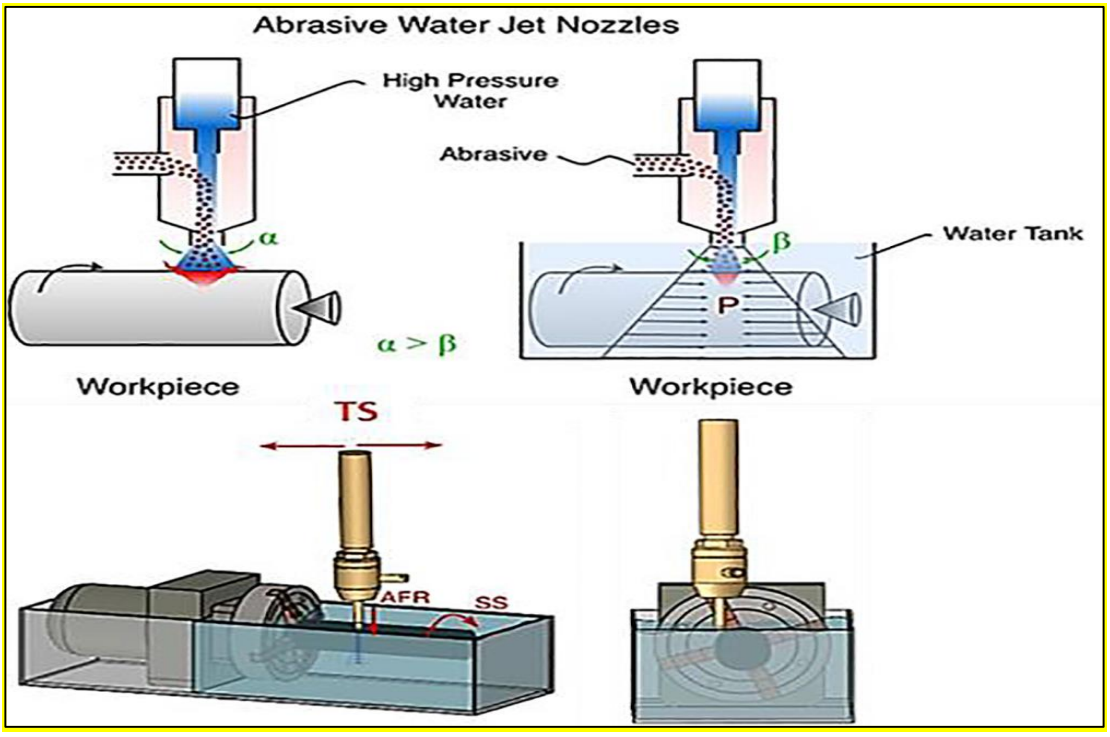

Figure 5.2. The behaviour of water jet in submerged cutting conditions and 3d drawing of submerged abrasive water jet process (Perspective and front side).

Figure 5.3. Submerged abrasive water jet experimental setup.

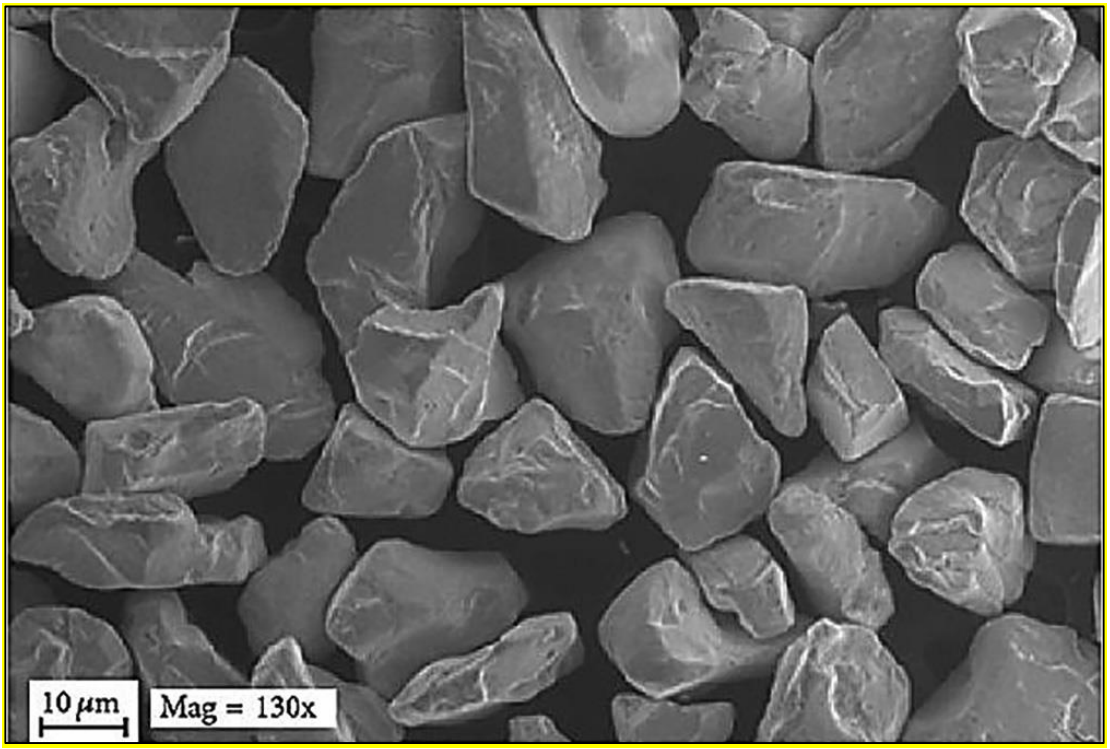

Figure 5.4. SEM image of the garnet abrasive material.

5.1.3. Experimental Design

In the experiments, TS, AFR and SS values were considered as input parameters (Table 5.2). Parameter levels were determined based on the preliminary tests and literature review, and three levels were determined for each parameter [94].

Surface roughness (Ra) and material removal rate (MRR) parameters were measured as output parameters (Table 5.2). The experiment was designed using full factorial design method, and a total of 27 different conditions ($n^k = 3^3$) were tested. Nozzle stand-off distance parameter was kept constant at a length of 2 mm. In Figure 5.5, the fixed-parameter defined by nozzle stand-off distance is shown schematically. Turning was done under the condition that the nozzle tip is tangent to the workpiece, and the cutting depth parameter was formed according to the scattering of the jet. In the literature, the nozzle stand-off distance parameter was defined as the depth-of-cut parameter, similar to that used in conventional turning [95].

This approach is important for analytical calculations. However, in the experimental study, it was determined that different diameter values were formed in each pass due to the changes in the manufacturing parameters depending on the design of the experiment. For this reason, the MRR parameter was calculated and analyzed as the output parameter by measuring the diameter values formed after each pass. However, considering the MRR values, it can be said that the depth-of-cut is approximately 1 mm. Mitutoyo SJ-301 type desktop profilometer was used for surface roughness (Ra) measurements. The cut-off length was determined as 0.8 mm. Three measurements were done for surface roughness, and the mean value is taken. To calculate the metal removal rate, the diameter of the workpiece before and after the machining is measured using a calliper, and MRR is calculated using Eq. (5.1) where, i is the test number, D_i is the diameter before the machining, D_i+1 is the diameter after machining, and h is the machined length. Noise measurement was performed by PCE-MSM 4 (±1.4 dB accuracy) equipment. The second-order variance analysis (ANOVA) is used to analyze the experimental results, and the significance levels were calculated by regression analysis. The ANOVA test provides a quantitative measurement of the effect of input parameters on the output parameters. Additionally, regression coefficient values (R-

Sq and R-Sq Adj.) are important to measure the statistical significance and adequacy of the experiment setup. Depending on the experience obtained for machinability, it can be said that the regression coefficient values 80% and more are enough for the AWJT process [96].

In the evaluation of the experimental results, the minimization criterion for Ra and the maximization criterion for MRR were considered. The optimum test conditions were determined using TOPSIS and VIKOR methods which are known to have high reliability and ease of application among the multi-criteria decisionmaking methods [97] [98] [99]. For Ra and MRR, a weight value of 0.5 was considered.

Table 5.2. Experimental input and output parameters.

Input parameters	Units	Level 1	Level 2	Level 3	Output parameters	Units
Travers speed (TS)	mm/min	40	140	240	Surface roughness	μm
Abrasive flow rate (AFR)	g/min	110	210	310	Material removal	mm^3/min
Spindle speed (SS)	rpm	100	200	300		

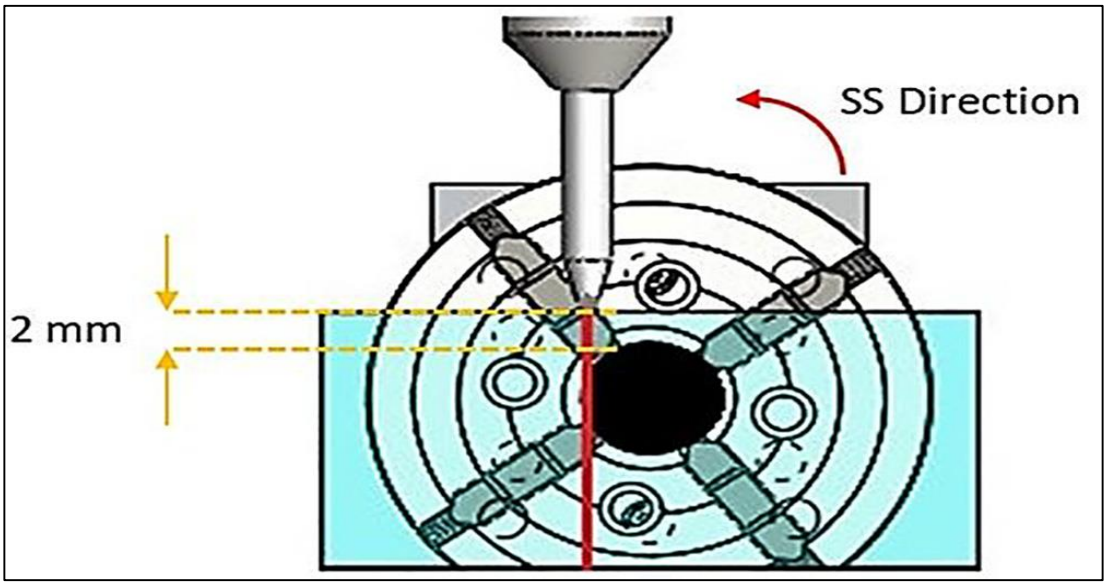

Figure 5.5. Schematic of nozzle stand-off distance parameter.

S parameters were used as optimum ideal, negative ideal and ideal parameter indicators, respectively. In solution Table of VIKOR, Ri, Fi, Qi parameters was used as the first solution coefficient, second solution coefficient and ideal parameter indicators, respectively. In the study, conventional AWJT results from the literature were used to compare the performance of the submerged AWJT process [94].

Normally, the comparison of underwater AWJT and conventional AWJT results had to be performed with the same parameters in both experiments. However, due to the resistance occurring under underwater conditions, it was not possible to reach high spindle speeds possible at the conventional method. Additionally, it was realized that sealing problem at high speeds would be a serious problem. For this reason, comparisons can be made by considering the nominal test values in both conditions.

$$MRR_i = \left(\pi.\left(D_i^2 - D_{i+1}^2\right)/_4\right).h \tag{5.1}$$

5.2. METHOD ANALYSIS

Analysis of variance (ANOVA) is considered a statistical test to detect the differences in means of the group when there are one parametric dependent variable and one or

more independent variables. At our study, we will give a brief review about ANOVA analysis test. The focus is on the conceptually based viewpoints associated with the use and explanation of ANOVA, with no coverage to the mathematical basics. Assumptions underlying ANOVA comprises the parametric data measures, normally distributed data, similar group variances, and independence of topics. Nevertheless, normality and variance assumptions are violated with impunity if sample sizes are appropriately big, and there are equal numbers of topics in every group. A statistically significant ANOVA is classically followed up with many comparisons procedures to determine which group means vary from each other [100].

5.3. TOPSIS METHOD

TOPSIS method uses two designated examples. In the first example, it is found that the best TOPSIS solution is neighbouring neither to the positive model solution nor the furthest from the negative ideal solution. In several methods on TOPSIS method stands as follows: "The ideal attitude is that the selected alternative must have the direct distance from the perfect positive solution and slowest distance from the perfect negative solution". Method for order presentation by comparison to the perfect solution (TOPSIS), TOPSIS method is a technique of order preference by the similarity to perfect solution that exploits the advantage standards/attributes and decreases the cost standards/attributes. In contrast, the negative model solution increases the cost standards /attributes and reduces the advantage standards /attributes [101].

5.4. VIKOR METHOD

VIKOR method comprises many standards optimization of complicated systems, which focuses on ranking and selecting from the set of substitutes between contradictory standards. VIKOR role is to discover many standards raking index based on a specific measure of familiarity to the optimal solution. It helps in solving the problems of MCDM associate with its two benefits; the first that it offers a maximum group value of the common and a less of the individual regret of the opponent. The compromise ranking of VIKOR has the four steps that n and m are the numbers of

standards and substitutes correspondingly. The mathematical procedure is presented in Figure 4.7. Step one and two discovers effectiveness measure and repentance measure for substitutes associate with each standard. Later, step three calculates the minimum and maximum quantities of step two results—the computation of *Qj* as the popular arrangement in step four prioritizes the substitutes [102].

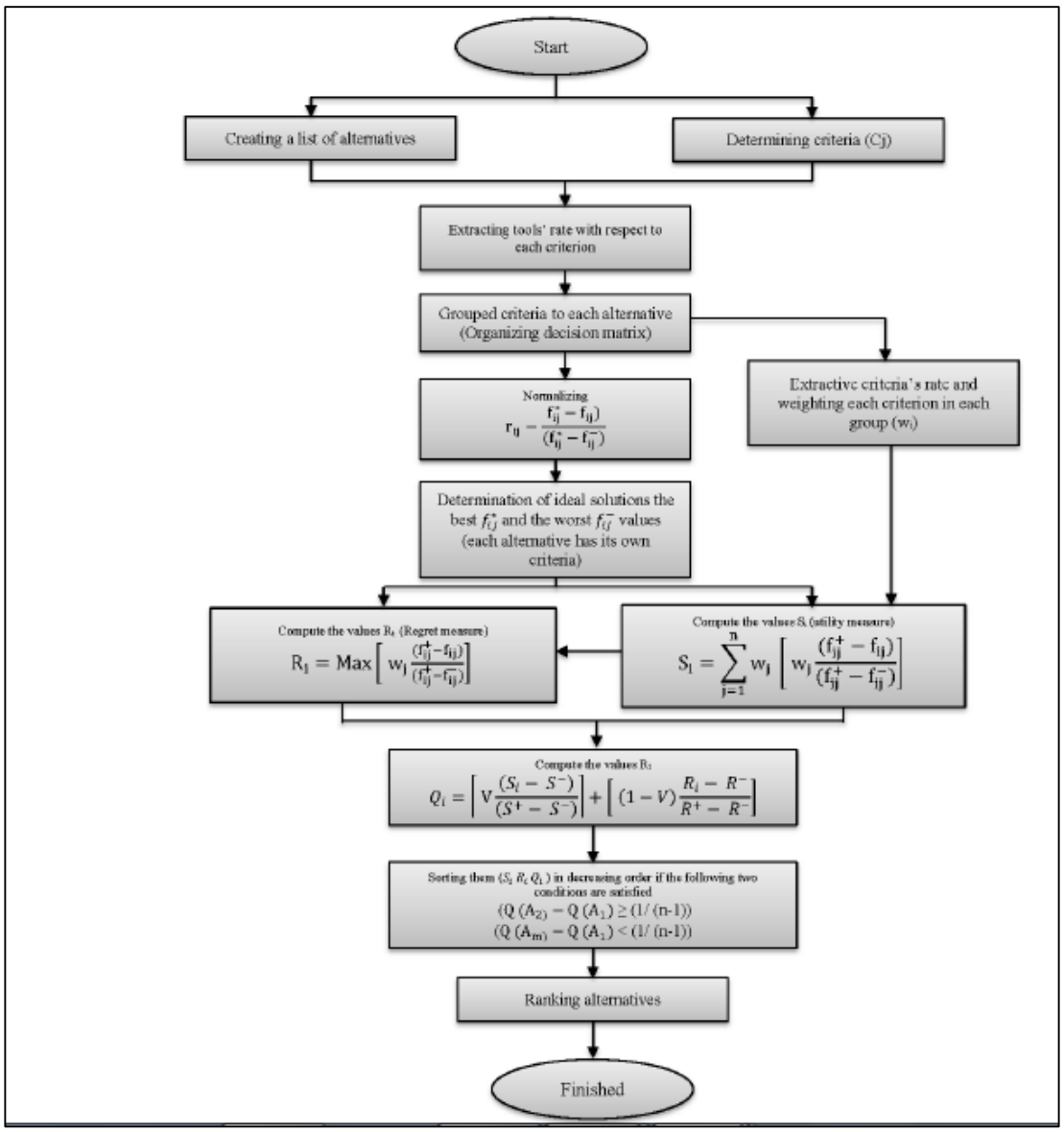

Figure 4.1. Diagram of modifying the VIKOR method [102].

PART 6

RESULTS AND DISCUSSION

6.1. THE IMPORTANCE AND ORIGINALITY OF THE STUDY

In the abrasive water jet (AWJ) process, which is a nontraditional material processing technology, engineering materials with high hardness and brittleness can be processed with high precision by erosive effect [103-109].

Thanks to the high pressure created in the AWJ process, ceramics, glass, rock, high hardness steels (>60 HRC) and composites can be processed [110-116].

In the water jet process, a rigid cutting can be performed by adding hard abrasive particles into the water jet. Also, since there is no thermal effect in the process, distortion, microstructure and mechanical softening based problems are not observed. No thermal effect is vital to increase the machinability of polymer materials. The disadvantages of the AWJ process are high noise generation (>100 dB), pressure-dependent water splash and conical edge formation over the kerf [117-118].

Generation of high heat and high operating temperatures during machining of engineering materials are inevitable. The generated energy by the friction between the workpiece and the cutting tool and the separation of atomic bonds during plastic deformation are the main reasons of the increasing temperature. Metallic materials have a high thermal conductivity coefficient compared to other engineering materials, so they are less affected by thermal deformation. However, in polymer materials, undesirable manufacturing problems arise due to high temperature such as distortion, increase in surface roughness, material plastering, build-up edge [119-122].

By optimizing the process parameters during the machining process of polymer materials, these faults can be minimized [91]. However, optimizing parameters is not enough to improve surface quality as a high amount of heat is generated during the machining applications due to high speed and load. Using cutting fluids is essential to remove heat from the workpiece. However, the negative effects of mineral and semi-synthetic cutting fluids on the environment and human health limit the use of them [123, 92, 124].

The use of vegetable-based cooling fluids in machining is limited since they have a low tribological performance at high temperatures due to their low thermo-oxidation resistance [125, 126]. For these reasons, it is necessary to use a process without heat generation in order to increase the machinability of the polymer materials. The water-jet process, in which cutting can be carried out without increasing the temperature, is very useful for increasing the machinability of polymer materials and improving the surface quality [115,127,128,34,21]. Kartal et al. [40], investigated the optimum parameters for minimum surface roughness (Ra) and maximum material removal rate (MRR) in the turning of lowdensity polyethylene material by experimental and statistical methods, and concluded that AWJ method is an effective method for machining polymers. In this study, three levels were determined for traverse speed (TS), abrasive flow rate (AFR) and spindle speed (SS), and a full factorial experimental design was established. According to the analysis results, 5 mm/min TS, 350 g/min AFR and 2500 min_1 SS were obtained as optimum parameters for minimum Ra (1.67 mm) and maximum MRR (14072.02 mm3/min). Eliminating the thermal effects during the AWJ machining of the polymer materials, machinability can be significantly improved [94]. However, there are problems associated with surface quality and ergonomics [129].

Surface roughness is highly effective in determining the fatigue life of the materials operating under dynamic loads. Low surface quality in the AWJT process is related to the explosion behavior of the water jet after it exits the nozzle. Due to the pressure change, the water jet is scattered along with the abrasive particles. Due to this scattering behavior, the rigidity of the cutting jet contacting the material decreases and the surface quality of the material is deteriorated. Furthermore, the AWJT process

produces noise and splash problems induced by high pressure. High-pressure AWJ produces noise at an unacceptable level (~110 dB) for workers' health [130,131]. To solve problems of surface quality and sound ergonomics, the scattering behavior in the jet nozzle should be controlled.

In this study, it has been hypothesized that the problems above can be solved by operating the jet nozzle at submerged conditions under hydrostatic pressure. Therefore, a submerged AWJT system was used, and machinability of castamide material was investigated as the novelty of the study. The aim of underwater turning is to ensure that the water jet under hydrostatic pressure is contacted to the workpiece material with a minimum scattering behavior and minimizing hypersonic water jet noise. This study is unique in the literature by using of the submerged AWJT apparatus for improving the machinability of castamide materials. Also, there are limited studies on the investigation of the machinability of polymer materials using submerged AWJT process. Castamide material was preferred as the test material due to its importance in engineering applications and its extensive use in machine design [93]. The experiments were carried out according to the full factorial design, and the experimental results were evaluated and optimized using statistical methods (variance and regression analyses, TOPSIS and VIKOR).

6.2. EXPERIMENTAL RESULTS AND DISCUSSION

Noise and splashing in the conventional AWJT process is given in Figure 6.1 (a), and the noise and machining conditions with the submerged AWJT are given in Figure 6.2 (b).

Figure 6.1. Process conditions of (a) Conventional AWJT and (b) Submerged AWJT.

The sound level was reduced from 108.8 dB to 86.1 dB by the submerged method. In addition, a stable machining zone was formed by avoiding splash. The experiments performed according to the full factorial experimental design and the obtained Ra and MRR values are given in Table 6.1, which shows that the lowest value for Ra is 1.46 mm which was achieved in the 6th test.

Table 6.1. Experimental results.

Experiment Number	NFR (mm/min)	AFR (g/min)	Spindle Speed (rpm)	Ra (μm)	MRR (mm^3/min)
1	10	50	100	2.89	142.79
2	10	50	200	2.81	149.88
3	10	50	300	1.92	154.1
4	10	250	100	2.56	154.88
5	10	250	200	2.11	158.6
6	10	250	300	1.46	169.07
7	10	450	100	1.52	182.25
8	10	450	200	1.61	192.52
9	10	450	300	1.95	215.93
10	30	50	100	4.25	109.94
11	30	50	200	3.27	117.13
12	30	50	300	3.97	120.94
13	30	250	100	3.81	125.93
14	30	250	200	3.17	126.46
15	30	250	300	3.37	127.77
16	30	450	100	2.57	132.11
17	30	450	200	2.68	135.39
18	30	450	300	3.07	141.89
19	50	50	100	5.46	79.76
20	50	50	200	5.46	84.93
21	50	50	300	5.04	85.63
22	50	250	100	4.27	88.01
23	50	250	200	4.92	88.82
24	50	250	300	4.89	94.9
25	50	450	100	4.49	96.65
26	50	450	200	4.4	99.73
27	50	450	300	4.28	103.71
Total Square root				354.642	481346.7768
Square root				18.83194095	693.7915946

Kartal and Yerlikaya [94] achieved a minimum of 1.73 mm roughness value in turning castamide with conventional AWJT. Results show a 15% increase in the surface quality for the submerged AWJT process. Kartal and Yerlikaya [94], achieved a maximum 212 mm3/min MRR value which was decreased to 200.93 mm3/min by a 5.22% decrease using submerged AWJT process (Table 5.3). MRR decreased due to the resistance caused by hydrostatic pressure under submerged conditions. However,

according to these results, it is difficult to say that the submerged AWJT process is effective or not. According to the experiences from the AWJ process, output parameters variation up to 20% could be caused by material in-homogeneity, local disorders in jet pressure, suction-based problems and machine movement. Therefore, uncertainties up to 20% are considered to lay within an interval of AWJ uncertainty and improvement of any qualitative or quantitative parameter within this range cannot be considered as a significant one. In this situation, according to the results, it can be said that the submerged AWJT process has similar characteristics in terms of Ra and MRR with the conventional AWJT process. However, reducing the noise and splashing problems in the underwater AWJT process makes an important difference. For this reason, submerged AWJT is more advantageous in general comparison. In addition, the possible causes of the results obtained for Ra and MRR were tried to be discussed, although they are considered within the uncertainty. The lower Ra formation in the submerged AWJT method can be explained by the expansion behaviour of the water jet shown in Figure 5.2. In the conventional AWJT process, water jet moves at high pressure through the nozzle [132,133], and when the water jet leaves the nozzle, it passes from a high-pressure zone to a low-pressure zone, and the jet expands. Because of this behaviour, the linear flow behaviour of the cutting jet deteriorates, and the stability is lost, and the pressure value gained for cutting the material is reduced due to its increased effect area. This can also be defined as a transition from laminar flow to turbulent flow. It is an expected result that as the flow behaviour deteriorates, Ra value is negatively affected. In the submerged AWJT process, water jet with a huge pressure (~3800 bar) in the nozzle passes into a hydrostatic pressure area which minimizes the expansion of water jet and provides a stable cutting operation. SEM images obtained for the conventional and submerged AWJT processes also support the results obtained for surface roughness (Figure 6.2). In the conventional AWJT process, because of the expanding water jet profile, it is expected that the abrasive particles in the water jet will be dispersed and that the micro-size particles stuck into the surface of the castamide material. In the submerged AWJT process, it is expected that more controlled dissemination of abrasive particles onto the surface of the workpiece due to the reduction of the water jet expansion.

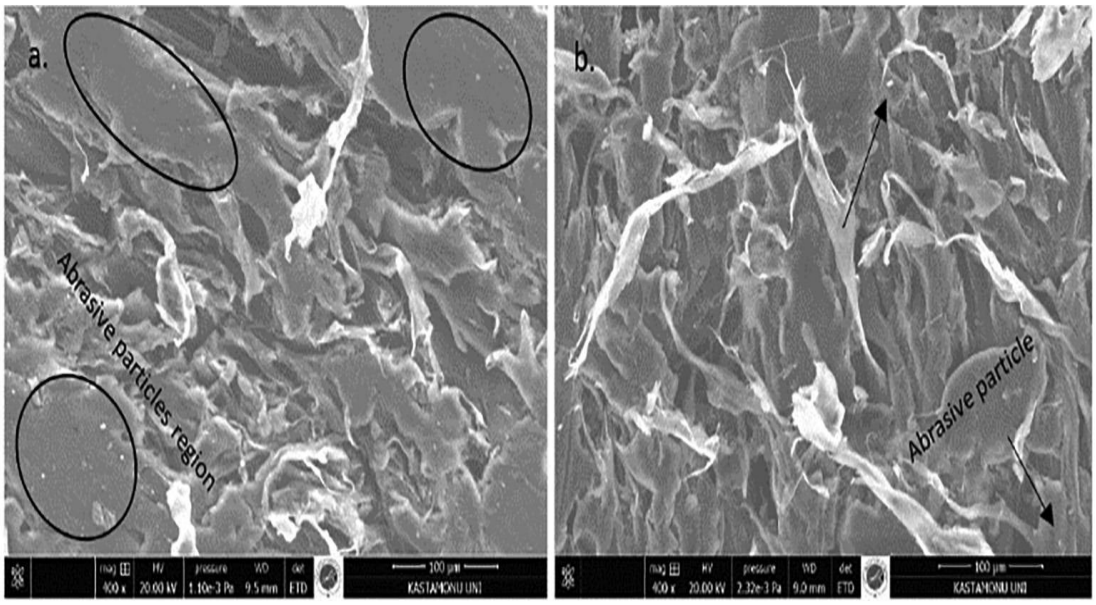

Figure 6.2. Surface SEM images of (a) Conventional AWJT, (b) Submerged AWJT (In conditions of 240 mm/min TS, 110 g/min AFR and 100 rpm Spindle Speed).

In Figure 6.2 (a), abrasive particles concentrated on the surface are shown. Figure 6.2 (b) shows that there are abrasive particles only at certain locations on the surface. SEM images were obtained for experimental conditions where surface roughness is the maximum. Images show that the submerged AWJT method is successful in reducing surface roughness. The behavior of abrasive particles in the jet is also important on the surface roughness. Abrasive particles break down significantly under high pressure. At this stage, large particles are drawn towards the slower outer part of the jet, while small particles are drawn towards the faster central part of the jet [110]. In this case, the abrasive effects of large particles decrease as they are exposed to more braking due to air friction. However, the significance of this effect should be discussed by material type. In the processing of steel materials, the effect on surface quality may decrease due to the decreasing energy. In polymer materials, even if the energy of the particles on the outer surface of the jet decreases, the outer particles will influence the material surface form due to the low strength of the polymer materials. In addition, braking abrasive particles when contacting the polymer material is important for surface quality. Particles stuck on the soft surface of polymer materials cause increased surface roughness. For this reason, the braking of particles in water instead of air and losing their energy with more friction effect is vital for reducing the surface roughness values

of polymer materials. In addition, even if the braking energy underwater is too high, the pressure value of the particles will be more than enough to process the polymer material.

6.2.1. Effect of Process Parameters on Ra

The effects of process parameters were determined by ANOVA, and surface roughness results were given in Table 6.2. The input parameters that are most effective on Ra value are the traverse speed (83.11%) and the abrasive flow rate (10.1%). Spindle speed (0.53%) has no significant effect on Ra (Table 6.2). The values obtained from the F test confirm the effect ratios and agrees with the literature [32, 134].

Two-way interaction of the parameters did not make a significant change on surface roughness. According to p values in Table 6.2, TS ($p = 0 < 0.05$) and AFR ($p = 0.002 < 0.05$) has statistically and physically significant effect on Ra while SS ($p = 0.487 > 0.05$) is not significantly effective.

Table 6.2. ANOVA results for surface roughness.

Source of Variance	**Degree of Freedom (DF)**	**Sum of Squares (SS)**	**Mean of Squares (MS)**	**F Ratio**	**P**	**Effect Rate (%)**
NFR	2	33.0761	16.5381	124.51	0.000	**83.11**
AFR	2	4.0189	2.0094	15.13	0.002	**10.1**
SS	2	0.2096	0.1048	0.79	0.487	**0.53**
NFR * AFR	4	0.1356	0.0339	0.26	0.899	**0.34**
NFR * SS	4	0.7853	0.1963	1.48	0.295	**1.97**
AFR * SS	4	0.5079	0.1270	0.96	0.481	**1.28**
Error	8	1.0626	0.1328			**2.67**
Total	26	39.7961				**100**
Significance	**R-Sq = 97.33%**				**R-Sq (adj) = 91.32%**	

Although the effect ratio of AFR parameter can be considered as low (10.1%), it is an important result that it has statistical and physical effect according to the p-value. The R-Sq (adj) value given in Table 5.4 for the surface roughness was found to be 91.32%.

This ratio proves the reliability of the test system when it is equal and over 80% [94, 135].

The statistical graphs obtained for the R-Sq (adj) value are given in Figure 6.3. According to the normal distribution graph given in Figure 6.3 (a), all experimental data are listed on the regression line. The histogram graph is given in Figure 6.3 (c) also shows behavior close to the normal distribution curve (Percentage deviation is 0.15% while the standard deviation is 1.237%) [136].

The difference between the experimental graph and the actual graph can be explained by the low significance data points shown in Figure 6.3 (b) and (d). These points negatively affecting the significance of the experimental data are produced by some unexplained factors during the experiment such as vibration, temperature variation etc.

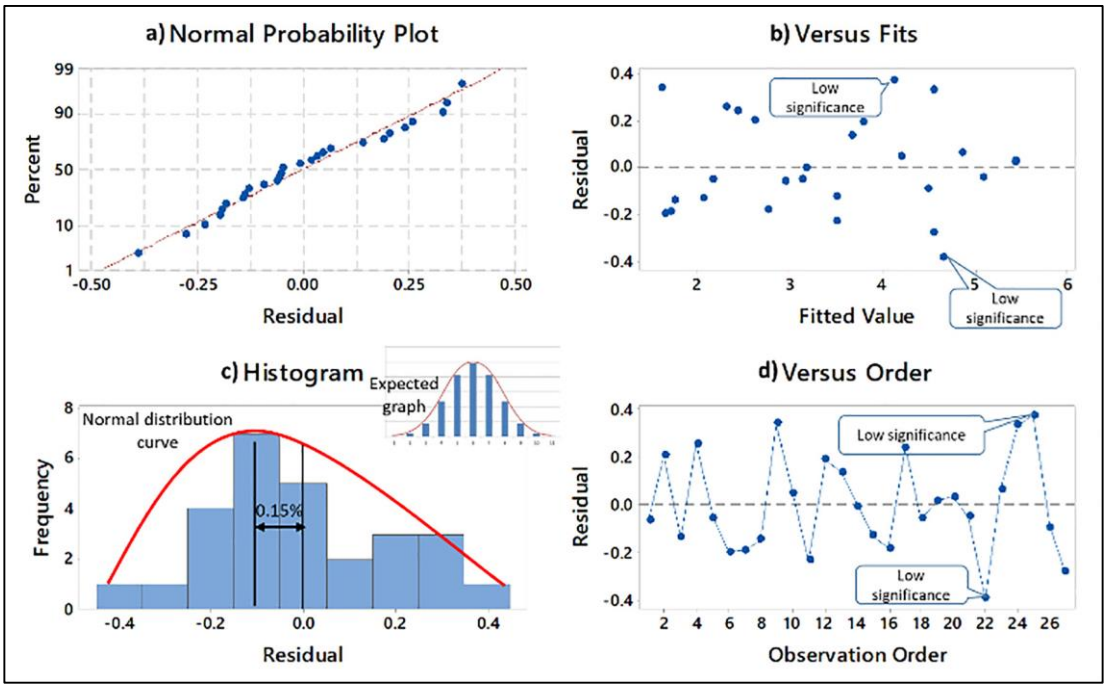

Figure 6.3. Statistical graphs for the reliability of Ra results.

Figure 6.4 gives the topography graphs obtained for the variation of Ra values according to the change of parameter levels. According to Figure 6.4, the surface roughness increased with the parameter TS, which had an effect of 83.11% on the surface roughness. Due to the increase in the traverse speed, the nozzle waiting time

required to process the castamide material will be reduced. In the AWJT process, the abrasive jet first applies a rough cutting process. Then, by increasing the waiting time of the nozzle, a finish material removal process is applied to the surface. Because of the decreased machining time due to increased TS, finish cutting process couldn't be applied which was required to achieve a low roughness value. Additionally, a spiral track is formed on the rotating workpiece depending on the linear movement of the nozzle. Increasing speed also increased the length between spiral tracks which increases the roughness. Kartal and Yerlikaya [94], found the effect ratio of TS parameter as 87.1% in conventional AWJ method. The effect of TS decreased by 4% in submerged machining conditions. Increasing TS negatively affects the Ra value. Therefore, decreasing the effect ratio of TS is an achievement for increasing machining speed. The effect rate of AFR parameter (10.1%) was found the same as Kartal and Yerlikaya [122]. Since the water contacts the workpiece under 3800 bar pressure, the effect of AFR parameter on Ra was found the same for both conventional and submerged systems. The correlation between the change in AFR value and the surface roughness values is consistent with the literature [122]. As the AFR value increased, surface roughness values decreased (Figure 6.4 (a) and (b)). With the increase of AFR, more abrasive particles contact the workpiece and better surface roughness is achieved. Due to the increased amount of abrasive, the cutting jet acts more rigidly and homogeneously on the cutting zone. It can be claimed that laminar flow can be achieved due to increased rigidity and homogeneity. Therefore, the increase in AFR ratio positively affected the surface quality. The effect rate of the SS parameter (0.53%) decreased compared to the results of Kartal and Yerlikaya [122] (1.1%). The hydrostatic pressure in the submerged system increases the friction force on the workpiece, making the rotation difficult. Therefore, the effect of SS parameter in submerged AWJT process decreased compared to that of the conventional AWJT process. Variation of SS parameters and the surface roughness indicate no significant correlation between the parameters (Figure 6.4 (b) and (c)). It can be claimed that the protective water film layer formed by centrifugal forces on the workpiece prevented the interaction between SS parameter and Ra.

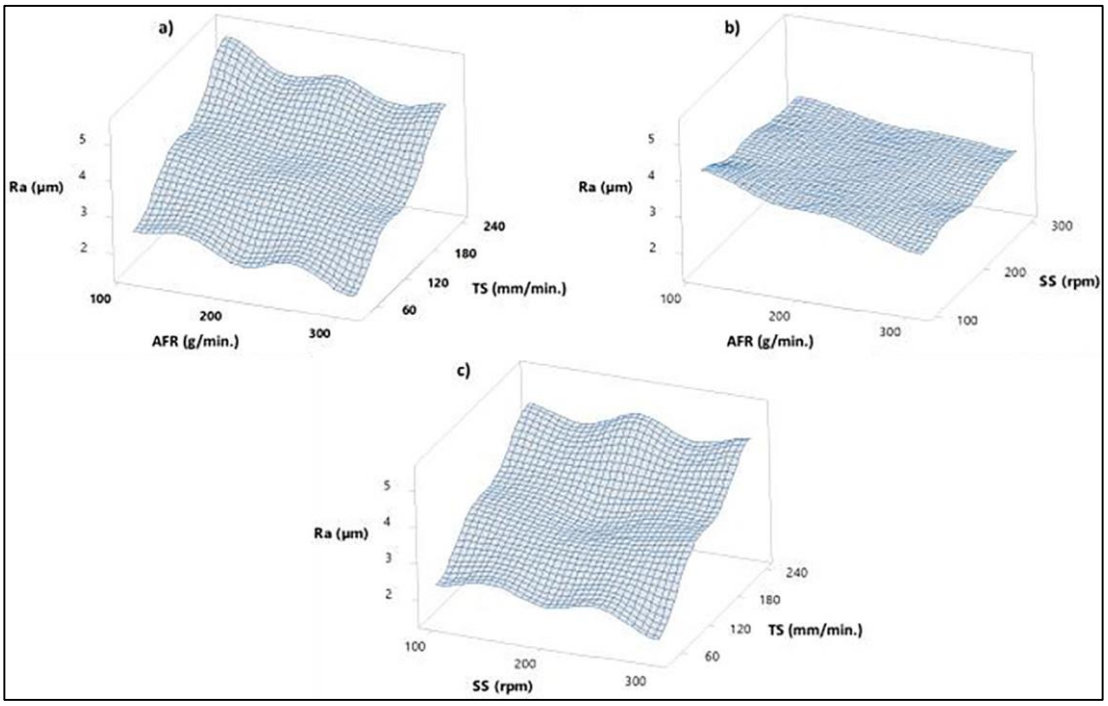

Figure 6.4. Topography images for understanding the effects of process parameters on Ra.

6.2.2. Effect of Process Parameters on Material Removal Rate (MRR)

The effect of machining parameters on the MRR was determined by ANOVA method (Table 6.3). According to Table 5.5, the effect rates of machining parameters TS, AFR, SS on MRR were determined as 85.56%, 10.26% and 1.10%, respectively. The values obtained from the F test confirm the effect rates. Kartal and Yerlikaya [94] found the effect ratio of TS, AFR and SS for the conventional AWJT as 82.56%, 11.36% and 1.73%, respectively. Based on the ANOVA results, no significant difference was found between the submerged and conventional AWJT. According to p values in Table 6.3, TS ($p = 0 < 0.05$), AFR ($p = 0 < 0.05$) and SS ($p = 0 < 0.05$) parameters has statistically and physically significant effect on MRR. Besides, the interaction of TS parameter with AFR ($p = 0 < 0.05$) and SS ($p = 0.002 < 0.05$) parameters was found to be statistically and physically important. As seen in Table 5.5, the R-Sq(adj) value for MRR was found as 99.89%.

Table 6.3. ANOVA results for material removal rate (MRR).

Source of Variance	Degree of Freedom (DF)	Sum of Squares (SS)	Mean of Squares (MS)	F Ratio	P	Effect Rate (%)
NFR	2	26172.6	13086.88	10079.88	0.000	**85.56**
AFR	2	3137.7	1568.9	1208.42	0.000	**10.26**
SS	2	336.3	168.2	129.53	0.000	**1.10**
NFR * AFR	4	858.8	214.7	165.37	0.000	**2.81**
NFR * SS	4	59.8	14.9	11.51	0.002	**0.19**
AFR * SS	4	13.2	3.3	2.54	0.122	**0.05**
Error	8	10.4	1.3			**0.03**
Total	26	30588.8				**100**
Significancy	**R-Sq = 99.97%**			**R-Sq (adj) = 99.89%**		

According to this value, the input parameters considered can fully explain the variation of the MRR parameter. The statistical graphs obtained for the R- Sq (adj) value are given in Figure 6.5. According to the normal distribution graph given in Figure 6.5 (a), all experimental data are distributed on the regression line. The histogram graph in Figure 6.5 (c) shows normal distribution curve behavior (Percentage deviation is 0% while the standard deviation is 34.30%). In Figure 6.5 (b) and (d), the distances between the test results and the regression line are graphically given. Test data distributed homogeneously along the center axis and the normal distribution curve in the histogram confirms the significance of the test data in the 95% confidence region.

Topographic graphs representing the variation of MRR values according to the change of parameter levels are given in Figure 6.5. According to Figure 6.6 (a) and (c), MRR value decreased by the increasing TS parameter, which is 85.56% effective on MRR. Machining time decreases with increasing TS. Due to the shorter machining time, the contact duration between the abrasive material and the castamide was reduced and thus the MRR values decreased. According to Figure 6.6 (a) and (b), MRR value increased by the increasing AFR. Increasing MRR value can be explained by the increasing flow rate of particles contacting the castamide material. As the AFR increases, the cutting

stability will increase due to increased jet rigidity. This can also be expressed as penetration to the determined depth of cut. Increased penetration enabled better material removal. Figure 6.6 (b) and (c) show that MRR didn't change by the SS parameter. TS and AFR parameters have high physical effects on MRR, and therefore the SS parameter didn't show a significant effect.

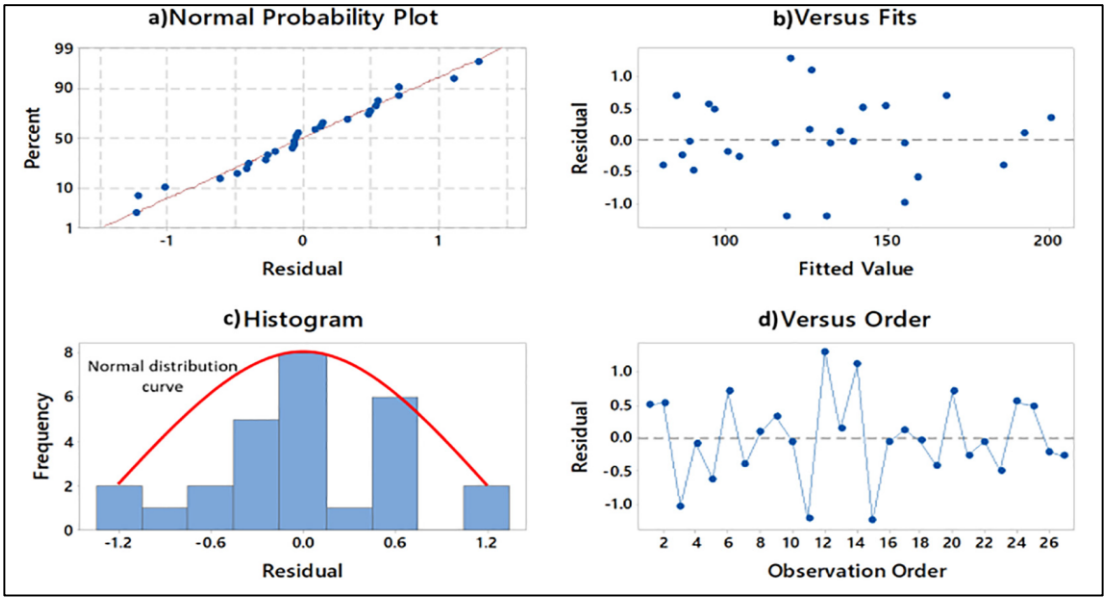

Figure 6.5. Statistical graphs for the reliability of MRR results.

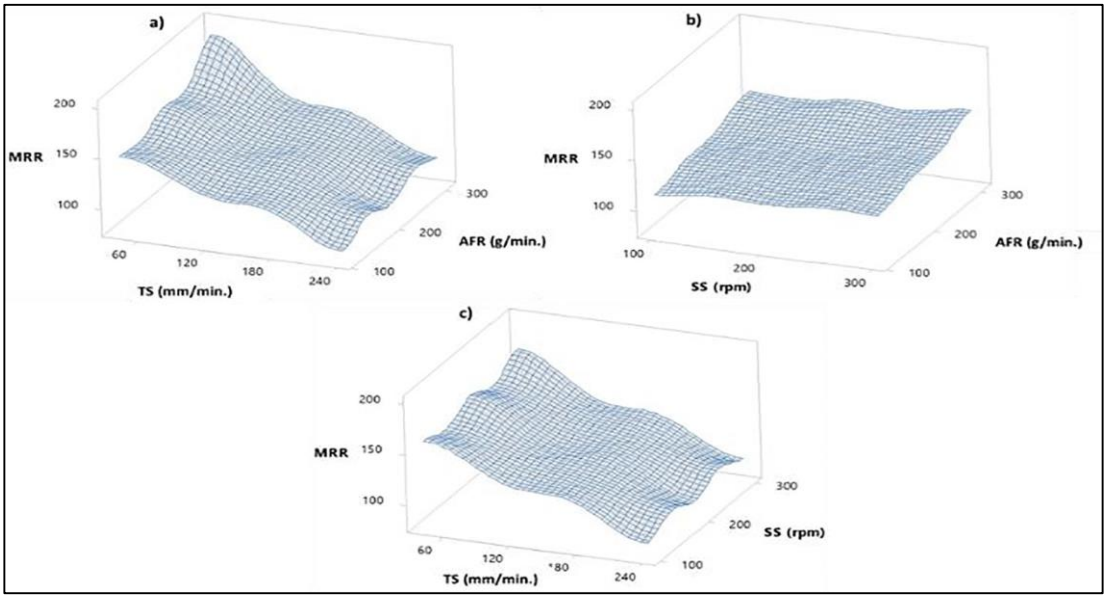

Figure 6.6. Topography images for understanding the effects of process parameters on MRR.

6.2.3. Optimization of Process Parameters

Optimum process parameters of submerged AWJT process are determined by TOPSIS and VIKOR methods. Minimization of Ra and maximization of MRR was considered as the goal functions. Solution steps were given for TOPSIS and VIKOR in Tables 6-13. Table 5.14 indicates that the optimum point in both TOPSIS and VIKOR methods is testing conditions of the number 9 (TS: 40 mm/min, the AFR is 310 g/min, SS 300 rpm). The Ra value measured in experiment 9 is 1.95 mm, and the calculated MRR is 200.93 mm^3 /min. Optimum conditions were obtained at minimum levels of TS and maximum levels of AFR and SS parameters. ANOVA and topography results agree with data obtained from optimum points. Therefore, the results obtained from TOPSIS and VIKOR methods are reliable. In addition, the same results obtained by two different methods increases reliability.

6.2.3.1. TOPSIS Method

TOPSIS method is one of the multi-criteria decision-making methods. The principle, optimum the point closest to the ideal solution and the farthest from the negative ideal solution is the determination [137]. TOPSIS method is an essential factor in complex decision problems has become an evaluation method. Its use is both academic and business. It covers a wide range of fields. TOPSIS method in five steps It is formed. TOPSIS method mathematically with the following steps it is summarized [138].

1. Matrix Equation is normalized to 6,1

$$n_{ij} = \frac{x_{ij}}{\sqrt{\sum_{i=1}^{m} x_{ij}^2}} j = 1,2,3,\dots,n; i = 1,2,3\dots,m \quad (6.1)$$

2. Normalized decision matrix elements are associated with equations. multiplied by weights and weighted normalized decision matrix Equation 6.2 created by

$$V_{ij} = n_{ij} w_{ij}\ j = 1,2,\dots,n; i = 1,2,3,\dots,m \quad (6.2)$$

3. Ideal solutions are calculated by Equation 5.4 and Equation 5.5.

$$\{V_1^+, V_2^+, Idots, V_n^+\}\{\max V_{ij} | j \in K), \left((MinV_{ij} | \in K') | i = 1,2, \dots, m \right)\} \quad (6.3)$$

$$\{V_1^-, V_2^-, Idots, V_n^-\}\{\max V_{ij} | j \in K), \left((MinV_{ij} | \in K') | i = 1,2, \dots, m \right)\} \quad (6.4)$$

K is the index set of utility criteria, and K 'is for negative criteria.

4. Optimum ideal (Equality 6.5) and negative ideal (Equality 6.6) values are below

$$s_i^+ == \left\{ \sum_{j=1}^{n} \left(V_{ij} - V_j^+ \right)^2 \right\}^{0.5} j = 1,2, \dots, n; i = 1,2,3, \dots m \quad (6.5)$$

$$s_i^- == \left\{ \sum_{j=1}^{n} \left(V_{ij} - V_j^- \right)^2 \right\}^{0.5} j = 1,2, \dots, n; i = 1,2,3, \dots m \quad (6.6)$$

5. For the ideal solution, proximity is evaluated by Equation 6.7

$$C_i = \frac{S_i^-}{S_i^+ + S_i^-} \; j = 1,2, \dots, n; i = 1,2,3, \dots, m; 0 \ll C_i \ll 1 \quad (6.7)$$

The highest Ci value is the ideal parameter for the TOPSIS Method

6.2.3.2. VIKOR Method

VIKOR method is another multi-criteria decision-making method. VIKOR method is close to ideal, providing maximum benefit and minimal damage for the majority determines a compromise solution. In recent years, the VIKOR method is multi-criteria and alternative has become a support tool with a wide range of uses in solving problems [138]. The VIKOR method is summarized mathematically as follows [138]:

1. The highest (xij) max and lowest (xij) min parameters are decided first it must be determined among all the criteria determined from the matrix.
2. Ei and Fi parameters are calculated according to Equality 6.8-6.9.

$$E_i = \sum_{j=1}^{n} w_j \left[w_i \left[\left(x_{ij}\right)_{max} - \left(x_{ij}\right) \right] / \left[\left(x_{ij}\right)_{max} - \left(x_{ij}\right)_{min} \right] \right] \quad (6.8)$$

$$E_i = max \left[w_i \left[\left(x_{ij}\right)_{max} - \left(x_{ij}\right) \right] / \left[\left(x_{ij}\right)_{max} - \left(x_{ij}\right)_{min} \right] \right] \quad (6.9)$$

3. Qi value is calculated according to Equation 6.10.

$$Q_i = \left(v\left(E_i - E_{i_{min}}\right) / \left(E_{i_{max}} - E_{i_{min}}\right) \right) + (1 - v) \left(\left(F - F_{i_{min}}\right) / \left(F_{i_{max}} - F_{i_{min}}\right) \right) \quad (6.10)$$

The variable v is called the group utility and is taken as approximately 0.5. Ei, Fi and Qi values are statistical weight coefficient values.

4. Ei, Fi and Qi values are sorted from small to large.
5. Acceptable (C1) and acceptable stability (C2) clusters are determined. In order for any alternative to be in the C1 cluster, the equation is shown in 6.11. must meet the condition.

$$(A_2) - (A_1) \geq DQ \quad (6.11)$$

Table 6.4. Rated Ra and MRR values for TOPSIS.

Experiment number	NFR (mm/min)	AFR (g/min)	Spindle Speed (rpm)	Rated Ra	Rated MRR
1	10	50	100	0.153462673	0.205811084
2	10	50	200	0.149214572	0.216030291
3	10	50	300	0.10195444	0.222112809
4	10	250	100	0.135939254	0.223237066
5	10	250	200	0.112043682	0.228598907
6	10	250	300	0.077527856	0.243689894
7	10	450	100	0.080713932	0.262686953
8	10	450	200	0.085493046	0.277489669
9	10	450	300	0.103547478	0.31123179
10	30	50	100	0.225680402	0.158462571
11	30	50	200	0.173641156	0.168825914
12	30	50	300	0.210812046	0.174317477
13	30	250	100	0.202315843	0.181509838
14	30	250	200	0.168331029	0.182273756
15	30	250	300	0.178951283	0.184161931
16	30	450	100	0.136470266	0.190417412
17	30	450	200	0.142311406	0.195145057
18	30	450	300	0.163020902	0.204513864
19	50	50	100	0.28993294	0.114962477
20	50	50	200	0.28993294	0.122414282
21	50	50	300	0.267630406	0.123423231
22	50	250	100	0.226742427	0.126853656
23	50	250	200	0.261258253	0.128021153
24	50	250	300	0.259665215	0.136784592
25	50	450	100	0.238424707	0.139306963
26	50	450	200	0.233645592	0.143746336
27	50	450	300	0.22727344	0.149482929

Table 6.5. Weighted Ra and MRR values for TOPSIS.

Experiment Number	NFR (mm/min)	AFR (g/min)	Spindle Speed (rpm)	Weighted Ra	Weighted MRR
1	10	50	100	0.076731337	0.102905542
2	10	50	200	0.074607286	0.108015145
3	10	50	300	0.05097722	0.111056405
4	10	250	100	0.067969627	0.111618533
5	10	250	200	0.056021841	0.114299453
6	10	250	300	0.038763928	0.121844947
7	10	450	100	0.040356966	0.131343476
8	10	450	200	0.042746523	0.138744835
9	10	450	300	0.051773739	0.155615895
10	30	50	100	0.112840201	0.079231286
11	30	50	200	0.086820578	0.084412957
12	30	50	300	0.105406023	0.087158738
13	30	250	100	0.101157921	0.090754919
14	30	250	200	0.084165515	0.091136878
15	30	250	300	0.089475642	0.092080966
16	30	450	100	0.068235133	0.095208706
17	30	450	200	0.071155703	0.097572528
18	30	450	300	0.081510451	0.102256932
19	50	50	100	0.14496647	0.057481238
20	50	50	200	0.14496647	0.061207141
21	50	50	300	0.133815203	0.061711615
22	50	250	100	0.113371214	0.063426828
23	50	250	200	0.130629127	0.064010577
24	50	250	300	0.129832608	0.068392296
25	50	450	100	0.119212353	0.069653481
26	50	450	200	0.116822796	0.071873168
27	50	450	300	0.11363672	0.074741465
Minimum				0.038763928	0.155615895
Maximum				0.14496647	0.057481238

Table 6.6. Optimum and negative ideal solution table for TOPSIS.

Experiment Number	NFR (mm/min)	AFR (g/min)	Spindle Speed (rpm)	Si+	Si-	Total
1	10	50	100	0.054152	0.05008	0.104232
2	10	50	200	0.048885	0.055484	0.10437
3	10	50	300	0.044709	0.062409	0.107118
4	10	250	100	0.04485	0.060066	0.104916
5	10	250	200	0.041614	0.064729	0.106344
6	10	250	300	0.033771	0.075643	0.109414
7	10	450	100	0.024275	0.084805	0.10908
8	10	450	200	0.016887	0.091713	0.108599
9	10	450	300	0.000169	0.10682	0.106989
10	30	50	100	0.081872	0.022782	0.104654
11	30	50	200	0.073512	0.030313	0.103825
12	30	50	300	0.072898	0.031243	0.104141
13	30	250	100	0.068754	0.035193	0.103947
14	30	250	200	0.06654	0.037352	0.103893
15	30	250	300	0.066107	0.037679	0.103786
16	30	450	100	0.061276	0.043615	0.104891
17	30	450	200	0.059093	0.045539	0.104632
18	30	450	300	0.055186	0.048802	0.103989
19	50	50	100	0.109414	0	0.109414
20	50	50	200	0.105688	0.003726	0.109414
21	50	50	300	0.102939	0.004355	0.107294
22	50	250	100	0.097755	0.006944	0.104699
23	50	250	200	0.100045	0.006735	0.106779
24	50	250	300	0.095517	0.01114	0.106657
25	50	450	100	0.092434	0.012836	0.10527
26	50	450	200	0.089836	0.015184	0.10502
27	50	450	300	0.08648	0.018242	0.104722

Table 6.7. Ideal solution table for TOPSIS.

Experiment Number	NFR (mm/min)	AFR (g/min)	Spindle Speed (rpm)	Pi	Rank
1	10	50	100	0.480469	9
2	10	50	200	0.531613	8
3	10	50	300	0.582622	6
4	10	250	100	0.572513	7
5	10	250	200	0.608681	5
6	10	250	300	0.691346	4
7	10	450	100	0.777458	3
8	10	450	200	0.844503	2
9	10	450	300	0.998418	1
10	30	50	100	0.21769	18
11	30	50	200	0.291959	17
12	30	50	300	0.300003	16
13	30	250	100	0.338566	15
14	30	250	200	0.359529	14
15	30	250	300	0.363046	13
16	30	450	100	0.415815	12
17	30	450	200	0.435234	11
18	30	450	300	0.469305	10
19	50	50	100	0	27
20	50	50	200	0.034053	26
21	50	50	300	0.040587	25
22	50	250	100	0.066322	23
23	50	250	200	0.063073	24
24	50	250	300	0.104448	22
25	50	450	100	0.12193	21
26	50	450	200	0.144582	20
27	50	450	300	0.174192	19

Table 6.8. Determination of maximum and minimum values for VIKOR method.

Experiment Number	NFR (mm/min)	AFR (g/min)	Spindle Speed (rpm)	Ra (μm)	MRR (mm^3/min)
1	10	50	100	2.89	142.79
2	10	50	200	2.81	149.88
3	10	50	300	1.92	154.1
4	10	250	100	2.56	154.88
5	10	250	200	2.11	158.6
6	10	250	300	1.46	169.07
7	10	450	100	1.52	182.25
8	10	450	200	1.61	192.52
9	10	450	300	1.95	215.93
10	30	50	100	4.25	109.94
11	30	50	200	3.27	117.13
12	30	50	300	3.97	120.94
13	30	250	100	3.81	125.93
14	30	250	200	3.17	126.46
15	30	250	300	3.37	127.77
16	30	450	100	2.57	132.11
17	30	450	200	2.68	135.39
18	30	450	300	3.07	141.89
19	50	50	100	5.46	79.76
20	50	50	200	5.46	84.93
21	50	50	300	5.04	85.63
22	50	250	100	4.27	88.01
23	50	250	200	4.92	88.82
24	50	250	300	4.89	94.9
25	50	450	100	4.49	96.65
26	50	450	200	4.4	99.73
27	50	450	300	4.28	103.71
Maximum				1.46	215.93
Minimum				5.46	79.76

Table 6.9. Weighted Ra and MRR values for VIKOR.

Experiment Number	NFR (mm/min)	AFR (g/min)	Spindle Speed (rpm)	Weighted Ra	Weighted MRR
1	10	50	100	0.17875	0.268561357
2	10	50	200	0.16875	0.242527723
3	10	50	300	0.0575	0.227032386
4	10	250	100	0.1375	0.224168319
5	10	250	200	0.08125	0.210508923
6	10	250	300	0	0.172064331
7	10	450	100	0.0075	0.123668943
8	10	450	200	0.01875	0.085958728
9	10	450	300	0.06125	0
10	30	50	100	0.34875	0.389182639
11	30	50	200	0.22625	0.362781817
12	30	50	300	0.31375	0.348791951
13	30	250	100	0.29375	0.330469266
14	30	250	200	0.21375	0.32852317
15	30	250	300	0.23875	0.323713006
16	30	450	100	0.13875	0.307777043
17	30	450	200	0.1525	0.295733275
18	30	450	300	0.20125	0.27186605
19	50	50	100	0.5	0.5
20	50	50	200	0.5	0.481016377
21	50	50	300	0.4475	0.47844606
22	50	250	100	0.35125	0.469706984
23	50	250	200	0.4325	0.466732761
24	50	250	300	0.42875	0.444407726
25	50	450	100	0.37875	0.437981934
26	50	450	200	0.3675	0.426672542
27	50	450	300	0.3525	0.412058456

Table 6.10. Calculation clusters for VIKOR method.

Experiment Number	NFR (mm/min)	AFR (g/min)	Spindle Speed (rpm)	Si	Ri
1	10	50	100	0.447311357	0.268561357
2	10	50	200	0.411277723	0.242527723
3	10	50	300	0.284532386	0.227032386
4	10	250	100	0.361668319	0.224168319
5	10	250	200	0.291758923	0.210508923
6	10	250	300	0.172064331	0.172064331
7	10	450	100	0.131168943	0.123668943
8	10	450	200	0.104708728	0.085958728
9	10	450	300	0.06125	0.06125
10	30	50	100	0.737932639	0.389182639
11	30	50	200	0.589031817	0.362781817
12	30	50	300	0.662541951	0.348791951
13	30	250	100	0.624219266	0.330469266
14	30	250	200	0.54227317	0.32852317
15	30	250	300	0.562463006	0.323713006
16	30	450	100	0.446527043	0.307777043
17	30	450	200	0.448233275	0.295733275
18	30	450	300	0.47311605	0.27186605
19	50	50	100	1	0.5
20	50	50	200	0.981016377	0.5
21	50	50	300	0.92594606	0.47844606
22	50	250	100	0.820956984	0.469706984
23	50	250	200	0.899232761	0.466732761
24	50	250	300	0.873157726	0.444407726
25	50	450	100	0.816731934	0.437981934
26	50	450	200	0.794172542	0.426672542
27	50	450	300	0.764558456	0.412058456
Si Ri+				0.06125	0.06125
Si Ri-				1	0.5

Table 6.11. Weighted coefficient values for VIKOR method.

Experiment Number	NFR (mm/min)	AFR (g/min)	Spindle Speed (rpm)	Qi	Rank
1	10	50	100	0.441877	19
2	10	50	200	0.393017	20
3	10	50	300	0.307851	22
4	10	250	100	0.345672	21
5	10	250	200	0.29287	23
6	10	250	300	0.185306	24
7	10	450	100	0.108373	25
8	10	450	200	0.051305	26
9	10	450	300	0	27
10	30	50	100	0.734129	10
11	30	50	200	0.624735	12
12	30	50	300	0.647945	11
13	30	250	100	0.606653	13
14	30	250	200	0.560789	15
15	30	250	300	0.566061	14
16	30	450	100	0.48615	16
17	30	450	200	0.473334	17
18	30	450	300	0.459388	18
19	50	50	100	1	1
20	50	50	200	0.989889	2
21	50	50	300	0.935994	3
22	50	250	100	0.870116	5
23	50	250	200	0.908418	4
24	50	250	300	0.869088	6
25	50	450	100	0.831711	7
26	50	450	200	0.806807	8
27	50	450	300	0.77438	9

Table 6.12. Ranking for optimum points.

Exp. No	**Topsis Method**				**Vikor Method**			
	S_i^+	S_i^-	C_i	**Rank**	ΣE_i	F_i	Q_i	**Rank**
1	0.054152	0.05008	0.480469	9	0.447311	0.268561	0.441877	19
2	0.048885	0.055484	0.531613	8	0.411278	0.242528	0.393017	20
3	0.044709	0.062409	0.582622	6	0.284532	0.227032	0.307851	22
4	0.04485	0.060066	0.572513	7	0.361668	0.224168	0.345672	21
5	0.041614	0.064729	0.608681	5	0.291759	0.210509	0.29287	23
6	0.033771	0.075643	0.691346	4	0.172064	0.172064	0.185306	24
7	0.024275	0.084805	0.777458	3	0.131169	0.123669	0.108373	25
8	0.016887	0.091713	0.844503	2	0.104709	0.085959	0.051305	26
9	**0.000169**	**0.10682**	**0.998418**	**1**	**0.06125**	**0.06125**	**0**	**27**
10	0.081872	0.022782	0.21769	18	0.737933	0.389183	0.734129	10
11	0.073512	0.030313	0.291959	17	0.589032	0.362782	0.624735	12
12	0.072898	0.031243	0.300003	16	0.662542	0.348792	0.647945	11
13	0.068754	0.035193	0.338566	15	0.624219	0.330469	0.606653	13
14	0.06654	0.037352	0.359529	14	0.542273	0.328523	0.560789	15
15	0.066107	0.037679	0.363046	13	0.562463	0.323713	0.566061	14
16	0.061276	0.043615	0.415815	12	0.446527	0.307777	0.48615	16
17	0.059093	0.045539	0.435234	11	0.448233	0.295733	0.473334	17
18	0.055186	0.048802	0.469305	10	0.473116	0.271866	0.459388	18
19	0.109414	0	0	27	1	0.5	1	1
20	0.105688	0.003726	0.034053	26	0.981016	0.5	0.989889	2
21	0.102939	0.004355	0.040587	25	0.925946	0.478446	0.935994	3
22	0.097755	0.006944	0.066322	23	0.820957	0.469707	0.870116	5
23	0.100045	0.006735	0.063073	24	0.899233	0.466733	0.908418	4
24	0.095517	0.01114	0.104448	22	0.873158	0.444408	0.869088	6
25	0.092434	0.012836	0.12193	21	0.816732	0.437982	0.831711	7
26	0.089836	0.015184	0.144582	20	0.794173	0.426673	0.806807	8
27	0.08648	0.018242	0.174192	19	0.764558	0.412058	0.77438	9

6.2.4. Regression Analyses for Obtaining Empiric Equations

Equation (6.12) was used for the Ra value determined based on the experimental results. A multilinear regression analysis (Equation. (6.13) was performed to predict the Ra and MRR [18, 140].

Since the parameter changes in Figure 6.1 and Figure 6.6 are linear, there is no need for expressions of the equation containing second-degree polynomials and interactions. Regression analysis was applied to experimental results to develop mathematical equations explaining the relationships between variables (Equation (6.14) and (Equation (6.15). Equations can be used for estimation and reliability tests. The TS, AFR and SS parameters were considered as independent variables, while Ra and MRR parameters were considered as dependent variables in the modeling studies. The equations were obtained as linear without interactions; i.e. less independent parameter was used for practical usage of equations [18, 140].

$$R_a = \frac{1}{L}\int_0^L |y(x)||dx| \tag{6.12}$$

$$R_a = \beta_0 + \sum_{i=1}^{k} \beta_i X_i + \sum_{i=1}^{k} \beta_{ii} X_i^2 + \sum\sum_{i<j} \beta_{ii} X_i X_j + \in_i \tag{6.13}$$

$$R_a(\mu m) = 2.715 + 13x10^{-3}TS - 4x10^{-3}AFR - 1x10^{-3}SS \tag{6.14}$$

$$MRR = 145.92 - 38.1 \times 10^{-2}TS + 13 \times 10^{-2}AFR + 43 \times 10^{-3}SS \tag{6.15}$$

6.2.5. Confirmation Tests

Confirmation tests were performed for optimum point and regression equations obtained from TOPSIS and VIKOR algorithm. In addition to the optimum value, two randomly determined test conditions were also considered to improve reliability. Error-values were calculated according to Equation (6.16). According to the confirmation tests in Table 6.13, a maximum of 13.07% and 8.49% error is determined

for the Ra and MRR respectively between the estimated value and the actual results. In addition, the regression equations were applied to all parameters in Table 6.13, and it was determined that the mean error is 9.99% for the Ra value and 3.72% for the MRR value. Cetin et al. [129] argue that 20% and less error indicates acceptable reliability. However, it is not correct to generalize these equations for the submerged AWJT process. It is stated in the literature that these equations have limited validity [141, 63,142,143]. An underwater AWJT process must be analyzed analytically to find general equations. In the literature, there are analytical equations developed for speed, diameter and manufacturing angles [51, 96, 100, 102, 106, 144, 145]. However, analytical models developed for Ra and MRR parameters are not sufficient.

On the other hand, there is an analytical model used in conventional turning for surface roughness. In Equation (6.17), f represents the tool feed rate, and r is the cutting tool radius. However, the usability of this equation for submerged AWJT is not possible. Although the feed rate and TS are the same parameters, a stable insert diameter is not available in the submerged AWJT. It can be claimed that this value is constantly changing according to pressure and abrasive particle behaviour. For this reason, only regression equations were used for reliability experiments in the study.

$$\%Error = |(Exp. - Pre.)/Exp| \times 100 \tag{6.16}$$

$$Ra = f^2/32.r \tag{6.17}$$

Table 6.13. Results of confirmation experiments and predicted values by regression equations.

Parameter	**Point**	**For Regression Analysis**		
		Experimental	**Predicted**	**Error (%)**
R_a	Optimum (NFR: 40 mm/min, AFR: 310 g/min, SS: 300 rpm)	*1.95*	*1.695*	*13.07*
	Random (NFR: 140 mm/min, AFR: 210 g/min, SS: 200 rpm)	*3.17*	*3.49*	*10.25*
	Random (NFR: 240 mm/min, AFR: 110 g/min, SS: 300 rpm)	*5.04*	*5.095*	*1.09*
MRR	Optimum (NFR: 40 mm/min, AFR: 310 g/min, SS: 300 rpm)	*200.93*	*183.88*	*8.49*
	Random (NFR: 140 mm/min, AFR: 210 g/min, SS: 200 rpm)	*127.46*	*128.48*	*0.80*
	Random (NFR: 240 mm/min, AFR: 110 g/min, SS: 300 rpm)	*85.63*	*81.68*	*4.61*

PART 7

CONCLUSIONS

This study clearly indicates that water jet machining reduces operational costs and reduces the processing time by reducing or eliminating the expensive secondary machining process. This process does not involve heat application to the materials, and it does not harm the workpiece. Abrasive water jet turning system was initially developed for operating underwater. This study is also conducted to handle issues like the splash and loud noise, which are observed in conventional AWJT systems, and they increase the plastic materials' machinability. The cutting surface remains clean and does not require additional treatment. Since it is environment-friendly, it does not create toxic or environmentally hazardous substances. It works at low tolerance, its sound level was reduced to 85dB, and besides, water splashes were prevented. In this study, optimum NFR, AFR and SS parameters were investigated to minimize surface roughness and maximize the chip removal rate in the underwater AWJT process. The quantitative effect of input parameters and optimum parameters (TOPSIS and VIKOR) was examined by statistical methods (ANOVA) and changing the Ra and MRR values according to the change in parameter levels, which were examined by graphical analysis. The obtained results are given below:

1. Under conventional AWJT conditions, the noise level was 108.8dB, which decreased to 86.1 dB using the submerged AWJT. Moreover, splashes were eliminated to form a stable machining zone.
2. Conventional AWJT showed a minimum of 1.73 μm Ra value, while the highest MRR value was 212 mm^3/min. In the submerged AWJT, the least Ra value was 1.46 μm while the highest MRR value was 200.93 mm^3/min.

3. ANOVA results show that TS, SS, and AFR parameters respectively affected the Ra value by 83.11%, 0.53%, and 1.10%. TS mainly affected Ra, and its value increased with increasing TS. Moreover, it was found that TS, SS, and AFR parameters respectively affected the MRR value by 85.56%, 1.10%, and 10.26%. Increasing TS and AFR parameters reduced the MRR values.
4. ANOVA results for conventional and submerged AWJT processes were similar.
5. R-Sq values (variance analysis) for Ra and MRR were 91.32% and 99.89%, respectively. It was confirmed that the obtained values were statistically sufficient.
6. The optimum test conditions (TOPSIS and VIKOR methods) were AFR: 310 g/min, TS: 40 mm/min, and SS: 300 rpm.
7. After validation tests for optimizing regression equations and TOPSIS, it was found that error rates were below 20%, which assures the reliability of the experimental design.

REFERENCES

1. Cad, M. E., & Student, C. M., "Parametric analysis of abrasives water jet machining of en8 material", ***Journal of Engineering Research and Application,*** *2*(3): 3029–3032 (2012).

2. Korat, M. M., & Acharya, G. D., "A Review on current research and development in abrasive waterjet machining", ***Journal of Engineering Research and Application,*** *4*(1): 423–432 (2014).

3. Sahu, R. K., Verma, S., & Mishra, S. K., "Optimization of parameters to minimize the skin friction coefficient in abrasive water suspension jet machining through TLBO", ***Advances in Production and Mechanical Engineering,*** *1*(4): 29–37 (2015).

4. Shah, R. V., & PATEL, D. M. "A study of Abrasive water jet Machining process On Granite Material", ***International Journal of Engineering Research and Applications (IJERA) ISSN,*** 2(3): 2248-9622 (2012).

5. Chandra, B., & Singh, J., "A study of effect of process parameters of abrasive jet machining", ***International Journal of Engineering Science and Technology,*** *3*(1): 12-17 (2011).

6. Selvan, M. C. P., & Raju, N. M. S., "Assessment of process parameters in abrasive waterjet cutting of granite", ***International Conference on Trends in Mechanical and Industrial Engineering (ICTMIE'2011),*** Bangkok, 140–144 (2011).

7. Kong, M. C., Axinte, D., & Voice, W., "Aspects of material removal mechanism in plain waterjet milling on gamma titanium aluminide", ***Journal of Materials Processing Technology,*** 210(3): 573–584 (2010).

8. Azmir, M. A., Ahsan, A. K., & Rahmah, A., "Effect of abrasive water jet machining parameters on aramid fibre reinforced plastics composite", ***International Journal of Material Forming,*** *2*(1): 37–44 (2009).

9. Wang, J., "A new model for predicting the depth of cut in abrasive waterjet contouring of alumina ceramics", ***Journal of Materials Processing Technology,*** *209*(5): 2314–2320 (2009).

10. Shaikh, A. A., & Ambardekar, V. S., "Predictive depth of cut model for abrasive water jet cutting of metal-polymer-metal laminate", ***International Journal of Emerging Technology and Advanced Engineering,*** 3(6): 2250-2459 (2013).

11. Zhong, Y., "A study of the cutting performance in multipass abrasive waterjet machining of alumina ceramics with controlled nozzle oscillation", ***The University of New South Wales,*** Australia, 24-31 (2008).

12. Xu, S., "Modelling the cutting process and cutting performance in abrasive waterjet machining with controlled nozzle oscillation", ***School of Engineering Systems Queensland University of Technology,*** Australia,1–205 (2006).

13. Kök, M., Kanca, E., & Eyercioğlu, Ö., "Prediction of surface roughness in abrasive waterjet machining of particle reinforced MMCs using genetic expression programming", ***The International Journal of Advanced Manufacturing Technology,*** *55*(9): 955–968 (2011).

14. Wang, J., "Depth of cut models for multipass abrasive waterjet cutting of alumina ceramics with nozzle oscillation", ***Frontiers of Mechanical Engineering in China,*** *5*(1): 19-32 (2010).

15. Shah, R. V., & Patel, D. M., "Abrasive water jet machining–The review", ***International Journal of Engineering Research and Applications,*** *2*(5): 803-806 (2012).

16. Wahaoil, C., "Maintenance Work Continues Inside the Tanks of Sidra Termina", https://www.wahaoil.ly/en/2020/03/4555/(2020).

17. Ergene, B., & Bolat, Ç., "A review on the recent investigation trends in abrasive waterjet cutting and turning of hybrid composites", ***Sigma: Journal of Engineering & Natural Sciences/Mühendislik ve Fen Bilimleri Dergis****,* 37 (3): 989-1016 (2019).

18. Çaydaş, U., & Hasçalik, A., "A study on surface roughness in abrasive waterjet machining process using artificial neural networks and regression analysis method", ***Journal of Materials Processing Technology,*** 202(3): 574–582 (2008).

19. Boud, F., Loo, L. F., & Kinnell, P. K., "The impact of plain waterjet machining on the surface integrity of aluminium 7475", ***Procedia Cirp,*** 13(2014): 382-386 (2014).

20. Akkurt, A., Kulekci, M. K., Seker, U., & Ercan, F., "Effect of feed rate on surface roughness in abrasive waterjet cutting applications", ***Journal of Materials Processing Technology,*** 147(3): 389–396 (2004).

21. Momber, A. W., & Kovacevic, R., "Principles of abrasive water jet machining", ***Springer Science & Business Media,*** New York, 20-25 (2012).

22. Palleda, M., "A study of taper angles and material removal rates of drilled holes in the abrasive water jet machining process", ***Journal of Materials Processing Technology,*** 189(3): 292–295 (2007).

23. Mutavgjic, V., Jurkovic, Z., Franulovic, M., & Sekulic, M., "Experimental investigation of surface roughness obtained by abrasive water jet machining", ***Experimental Investigation of Surface Roughness Obtained by Abrasive Water Jet Machining,*** 2(2): 73–76 (2011).

24. Hocheng, H., & Chang, K. R., "Material removal analysis in abrasive waterjet cutting of ceramic plates", ***Journal of Materials Processing Tech.,*** *40*(3): 287–304 (1994).

25. Azmir, M. A., & Ahsan, A. K., "A study of abrasive water jet machining process on glass/epoxy composite laminate", ***Journal of Materials Processing Technology,*** 209(20): 6168–6173 (2009).

26. Hascalik, A., Çaydaş, U., & Gürün, H., "Effect of traverse speed on abrasive waterjet machining of Ti-6Al-4V alloy", ***Materials and Design,*** 28(6): 1953–1957 (2007).

27. Khan, A. A., & Haque, M. M., "Performance of different abrasive materials during abrasive water jet machining of glass", ***Journal of Materials Processing Technology,*** 191(3): 404–407 (2007).

28. Jegaraj, J. J. R., & Babu, N. R., "A strategy for efficient and quality cutting of materials with abrasive waterjets considering the variation in orifice and focusing nozzle diameter", ***International Journal of Machine Tools and Manufacture,*** 45(13): 1443–1450 (2005).

29. Wang, J., & Wong, W. C. K., "A study of abrasive waterjet cutting of metallic coated sheet steels", ***International Journal of Machine Tools and Manufacture,*** 39(6): 855–870 (1999).

30. Ray, P. K., & Paul, A. K., "Some studies on abrasive jet machining", ***Fellow Department if Mechanical Engineering Regional Engineering College,*** Rourkela**,** 27-29 (1987).

31. Kartal, F., "A review of the current state of abrasive water-jet turning machining method", ***The International Journal of Advanced Manufacturing Technology,*** 88(4): 495–505 (2017).

32. Hashish, M., "Macro characteristics of AWJ turned surfaces", ***WJTA American Waterjet Conf Minnesota Paper No4***, Washington, USA, 1–14 (2001).

33. Zhong, Z. W., & Han, Z. Z., "Turning of glass with abrasive waterjet", ***Materials and Manufacturing Processes,*** 17(3): 339–349 (2002).

34. Andersson, U., Holmqvist, G., Öjmertz, K. M. C. "Abrasıve Waterjet Used As A Tool for Producıng Materıals Test Specımens" ***WJTA American Waterjet Conference,*** Houston, Texas, 17-19 (2003).

35. Uhlmann, E., Flögel, K., Kretzschmar, M., & Faltin, F., "Abrasive waterjet turning of high performance materials", ***Procedia CIRP,*** 1(1): 409–413 (2012).

36. Axinte, D. A., Stepanian, J. P., Kong, M. C., & McGourlay, J., "Abrasive waterjet turning-An efficient method to profile and dress grinding wheels", ***International Journal of Machine Tools and Manufacture,*** 49(3–4): 351–356 (2009).

37. Zohourkari, I. & Zohoor, M., "Mathematical modeling of abrasive waterjet turning of ductile materials", **In *Engineering Systems Design and Analysis***, 49(187): 825-830 (2010).

38. Kartal, F, & Gökkaya, H., "Aşındırıcı Su Jeti ile Tornalama Deney Düzeneği Tasarımı", ***International Iron& Steel Symposium,*** Karabük, Türkiye, 20-25 (2012).

39. Kartal, F., Gökkaya, H., & Nalbant, M., "Turning of (Cu-Cr-Zr) alloy with abrasive water jet", ***In 21st International Conference on Water Jetting,*** Ottawa, Canada, 15-21 (2012).

40. Kartal, Fuat, Çetin, M. H., Gökkaya, H., & Yerlikaya, Z., "Optimization of abrasive water jet turning parameters for machining of low density polyethylene material based on experimental design method", ***International Polymer Processing,*** 29(4): 535–544 (2014).

41. Kartal, F., & Gökkaya, H., "Aısı 1040 Çeliğinin Aşındırıcı Su Jeti İle tornalama İşleminde İşleme Paremetrelerinin Talaş Kaldırma Hacmine Ve Kesme Derinliğine Etkisi", ***Pamukkale Üniversitesi Mühendislik Bilimleri Dergisi,*** Turkey, 20(1): 20-24 (2013).

42. Hloch, S., Hlaváček, J., Vasilko, K., Cárach, J., Samardžić, I., Kozak, D., & Klichová, D., "Abrasive waterjet (AWJ) titanium tangential turning evaluation", ***Metalurgija,*** 53(4): 537-540 (2014).

43. Li, W. Y., Wang, J., & Ali, Y. M., "An experimental study of radial-mode abrasive waterjet turning of steels", ***Materials Science Forum,*** 6(8): 166–170 (2012).

44. Zohourkari, I., Zohoor, M., & Annoni, M., "Investigation of the effects of machining parameters on material removal rate in abrasive waterjet turning", ***Advances in Mechanical Engineering,*** Ukrain, 20-23 (2014).

45. Kartal, F., & Gökkaya, H., "Effect of abrasive water jet turning process parameters on surface roughness and material removal rate of AISI 1050 steel", ***Materials Testing,*** 57(9): 773-782 (2015).

46. Hashish, M., & Du Plessis, M. P., "Prediction equations relating high velocity jet cutting performance to stand off distance and multipasses", ***Dept. of Mechanical Engineering, Concordia University,*** Montreal, Canada , 20-35 (1979).

47. Chen, L., Siores, E., & Wong, W. C. K., "High-pressure abrasive waterjet erosion process", ***Proc. Australasian Conf. Manufacturing,*** Seoul, Korea, 642–647 (1996).

48. Vikram, G., & Ramesh Babu, N., "Modelling and analysis of abrasive water jet cut surface topography", ***International Journal of Machine Tools and Manufacture,*** 42(12): 1345–1354 (2002).

49. Çaydaş, U., & Hascalık, A., "A study on surface roughness in abrasive waterjet machining process using artificial neural networks and regression analysis method", ***Journal of Materials Processing Technology,*** 202(3): 574-582 (2008).

50. Aich, U., Bandyopadhyay, A., & Banerjee, S., "State of the Art—Review on Abrasive Water Jet Machining Process", ***International Review of Mechanical Engineering,*** 7(7): 1471-1494 (2013).

51. Manu, R., & Babu, N. R., "An erosion-based model for abrasive waterjet turning of ductile materials", ***Wear,*** 266(12): 1091–1097 (2009).

52. Selvan, M. C. P., & Raju, N. M. S., "Analysis of surface roughness in abrasive waterjet cutting of cast iron", ***International Journal of Science, Environment and Technology,*** 1(3): 174-182 (2012).

53. Borkowski, P. J., "Application of abrasive-water jet technology for material sculpturing", ***Transactions of the Canadian Society for Mechanical Engineering,*** 34(4): 389–400 (2010).

54. Rajyalakshmi, M., & Suresh Babu, P., "Abrasive Water Jet Machining - A review on current development", ***International Journal of Science Technology & Engineering***, 2(12): 428–434 (2016).

55. Hocheng, H., Tsai, H. Y., Shiue, J. J., & Wang, B., "Feasibility study of abrasive-waterjet milling of fiber-reinforced plastics", ***Journal of Manufacturing Science and Engineering, Transactions of the ASME,*** 119(2): 133–142 (1997).

56. Arola, D., & Ramulu, M., "Material removal in abrasive waterjet machining of metals a residual stress analysis", ***Wear,*** 211(2): 302–310 (1997).

57. Hloch, Sergej, & Rimar, M., "Design of experiments applied on abrasive waterjet factors sensitivity identification", ***Nonconventional Technologies Review,*** 2(2): 1454 (2005).

58. Zhu, H. T., Huang, C. Z., Wang, J., Li, Q. L., & Che, C. L., "Experimental study on abrasive waterjet polishing for hard-brittle materials", ***International Journal of Machine Tools and Manufacture,*** 49(8): 569–578 (2009).

59. Anil, J., Sandeep, S., Munish, K., "A literature review on the abrasive water jet machining - awjm process", ***International Journal of Engineering Sciences,*** 3(4): 22-69 (2016).

60. Oiseth, S. K., Krozer, A., Lausmaa, J., & Kasemo, B., "Ultraviolet light treatment of thin high-density polyethylene films monitored with a quartz crystal microbalance", ***Journal of Applied Polymer Science,*** 92(5): 2833–2839 (2004).

61. Duvall, D. E., & Edwards, D. B., "Oxidative degradation of high density polyethylene pipes from exposure to drinking water disinfectants", ***ESI Report,*** Aurora, Canada, 1-75 (2009).

62. Singh Butola, B. & Joshi, M., "Photostability of HDPE Filaments Stabilized with UV Absorbers (UVA) and Light Stabilizers (HALS)", ***Journal of Engineered Fibers and Fabrics***, 8(1): 15-58 (2013).

63. Kamweru, P. K., Ndiritu, F. G., Kinyanjui, T., Muthui, Z. W., & Gichuki, R., "UV Absorption and dynamic mechanical analysis of polyethylene films", ***International Journal of Physical Sciences,*** 9(24): 545–555 (2014).

64. Brandalise, R. N., Zeni, M., Martins, J. D., & Forte, M. M., "Morphology, mechanical and dynamic mechanical properties of recycled high density polyethylene and poly (vinyl alcohol) blends", ***Polymer Bulletin,*** 62(1): 33-43 (2009).

65. Barbosa, A. P., Costa, L. L., Portela, T. G. R., Moura, E. A., Del Mastro, N. L., Satyanarayana, K. G., & Monteiro, S. N., "Effect of electron beam irradiation on the mechanical properties of buriti fiber", ***Matéria (Rio de Janeiro),*** 17(4): 1135-1143 (2012).

66. Xia, W., Zhao, D. A., Guo, J., & Chen, B., "Research on the abrasive water-jet cutting machine information fusion fault diagnosis system based on fuzzy neural network", ***In 2010 International Conference on Biomedical Engineering and Computer Science,*** 3(4): 1-4 (2010).

67. Fredin, J., & Jönsson, A., "Experimentation on piercing with abrasive waterjet", ***World Academy of Science, Engineering and Technolgy,*** 5(2): 11-21 (2011).

68. Aich, U., Banerjee, S., Bandyopadhyay, A., & Das, P. K., "Abrasive water jet cutting of borosilicate glass", ***Procedia Materials Science,*** 6(5): 775-785 (2014).

69. Prasad, K. & Chakraborty, S., "A decision-making model for non-traditional machining processes selection", ***Decision Science Letters,*** 3(4): 467-478 (2014).

70. Choudhary, S. K., & Jadoun, R. S., "Current advanced research development of electric discharge machining (EDM): A review", ***International Journal of Research in Advent Technology,*** 2(3): 273-297 (2014).

71. Ho, K. H., & Newman, S. T., "State of the art electrical discharge machining (EDM)", International ***Journal of Machine Tools and Manufacture,*** 43(13): 1287-1300 (2003).

72. Anurag, R., Anirudh V, Nanjundeswaraswamy, D. S., "Chemical machining process - an overview", ***Published in International Research Journal of Innovations in Engineering and Technology (IRJIET),*** 3(11): 37-39 (2019).

73. Pandilov, Z., "Application of electro chemical machining for materials used in extreme conditions", ***In IOP Conf Ser Mater Sci Eng***, 3(29): 12-14 (2018).

74. Thoe, T. B., Aspinwall, D. K., & Wise, M. L. H., "Review on ultrasonic machining", ***International Journal of Machine Tools and Manufacture,*** *38*(4): 239-255 (1998).

75. Kataria, R., Kumar, J. & Pabla, B. S., "A review on ultrasonic machining", ***International Journal of Emerging Trends in Research,*** 1(2): 24-34 (2016).

76. Dubey, A. K., & Yadava, V., "Laser beam machining—a review", ***International Journal of Machine Tools and Manufacture,*** 48(6): 609-628 (2008).

77. Muangpool, T., & Pullteap, S., "Reviews on laser cutting technology for industrial applications", ***Third International Conference on Photonics Solutions (ICPS2017),*** 107(14): 107-140 (2018).

78. Mehta, J. N., Wadgaokar, R., Khatal, A. & Chavan, M., "Working model of water jet cutting system on low pressure", ***International Journal of Students Research in Technology & Management,*** 1(2): 242-252 (2013).

79. Khushaal, B., Tejas, H.S., Preran, K., Abhishek, S., Saqlain, I., Nanjundeswaraswamy, T. S. "Abrasive water jet machining", ***International Research Journal of Innovations in Engineering and Technology (IRJIET)*** 3(11): 61-65 (2019).

80. Benedict, G. F., "Nontraditional manufacturing processes", ***CRC Press,*** Florida, USA, 10-51 (1987).

81. Badgujar, P. P., & Rathi, M. G., "Abrasive Water jet Machining-A State of Art", ***IOSR Journal of Mechanical and Civil Engineering (IOSR-JMCE) e-ISSN,*** 3(2): 2278-1684 (2014).

82. Ebeid, S. J., Mahmoud, M., Sayed, M. M., & Atia, M. R. A., "Prediction of abrasive water jet plain milling process parameters using artificial neural networks", ***Journal of Machinery Manufacturing and Automation,*** 3(3):56- 73 (2014).

83. Kartal, F., "Design Optimization of Machining Parameters for AWJ Turning Operations of 718 Inconel Super alloy Based on the Taguchi", ***Uluslararası Muhendislik Arastirma ve Gelistirme Dergisi,*** 10(2): 148–156 (2018).

84. Hashish, M. "Turning with abrasive-waterjets—a first investigation", ***Journal of Manufacturing Science and Engineering,*** 109(4): 281-290 (1987).

85. Namazi, H., “Polymers in our daily life”, ***BioImpacts: BI,*** 7(2): 73 (2017).

86. Shradha, T., Lalit, S. & Vijay, S., “Miraculous adjuvants: the pharmaceutical polymers shradha tomar”, ***International Research Journal of Pharmacy,*** 7(7): 10-18 (2016).

87. Mark, J. E., “Physical properties of polymers handbook”, ***Springer,*** New York, 825 (2007).

88. Ünver, K. H., “Polymers as design materials for toy industry”, ***Master Thesis, Izmir Institute of Technology,*** Izmir, Turkey, 20-31 (1998).

89. Brahim, I. D., Jamiru, T., Sadiku, E. R., Hamam, A., & Kupolati, W. K., “Applications of polymers in the biomedical field”, ***Current Trends in Biomedical Engineering & Biosciences***, 4(5): 102-104 (2017).

90. Stein, R. S., “Polymer Science and Engineering-The Shifting Research Frontiers”, ***Journal of Polymer Science Part A: Polymer Chemistry,*** 32(16): 3215-3221 (1994).

91. Kechagias, J., Petropoulos, G., Iakovakis, V., & Maropoulos, S., "An investigation of surface texture parameters during turning of a reinforced polymer composite using design of experiments and analysis", ***International Journal of Experimental Design and Process Optimisation,*** *1*(3): 164 (2009).

92. Sales, W. F., Diniz, A. E., & Machado, Á. R., "Application of cutting fluids in machining processes", ***Journal of the Brazilian Society of Mechanical Sciences,*** 23(2): 227–240 (2001).

93. Bozdemir, M., & Aykut, Ş., "Optimization of surface roughness in end milling Castamide", ***The International Journal of Advanced Manufacturing Technology,*** 62(8): 495–503 (2012).

94. Kartal, Fuat, & Yerlikaya, Z., "Investigation of surface roughness and MRR for engineering polymers with the abrasive water jet turning process", ***International Polymer Processing,*** *31*(3): 336–345 (2016).

95. Hlavácˇ, L.M., Palicˇka, P., “Testing of parameters for turning by abrasive water jets”, ***In Proceedings of the 18th International Conference on Water Jetting,*** Gdansk, Poland, 123–128 (2020).

96. Cetin, M. H., Ozcelik, B., Kuram, E., & Demirbas, E., "Evaluation of vegetable based cutting fluids with extreme pressure and cutting parameters in turning of AISI 304L by Taguchi method", ***Journal of Cleaner Production,*** 19(18): 2049–2056 (2011).

97. Alvali, G.T. “Application of Engineering and Economy Approaches to the Transport Technology: A Case Study of Freight Wagon Bogie”, Karabuk University, Karabuk, Turkey, 12-19 (2019).

98. Jahan, A., Edwards, K. L., & Bahraminasab, M., "Multi-criteria Decision Analysis, For Supporting the Selection of Engineering Materials in Product Design", ***Butterworth-Heinemann,*** USA, 34-41 (2013).

99. Hwang, C.-L., Yoon, K., "Multiple Attribute Decision Making Methods and Applications", ***Springer,*** New York, USA, 21-26 (1981).

100. Sawyer, S. F., "Analysis of variance: the fundamental concepts", ***Journal of Manual & Manipulative Therapy,*** 17(2): 27-38 (2009).

101. Pavić, Z. & Novoselac, V., "Notes on TOPSIS method", ***International Journal of Research in Engineering and Science,*** 1(2): 5-12 (2013).

102. Mardani, A., Zavadskas, E. K., Govindan, K., Amat Senin, A. & Jusoh, A., VIKOR technique: A systematic review of the state of the art literature on methodologies and applications. ***Sustainability,*** 8(1): 37 (2016).

103. Karakurt, I., Aydin, G. & Aydiner, K., "Analysis of the kerf angle of the granite machined by abrasive waterjet (AWJ)", ***Indian Journal of Engineering and Materials Sciences***, *18*(6): 435–442 (2011).

104. Hlaváč, Libor M, Hlaváčová, I. M., Geryk, V., & Plančár, Š., "Investigation of the taper of kerfs cut in steels by AWJ", ***The International Journal of Advanced Manufacturing Technology,*** *77*(12): 1811–1818 (2015).

105. Aydin, G., Karakurt, I. & Aydiner, K., "Prediction of the cut depth of granitic rocks machined by abrasive waterjet (AWJ)", ***Rock Mechanics and Rock Engineering,*** *46*(5): 1223–1235 (2013).

106. Aydin, G., Karakurt, I. & Aydiner, K., "An investigation on surface roughness of granite machined by abrasive waterjet", ***Bulletin of Materials Science,*** *34*(4): 985–992 (2011).

107. Karakurt, I., Aydin, G. & Aydiner, K., "A machinability study of granite using abrasive waterjet cutting technology", ***Gazi University Journal of Science,*** *24*(1): 143–151 (2011).

108. Strnadel, B., Hlaváč, L. M. & Gembalová, L., "Effect of steel structure on the declination angle in AWJ cutting", ***International Journal of Machine Tools and Manufacture,*** 64(2): 12–19 (2013).

109. Karakurt, I., Aydin, G., & Aydiner, K., "An investigation on the kerf width in abrasive waterjet cutting of granitic rocks", ***Arabian Journal of Geosciences,*** *7*(7): 2923–2932 (2014).

110. Hlaváč, Libor M, Gembalová, L., Štěpán, P., & Hlaváčová, I. M., "Improvement of abrasive water jet machining accuracy for titanium and TiNb alloy", ***The International Journal of Advanced Manufacturing Technology,*** *80*(12): 1733–1740 (2015).

111. Karakurt, I., Aydin, G., & Aydiner, K., "An experimental study on the depth of cut of granite in abrasive waterjet cutting", ***Materials and Manufacturing Processes,*** 27(5): 538–544 (2012).

112. Hlavac, L. M., Spadło, S., Krajcarz, D., & Hlavacova, I. M., "Influence traverse speed on surface quality after water-jet cutting for hardox steel", ***METAL 2015 - 24th International Conference on Metallurgy and Materials, Conference Proceedings,*** Brno, Czech Republic, 723–728 (2015).

113. Gudimetla, P., Wang, J., & Wong, W., "Kerf formation analysis in the abrasive waterjet cutting of industrial ceramics", ***Journal of Materials Processing Technology,*** 128(3): 123–129 (2002).

114. Hlaváč, Libor M., Krajcarz, D., Hlaváčová, I. M., & Spadło, S., "Precision comparison of analytical and statistical-regression models for AWJ cutting", ***Precision Engineering,*** 50(2): 148–159 (2017).

115. Hlaváč, L. M., Hlaváčová, I. M., Gembalová, L., Kaličinský, J., Fabian, S., Měšťánek, J., Kmec, J., & Mádr, V., "Experimental method for the investigation of the abrasive water jet cutting quality", ***Journal of Materials Processing Technology,*** 209(20): 6190–6195 (2009).

116. Hlaváč, Libor M, Kocich, R., Gembalová, L., Jonšta, P., & Hlaváčová, I. M., AWJ cutting of copper processed by ECAP", ***The International Journal of Advanced Manufacturing Technology,*** *86*(4): 885–894 (2016).

117. Selvan, M. C. P., Raju, N. M. S., & Rajavel, R., "Effects of Process Parameters on Depth of Cut in Abrasive Waterjet Cutting of Cast Iron", ***International Journal of Scientific & Engineering Research,*** 2(9): 1–5 (2011).

118. Karakurt, I., Aydin, G., & Aydiner, K., "A study on the prediction of kerf angle in abrasive waterjet machining of rocks", ***Proceedings of the Institution of Mechanical Engineers, Part B: Journal of Engineering Manufacture,*** 226(9): 1489–1499 (2012).

119. Takeyama, H., & Iijima, N., "Machinability of glassfiber reinforced plastics and application of ultrasonic machining", ***CIRP Annals,*** 37(1): 93–96 (1988).

120. Weinert, K., & Kempmann, C., "Cutting temperatures and their effects on the machining behaviour in drilling reinforced plastic composites", ***Advanced Engineering Materials,*** *6*(8): 684–689 (2004).

121. König, W. & Grass, P. "Quality definition and assessment in drilling of fibre reinforced thermosets", ***CIRP Ann,*** 38 (2): 119–124 (1989).

122. Chen, W.C. "Some experimental investigations in the drilling of carbon fiberreinforced plastic (CFRP) composite laminates", ***Int. J. Mach. Tools Manuf,*** 3(7): 1097–1108 (1997).

123. Zimmerman, J. B. “Formulation Evaluation of Emulsifier Systems For Petroleumand Bio-Based Semi-Synthetic Metalworking Fluids”, ***University of Michigan,*** 20-25 (2003).

124. Yücel, E., Günay, M., Ayyıldız, M., Erkan, Ö. & Kara, F., “Talas_lı _Imalatta Kullanılan Kesme Sıvılarının _Insan Sag˘lıg˘ına Etkileri Ve Sürdürülebilir Kullanımı”, ***In: 6th International Advanced Technologies Symposium (IATS’11),*** Elazıg, Turkey,116–121 (2011).

125. Pillay, D.S., Sidik, N.A.C., “Tribological properties of biodegradable nanolubricant”, ***J. Adv. Res. Fluid Mech. Thermal Sci.*** 3(2): 1–13 (2017).

126. Mang, T., Dresel, W. “Lubricants and Lubrication”, ***Weinheim,*** Germany, 10-15 (2007).

127. Liu, H., Wang, J., Kelson, N., & Brown, R. J., “A study of abrasive waterjet characteristics by CFD simulation”, ***J. Mater. Process. Technol.*** 153(154): 488–493 (2004).

128. Ma, C., & Deam, R. T., "A correlation for predicting the kerf profile from abrasive water jet cutting", ***Experimental Thermal and Fluid Science,*** *30*(4): 337–343 (2006).

129. Kumar, K., Zindani, D., & Davim, J. P., "Advanced Machining and Manufacturing Processes", ***Springer,*** New York, USA, 31-35 (2018).

130. Kalla, D. K., Zhang, B., Asmatulu, R., & Dhanasekaran, P. S., "Current research trends in abrasive waterjet machining of fiber reinforced composites", ***Materials Science Forum,*** *7(13)*: 37–42 (2012).

131. Radvanská, A., Ergić, T., Ivandić, Ž., Hloch, S., Valicek, J., & Mullerova, J., "Technical possibilities of noise reduction in material cutting by abrasive water-jet", ***Strojarstvo,*** 51(4): 347–354 (2009).

132. Hashish, M., Steele, D. E., & Bothell, D. H., "Machining with super-pressure (690 MPa) waterjets", ***International Journal of Machine Tools and Manufacture,*** 37(4): 465–479 (1997).

133. Ansari, A. I., Hashish, M., & Ohadi, M. M., "Flow visualization study of the macromechanics of abrasive-waterjet turning", ***Experimental Mechanics,*** 32(4): 358–364 (1992).

134. Lohar, S. R., & Kubade, P. R., "Investigation of effect of abrasive water jet machining process parameters on performance characteristics of high carbon high chromium steel", ***International Advanced Research Journal in Science, Engineering and Technology,*** 4(2): 152–158 (2017).

135. Montgomery, D., "Montgomery Design and Analysis of Experiments", ***John Wiley & Sons,*** New Jersy, USA, 22-25 (1997).

136. Wang, J., "Abrasive waterjet machining of polymer matrix composites–cutting performance, erosive process and predictive models", ***The International Journal of Advanced Manufacturing Technology,*** *15*(10): 757–768 (1999).

137. Unal, O., & Maleki, E., "Shot peening optimization with complex decision-making tool: Multi criteria decision-making", ***Measurement,*** 125 (2), 133-141 (2018).

138. Khorshidi, R. & Hassani, A., "Comparative analysis between TOPSIS and PSI methods of materials selection to achieve a desirable combination of strength and workability in Al/SiC composite", ***Materials & Design***, 52(2), 999-1010 (2013).

139. İnternet: "Bütünleşik AHP TOPSIS-VIKOR Uygulaması", **https://www.slideshare.net/ahmetsonmez37/btnleik-ahp-topsisvikor-uygulamas/** (2018).

140. Valíček, J., Hloch, S., & Kozak, D., "Surface geometric parameters proposal for the advanced control of abrasive waterjet technology", ***The International Journal of Advanced Manufacturing Technology,*** 41(4): 323 (2009).

141. Hloch, S., Fabian, S., & Straka, L., "Factor analysis and mathematical modelling of AWJ cutting", ***Proceedings of the International Conference of DAAAM Baltic*** , 2(2): 127–132 (2006).

142. Aydin, G., Karakurt, I., & Hamzacebi, C., "Artificial neural network and regression models for performance prediction of abrasive waterjet in rock cutting", ***The International Journal of Advanced Manufacturing Technology,*** *75*(12): 1321–1330 (2014).

143. Hloch, S, Gombár, M., Fabian, S., & Straka, L., "Factor analysis of abrasive waterjet process factors influencing the cast aluminum surface roughness", ***Manufacturing Science and Technology.*** *Malaysia*, 145–149 (2006).

144. Hlaváč, Libor M, Strnadel, B., Kaličinský, J., & Gembalová, L., "The model of product distortion in AWJ cutting", ***The International Journal of Advanced Manufacturing Technology,*** 62(4): 157–166 (2012).

145. Hlaváč, Libor M, Hlaváčová, I. M., & Geryk, V., "Taper of kerfs made in rocks by abrasive water jet (AWJ)", ***The International Journal of Advanced Manufacturing Technology***, 88(4): 443–449 (2017).

RESUME

Salem A. Basher Ibrahim was born in Agala, Libya, in 1973. He received his early education in Tripoli where he finished his high school education at Ajdabiya High School. Then, he took admission in an undergraduate program offered by The Faculty of Mechanical Engineering, Libyan Department of Construction Engineering, in 2005. From 2005 to 2007, he performed at a consulting office where he used his engineering design skills and supervised several teams and projects, which were going on in Libya. In 2007-2008, he undertook Tripoli International Airport project, and accomplished it with a French organization APAV. From 2009 to 2010, he initiated his work as a civil engineer at the Savings Company, which was dealing with major investments in real estate and construction where he supervised several real estate projects. Since 2010, he is working for the Savings and Real Estate Investment Bank as a civil engineer. To accomplish his MSc, he moved to Turkey where he took admission in Karabük University in 2017.

CONTACT INFORMATION

Address : Graduate School of Mechanical Engineering
Demir-Çelik Campus
Karabük University, Karabuk City, Turkey
E-mail : salemibrahim114@yahoo.com
Phone : 00905439178647- 00218914354403

WORK EXPERIENCE

1996 - 1998	Eni (Agaco) Oil Company Limited H.V.A.C (Heating, Ventilation and Air-Conditioning) Technician
1998 – 2005	Eni (Agaco) Oil Company Limited H.V.A.C Engineer Promoted after gaining problem-solving experience, and Higher Diploma

DUTIES AND RESPONSIBILITIES

- Supervise maintenance activities before failure to assure job performance according to the standards
- Perform and observe all tests and checks relevant to maintenance and installation activities
- Evaluate technical equipment and study electric diagrams
- Allocate job requests and issue work orders to employees after completion of jobs
- Organize and file all personal documents and fill up timesheets for each employee.

EDUCATIONAL CAREER

After performing several years for Oil Sector, I became an educator, and joined Mrada Mechanical Engineering Department Higher Institute of Comprehensive Professions as a lecturer of Mechanical Engineering.

SPECIFIC KNOWLEDGE & SKILLS

- Arabic and English language skills
- Obtained ICDL certificate; so, I am proficient in using computers (specifically Microsoft Office & internet applications).
- Team building and development skills
- Plants and machinery overhauling
- HVAC system troubleshooting
- Spare parts' analysis

HOBBIES

Football, travel, watching movies and reading.